VNIVERSITAT DE VALÈNCIA
525 anys 1499 - 2024
Doctoral Program in Physiology
Department of Physiology
Faculty of Medicine and Odontology

ROLE OF T-TYPE VOLTAGE-GATED CALCIUM CHANNELS ON VASCULAR TONE

International Doctoral Thesis

Andrea Suárez Fortea

Under the supervision of:

Dr. María Dolores Mauricio Aviñó

Dr. Eva Serna García

Dr. Solanye Jacqueline Guerra Ojeda

Valencia, July 2024

Dr. María Dolores Mauricio Aviñó, professor at the Department of Physiology, Faculty of Medicine and Odontology, University of Valencia.

Dr. Eva Serna García, professor at the Department of Physiology, Faculty of Medicine and Odontology, University of Valencia.

Dr. Solanye Jacqueline Guerra Ojeda, postdoctoral researcher at the Department of Physiology, Faculty of Medicine and Odontology, University of Valencia.

Certify that:

The present dissertation, entitled "**Role of T-type Voltage-Gated Calcium Channels on vascular tone**", has been written by **Andrea Suárez Fortea** under their supervision. This manuscript corresponds to the Doctoral Program with International Mention in Physiology of the University of Valencia.

In recognition whereof, we sign the present certificate in Valencia, July 2024.

MARIA DOLORES MAURICIO AVIÑO - NIF:53204038R

Firmado digitalmente por MARIA DOLORES MAURICIO AVIÑO - NIF:53204038R
Fecha: 2024.07.05 12:47:16 +02'00'

Dr. María Dolores Mauricio Aviñó

EVA| SERNA| GARCIA

Firmado digitalmente por EVA|SERNA| GARCIA
Fecha: 2024.07.05 12:58:20 +02'00'

Dr. Eva Serna García

SOLANYE JACQUELINE| GUERRA| OJEDA

Firmado digitalmente por SOLANYE JACQUELINE| GUERRA|OJEDA
Fecha: 2024.07.05 13:02:16 +02'00'

Dr. Solanye Jacqueline Guerra Ojeda

To all animals used for science

Fundings

Personal fundings

- Grant of a scholarship for the stay of staff in predoctoral training in INCLIVA research groups within the program "*Intramural INCLIVA para estancias formativas en centros de prestigio"* from the Health Research Institute INCLIVA. This stay with a total duration of 4 months was performed in the Albert Einstein College of Medicine located in New York (USA) from 01/09/2023 to 01/01/2024 under the supervision of Dr. Sibinga, MD.

Project fundings

- Consellería de Innovación, Universidades, Ciencia y Sociedad Digital for the promotion of scienfic research, technological development and innovation in the Valencian Community
    - Title: Utilidad de la estabilización de la homeostasis de calcio intracelular en el control de los procesos fibrilatorios.
    - Ref: Promoteo/2018/078

- Universitat de Valencia
    - Title: Estudio del papel de los canales de calcio activados por voltaje de tipo T en diferentes lechos vasculares en un modelo animal de hipertensión arterial y en la vena safena humana.
    - Ref: UV-INV-AE-1544052.

Acknowledgements

Because most of the people I mention here are native Spanish speakers, please let me write this section in Spanish.

Me gustaría expresar mi más profundo agradecimiento a todas las personas que han sido parte de este emocionante viaje. Sin vosotros, no habría llegado hasta aquí.

En primer lugar, a mis tutoras: he tenido la gran suerte de poder trabajar codo con codo con vosotras y os digo de corazón que sois maravillosas. A la Dra. Eva Serna, gracias por darme la oportunidad de comenzar mi camino en investigación. Eres capaz de contagiar tu pasión por la ciencia a todo el que está a tu alrededor, y desde luego, conmigo lo has conseguido. Gracias por creer en mi desde el primer momento. A la Dra. María Dolores Mauricio, mi mami de laboratorio. Has estado a mi lado en los momentos buenos y en los no tan buenos. Gracias por cuidar de que todos estemos bien, de que las cosas se hagan bien, y por toda esa glucosa que nos traes para sobrevivir a las jornadas intensivas de experimentos. A la Dra. Solanye Guerra, siempre dispuesta a ayudar a todo aquel que lo necesite, eres una enciclopedia humana. Gracias infinitas por aconsejarme en todo, por ayudarme a desentrañar los oscuros secretos del western blot y, sobre todo, por ser amiga.

Al Dr. José Mª Vila, por transmitirme tus sabios conocimientos sobre ciencia y lo que no es ciencia, por ser tan amable conmigo desde el primer día. Y por supuesto, por las naranjas de tu huerto.

A todos los compañeros de laboratorio que han compartido conmigo esas jornadas maratonianas de baño de órganos durante estos cuatro años. A David y Begoña, por ayudarme en parte del procedimiento experimental de esta tesis. Gracias por los todos los recuerdos y anécdotas que me hacen llorar de la risa. En especial a Alicia, quien me ha acompañado durante esta montaña rusa de emociones que es escribir una tesis doctoral. Gracias por todos los momentos que hemos compartido, por las risas y por los llantos, dentro y fuera del laboratorio, aderezados con un poquito de musiquita y otro poquito de olor a isoflurano.

Al Grupo de Investigación de Electrofisiología Cardiaca Experimental (GRELCA) del Departamento de Fisiología de la Universitat de València, por haber puesto a nuestra disposición el modelo experimental de conejo y su quirófano para la extracción de muestras. Gracias a los doctores Óscar y Patricia por la amabilidad con la que nos tratan cada vez que nos acercamos a su laboratorio.

Al Departamento de Fisiología de la Universitat de València, en especial al personal de secretaría por su eficacia y ayuda en todos los trámites. Especialmente a Inma, por alegrarnos las mañanas con sus charlas, siempre con una sonrisa. Te echamos mucho de menos. También agradecer a la Dra. Rosario Salvador, coordinadora del Programa de Doctorado en Fisiología, por su ayuda y amabilidad en la preparación los trámites de depósito de esta tesis.

Al Instituto de Investigación Sanitaria (INCLIVA) por subvencionar parte de mis gastos durante mi estancia predoctoral. Asimismo, me gustaría expresar mi agradecimiento también al Grupo de Investigación del Dr. Nicholas Sibinga en el Albert Einstein College de Nueva York, por acogerme

con tanta amabilidad durante mis meses de estancia y enseñarme nuevas técnicas de investigación. Sin duda, esa experiencia ha sido una de las mejores de mi vida, con la que he crecido a todos los niveles, personal y profesionalmente.

A mis amigos, por apoyarme y seguirme siempre, allá donde vaya, hasta el otro lado del charco. Gracias por estar ahí cuando lo he necesitado, por escucharme hablar de ciencia a todas horas y aguantar todos mis estados durante la escritura de esta tesis doctoral.

A Julio, mi compañero de viaje. Gracias por acompañarme allá donde la vida nos lleve, por entenderme, animarme, apoyarme, por sacar mi mejor versión. Por crear un hogar junto a mí.

Gracias también a mi familia: a mi madre, por enseñarme a ser valiente y volar alto, a hacer frente a todo lo que to que nos depare la vida, siempre con una sonrisa. A mi hermana Susana, mi pequeño gran apoyo. Aunque no lo creas, eres mi ejemplo a seguir. A mi abuela, por animarme a seguir adelante, por intentar entender qué son los canales de calcio. Por creer en mí.

Las ausencias nos acompañan incluso más que las presencias. A quien está, lo vemos en el espacio que ocupa; a quien no, lo vemos en todas partes. Papá, gracias por empujarme a empezar este doctorado, espero que te sientas orgulloso. Soy quien soy gracias a ti.

ABSTRACT

Abstract

Introduction

The endothelium plays a crucial role in regulating vascular tone by the release of relaxant and contractile substances. Endothelial NO, produced by eNOS, causes dilation by activating sGC and increasing cGMP. The endothelium and external factors, such as the sympathetic nervous system, regulate vascular smooth muscle cell function. Endothelial dysfunction implies a loss of vasodilator capacity, mainly due to a decreased NO bioavailability, and it is commonly present in cardiovascular diseases.

Ca^{2+} is an extremely versatile signalling molecule that influences a variety of cellular processes. Many pathways are involved in Ca^{2+} homeostasis at the vascular level. Several types of Ca^{2+} channels present in cell membranes regulate Ca^{2+} flow. In addition, the sarcoplasmic reticulum and mitochondria allow Ca^{2+} release and reuptake. The coordinated action of all these cellular mechanisms is essential for vascular homeostasis. L-type VGCCs are the main pathway for calcium influx in smooth muscle cells and cause vasoconstriction. Additionally, studies have found T-type VGCCs expressed alongside L-type VGCCs in different vascular beds. T-type VGCCs are characterised by activation at lower depolarisation levels compared to L-type VGCCs, have faster kinetics and are mainly expressed in the nervous system and cardiac pacemakers, playing a key role in cellular excitability. Currently, three subtypes of T-type VGCCs are known: $Ca_V3.1$, $Ca_V3.2$ and $Ca_V3.3$. In the cardiovascular system, the predominant subtypes of these channels are $Ca_V3.1$ and $Ca_V3.2$. Their activation has been associated to

vasoconstriction. However, some authors also reported their implication in vasodilation.

The myogenic response involves constriction and dilation of blood vessels in response to changes in intraluminal pressure, contributing to the mechanism of autoregulation of blood flow. Both L-and T-type VGCCs are involved in this response, with the L-type playing a predominant role. In recent years, studies have increasingly demonstrated the involvement of T-type VGCCs in the myogenic response, especially resistance vascular beds at lower pressures (40 - 80 mmHg). Overall, the contribution of T-type VGCCs to the myogenic response appears to be minor compared to the participation of L-type VGCCs.

On the other hand, vascular oxidative stress could lead to increased expression and contribution of T-type VGCCs over L-type VGCCs, leading to increased vascular tone. Since cardiovascular diseases are associated to oxidative stress, blocking T-type VGCCs may offer advantages over blocking L-type VGCCs. In addition, some authors suggest that NO deficiency may activate T-type VGCCs. Since endothelial dysfunction is an underlying feature of cardiovascular diseases, T-type VGCCs antagonists could become a therapeutic alternative in these diseases.

Cardiovascular diseases are currently the leading cause of death worldwide. In Spain, around 120,000 people died from cardiovascular causes in 2020, accounting for almost 25 % of all deaths in the country. Hypertension is an important risk factor for global mortality. It is related to cardiovascular diseases, such as atherosclerosis or myocardial infarction, contributing directly to the increased risk of stroke and ischaemic heart disease. It is also

considered a risk factor for the development of cardiovascular diseases along with other factors.

Hypertension is now a global public health problem which, according to the latest WHO report, causes around 9 million deaths per year, and its incidence is increasing. The number of cases has risen from 594 million in 1975 to approximately 1.3 billion people by 2021. Adequate control of hypertension has been shown to reduce the rate of myocardial infarction by 24 % and stroke mortality by 42 %.

In cardiovascular diseases such as hypertension, vascular dysfunction occurs due to several triggering mechanisms, including oxidative stress and calcium-related pathways. Elevated Ca^{2+} channel activity can lead to excessive vasoconstriction and hypertension. L-type VGCCs blockers, such as DHPs, are an effective treatment for hypertension. However, one of the main side effects is the development of peripheral malleolar oedema, forcing many patients to discontinue treatment. The oedema produced by L-type VGCCs blockers occurs due to inhibition of the myogenic response, which results in increased dilation of the precapillary vessels and thus increased hydrostatic pressure in the capillary. Since T-type VGCCs play a minor role in myogenic tone, it would be expected that blockers of these channels would be good candidates for treating hypertension without causing oedemas. A better understanding of the function of T-type VGCCs in vascular smooth muscle and endothelial cells is the basis for the rational development of new antihypertensive drugs with fewer side effects. In fact, several clinical studies show that combined treatment with L- and T-type VGCC blockers proves to be more effective than conventional L-type blockers alone.

Finally, oestrogens can inhibit L-type VGCCs, so it would not be surprising if they could also affect T-type VGCCs. Understanding the role and regulation of T-type VGCCs in different sexes could lead to the development of new personalised therapies for the treatment of hypertension or other cardiovascular diseases.

Hypothesis and aims

Under physiological conditions, NO could down-regulate the function of T-type VGCCs. Therefore, in the presence of endothelial dysfunction, which mainly results in a deficit of NO release, these channels might become more active. Since we hypothesise that their function is mainly vasoconstrictor, they might worsen the prognosis of hypertension. In addition, the role of T-type VGCCs might vary according to sex, as has been shown for L-type VGCCs.

The overall aim of this thesis is to determine the vascular function and expression of T-type VGCCs under physiological conditions and in hypertension, as well as whether sex can modulate this function. The specific aims are: 1. Determine the involvement of T-type VGCCs in the contractile response to phenylephrine and angiotensin II in the aorta and renal artery of healthy rabbits and assess whether the absence of NO influences the α_1-adrenergic response. 2. Investigate the role of T-type VGCCs in the endothelium-dependent and -independent relaxant response in healthy rabbit aorta and renal artery. 3. Analyse the protein expression levels of T-type VGCCs in the aorta and renal artery of healthy rabbits and explore possible co-localisation between T-type VGCCs and eNOS. 4. Examine whether the

function and expression of T-type VGCCs are altered in a model of hypertension and determine whether these alterations are influenced by sex.

Material and methods

To determine vascular function and expression of T-type VGCCs under physiological conditions, male healthy rabbits were used. To study the role of T-type VGCCs in hypertension, male and female hypertensive rats (SHR model) and its normotensive control (WKY) were used.

For vascular reactivity measurements, the rabbit aorta and renal artery were mounted in an organ bath, while the rat renal artery was mounted in a wire myograph. Concentration-response curves were performed for phenylephrine, angiotensin II, acetylcholine and sodium nitroprusside. The involvement of T-type VGCCs and NO was assessed by incubating arterial rings with nickel chloride, a T-type VGCC blocker, and L-NAME, a NOS inhibitor.

Protein expression of rabbit arteries was analysed by Western blot using antibodies specific for Cav3.1 and Cav3.2. The localisation of these two subtypes in the endothelium of renal artery and their possible colocalisation with eNOS, was determined by immunohistochemistry.

For gene expression studies, intrarenal arteries from rats were used. After isolation, the arteries were extracted from trizol reagent. RT-PCR analysis was then performed using pre-designed TaqMan gene expression assays for the target genes *$Ca_V3.1$*, *$Ca_V3.2$* and *Nos3*, as well as for the housekeeping gene *Gapdh*.

Flow cytometry experiments were carried out using the fluorochromes DAF-FM Diacetate, Dihydrorhodamine 123 and Dihydroethidium.

Statistical analyses were performed with Microsoft Excel and GraphPad Prism. For comparison of the different groups and experimental conditions, *P*-values were generated by one-way or two-way analysis of variance (ANOVA) or Student's *t*-test.

Results

We performed concentration-response curves to phenylephrine in the presence of L-NAME to examine whether there was NO release in response to α_1-adrenergic receptor stimulation in the aorta and renal artery of healthy rabbits. L-NAME enhanced the contractile response to phenylephrine in both the aorta and renal artery, increasing pCE_{50} and Emax, indicating that NO attenuates adrenergic contraction in these two vascular beds. Subsequently, we performed concentration-response curves to phenylephrine and angiotensin II in the presence of nickel chloride. In both cases, the curves were shifted to the right, indicating that T-type VGCCs participate in the contraction induced by these agonists. Furthermore, to test the hypothesis that NO could modulate the activity of T-type VGCCs, the phenylephrine curves were performed in the presence of L-NAME and nickel chloride. The results showed that in the absence of NO, the contribution of T-type VGCCs in this response was significantly increased only in the renal artery.

In addition, we investigate the role of T-type VGCCs in both endothelium-dependent and -independent arterial relaxation. In the aorta, nickel chloride did not affect the relaxation of acetylcholine or sodium

nitroprusside. However, in the renal artery, nickel chloride reduced the response to acetylcholine but not to sodium nitroprusside. The blockade induced by nickel chloride on acetylcholine response was similar to that induced by L-NAME. Moreover, co-incubation of nickel chloride plus L-NAME did not show a synergic blockade compared to that induced by nickel chloride or L-NAME separately, suggesting that T-type VGCCs-mediated relaxation might share the same vasodilator pathway as NO.

Protein expression of $Ca_V3.1$ and $Ca_V3.2$ subtypes in the aorta and renal artery of healthy rabbits revealed no significant differences between the two vessels. On the other hand, results obtained by immunohistochemistry indicated that both subtypes were localised in rabbit renal artery endothelium and that there was a colocalisation between $Ca_V3.1$ and eNOS.

Based on our findings in healthy renal rabbit arteries, we focused on this vascular bed to study the role of these channels in hypertension. The study was performed in both male and female SHR model, taking the WKY rats as a normotensive control.

To test whether the vascular tissue of the SHR model might be more exposed to oxidative stress than that of WKY rats, we measured basal intracellular levels of ROS in circulating white blood cells. Our results indicated that in male SHR, there was an increased production of H_2O_2 and $ONOO^-$ in both leukocytes and neutrophils. These results suggest that the vascular tissue of male SHR would be more exposed to oxidative stress than that of females.

To test whether hypertension caused vascular dysfunction in the SHR model, concentration-response curves to acetylcholine and sodium

nitroprusside were performed in the renal artery. The results showed that the renal artery from the SHR model had endothelial dysfunction in both males and females without impairment of endothelium-independent vasodilator capacity. On the other hand, curves to phenylephrine were performed in the study groups. The results showed that hypertension did not modify the contractile response to phenylephrine in males. However, in females, a greater sensitivity to phenylephrine was found in SHR. Hypertension reduced NO production in response to phenylephrine, especially in females.

To study the involvement of T-type VGCCs in the response to phenylephrine, concentration-response curves were performed in the presence of nickel chloride. Furthermore, to test the hypothesis that NO might modulate T-type VGCCs activity, the curves were performed in the presence of L-NAME and nickel chloride. Our results showed that T-type VGCCs contribute to phenylephrine-induced contraction in the renal artery of both male and female rats. Hypertension increased the involvement of T-type VGCCs only in female rats. In the absence of NO, the involvement of T-type VGCCs increased in female WKY. In both SHR groups and male WKY, incubation with L-NAME did not enhance nickel chloride blockade, which was consistent with a scarce NO release in response to phenylephrine in these groups.

In addition, we measured gene expression of the predominant vascular territory subtypes of T-type VGCCs (*$Ca_V3.1$* and *$Ca_V3.2$*) and *Nos3* in rat intrarenal arteries of both male and female WKY and SHR groups by RT-PCR. The mRNA expression of both *$Ca_V3.1$* and *$Ca_V3.2$* was significantly higher in male SHR compared to WKY rats of the same sex, while in females,

it was significantly lower in SHR compared to WKY rats. On the other hand, the *eNos* expression was significantly higher in male SHR compared to WKY rats of the same sex. In females, no changes in *Nos3* gene expression were observed. In addition, the results showed a positive correlation between *$Ca_V3.1$* and *$Ca_V3.2$* and *Nos3* gene expression.

Overall, these results indicate a different role for T-type VGCCs depending on sex and a different regulation in response to hypertension between males and females.

Discussion

The regulation of vascular tone by T-type VGCCs is complex. Initially, $Ca_V3.1$ subtype function was linked to vasoconstriction and $Ca_V3.2$ to vasodilation. However, murine models deficient in $Ca_V3.1$ or $Ca_V3.2$ have shown that both subtypes are involved in both vasoconstriction and vasodilation, depending on the vascular bed.

Our results show that T-type VGCCs are involved in both α_1-adrenergic and angiotensin II vasoconstriction in rabbit aorta and renal artery under physiological conditions. In the absence of NO, the participation of T-type VGCCs in response to phenylephrine increases in the renal artery but not in the aorta indicating the modulation of these channels by NO. Moreover, these channels are involved in endothelium-dependent vasodilation in the renal artery, where there is an endothelial colocalisation between $Ca_V3.1$ and eNOS underlying the disruption of healthy vasodilation when T-type VGCCs are blocked. These results support the hypothesis that Ca^{2+} influx through $Ca_V3.1$ may activate eNOS.

Because the function of T-type VGCCs seems to be more relevant in the renal artery, we focus on this artery to study the role of these channels in hypertension in both sexes. We observed that hypertension induces endothelial dysfunction in both sexes and increase sensitivity to phenylephrine only in females. In the absence of NO, the response to phenylephrine was similar between females WKY and SHR, pointing to a crucial role of NO in α_1-adrenergic contraction for female WKY, which is lost in SHR. Therefore, T-type VGCCs become more active in hypertensive females, probably due to a decreased NO release.

Finally, the increased oxidative stress in male SHR may also increase the gene expression of *$Ca_V3.1$* and *$Ca_V3.2$*, as described by other authors. The increased *Nos3* expression in hypertensive males could be interpreted as an attempt to compensate for the oxidative stress. Furthermore, the positive correlation between gene expression of the T-type VGCCs subtypes with *Nos3* could explain the increased gene expression of both T-type VGCCs and *Nos3* observed in male SHR. Paradoxically, this overexpression does not translate into increased vascular involvement of T-type VGCCs or increased NO release.

On the other hand, in females, gene expression of T-type VGCCs decreases despite their increased participation in the adrenergic response. Precisely, this could be the cause of such underexpression, i.e., the increased activity of T-type VGCCs in hypertensive females would exert an inhibitory effect on *Cav3.1* and *Cav3.2* gene expression that would explain the underexpression shown by this group. Hypertension does not change *Nos3* gene expression in females despite the lower NO participation. This finding

would indicate the inability of hypertensive females to up-regulate *Nos3* gene expression, leading to endothelial dysfunction and increased sensitivity to phenylephrine.

The function and modulation of T-type VGCCs under physiological conditions and in hypertension, especially their sex-specific effects and their relationship with NO, have been explored in this PhD thesis, providing new insights into their role in the regulation of vascular tone.

RESUMEN

Resumen

Introducción

La pared arterial está constituida por tres capas: la túnica íntima, la túnica media y la túnica externa. El endotelio, localizado en la túnica íntima, libera sustancias vasoactivas que son capaces de regular el tono de los vasos sanguíneos, principal determinante de la presión arterial. La activación de la óxido nítrico sintasa endotelial (eNOS) produce óxido nítrico (NO), un potente vasodilatador que provoca la conversión de GTP en GMPc conduciendo a la relajación de los vasos sanguíneos. La función de las células musculares lisas vasculares está regulada por el endotelio y por otros factores externos como el sistema nervioso simpático, que desempeña un papel crucial en la regulación de la presión arterial y el flujo sanguíneo. En condiciones fisiológicas, el endotelio libera también sustancias vasoconstrictoras; ante una disfunción endotelial, nos encontramos con un desequilibrio entre la producción de las sustancias vasoconstrictoras y vasodilatadoras que puede conducir a una pérdida de la capacidad vasodilatadora y a un estado de hipercontractilidad. Esta situación está comúnmente presente en las enfermedades cardiovasculares.

El Ca^{2+} es una molécula de señalización extremadamente versátil que influye en diversos procesos celulares. Son muchas las vías que intervienen en la homeostasis del Ca^{2+} a nivel vascular. La entrada y salida de Ca^{2+} del citoplasma es posible gracias a varios tipos de canales de Ca^{2+} presentes en las membranas celulares. Además, el retículo sarcoplásmico, así como las mitocondrias, permiten la liberación de Ca^{2+} y su recaptación. La acción

coordinada de todos estos mecanismos celulares es esencial para la homeostasis vascular.

La principal entrada de Ca^{2+} en las células musculares lisas vasculares se produce a través de los canales de Ca^{2+} dependientes de voltaje (VGCCs, por sus siglas en inglés), que se abren cuando la membrana celular se despolariza, permitiendo la entrada de Ca^{2+} y provocando la vasoconstricción. Estos canales se clasifican en dos grandes grupos, en función de los voltajes a los que se activan, que se dividen a su vez en tres familias principales: Ca_V1 (comúnmente llamados de tipo L) y Ca_V2 (tipo N, P/Q y R), activados por altos voltajes, y Ca_V3 (tipo T), que se activa a bajos voltajes. La mayor o menor abundancia en las distintas poblaciones de estos canales varía a lo largo del árbol vascular. Los VGCCs de tipo L constituyen la principal vía de entrada de Ca^{2+} en las células musculares lisas vasculares, regulando la respuesta miogénica y la presión arterial. Sin embargo, otros subtipos de VGCCs, como los de tipo T, también están presentes en el sistema vascular. Cada vez más estudios describen la expresión de VGCC de tipo T además de los de tipo L en diferentes lechos vasculares de distintas especies.

Los VGCC de tipo T se caracterizan por activarse a niveles de despolarización más bajos comparados con los de tipo L, poseer una cinética más rápida y expresarse principalmente en el sistema nervioso y en los marcapasos cardíacos, desempeñando un papel fundamental en la excitabilidad celular. Actualmente, se conocen tres subtipos de los VGCCs de tipo T: $Ca_V3.1$, $Ca_V3.2$ y $Ca_V3.3$. En el sistema cardiovascular, los subtipos predominantes de estos canales son $Ca_V3.1$ y $Ca_V3.2$. La entrada de Ca^{2+} a través de estos canales se ha relacionado con la vasoconstricción, aunque

también algunos autores han demostrado su participación en mecanismos de relajación vascular.

La respuesta miogénica implica la constricción y dilatación de los vasos sanguíneos en respuesta a cambios en la presión intraluminal, contribuyendo al mecanismo de autorregulación del flujo sanguíneo. En esta respuesta participan tanto los canales de Ca^{2+} de tipo L como los de tipo T, siendo los primeros los que desempeñan un papel predominante. En los últimos años han ido apareciendo estudios que demuestran la implicación de los VGCCs de tipo T en la respuesta miogénica en algunos lechos vasculares, especialmente de resistencia. En lechos vasculares específicos, como las arterias cerebrales y mesentéricas, los VGCCs de tipo T contribuyen a la regulación del tono miogénico a presiones más bajas (40-80 mmHg). En líneas generales, la contribución de los VGCCs de tipo T a la respuesta miogénica parece ser minoritaria comparada con la participación de los VGCCs de tipo L.

Por otra parte, el estrés oxidativo vascular podría conducir a una mayor expresión y contribución de los VGCC de tipo T sobre los de tipo L, lo que llevaría a un aumento del tono vascular. Puesto que las enfermedades cardiovasculares cursan con estrés oxidativo, el bloqueo de los VGCCs de tipo T podría ofrecer ventajas sobre el bloqueo de los VGCCs de tipo L. Además, algunos autores sugieren que, en situación de déficit de NO, la activación de los VGCCs de tipo T podría verse incrementada. Puesto que la disfunción endotelial es una característica subyacente de las enfermedades cardiovasculares, los antagonistas de los VGCCs de tipo T podrían convertirse en una alternativa terapéutica en dichas enfermedades.

Las enfermedades cardiovasculares constituyen actualmente la principal causa de muerte a nivel mundial. En España, alrededor de 120.000 personas murieron por causas cardiovasculares en 2020, lo que supone casi el 25 % de las muertes totales del país. La hipertensión arterial es un importante factor de riesgo de mortalidad global y está relacionada con enfermedades cardiovasculares, como la aterosclerosis o el infarto de miocardio, contribuyendo directamente al aumento del riesgo de sufrir ictus, cardiopatía isquémica y otras enfermedades cardiovasculares. Además, se considera un factor de riesgo para el desarrollo de estas enfermedades junto con otros factores como las dislipidemias, el tabaquismo, los malos hábitos alimentarios, el consumo de alcohol, el sedentarismo, la obesidad, la diabetes, la edad avanzada o los antecedentes familiares.

La hipertensión constituye, hoy en día, un problema de salud pública mundial que, según cifras de la OMS, causa alrededor de 9 millones de muertes al año, y su incidencia va en aumento. El número de casos ha pasado de 594 millones en 1975 a 1.130 millones en 2015, afectando aproximadamente a 1.300 millones de personas en 2021. La prevalencia de la hipertensión aumenta con la edad y provoca una afectación sistémica secundaria con efectos renales, cerebrovasculares y cardíacos. Se ha demostrado que un control adecuado de la hipertensión reduce la tasa de infartos de miocardio en un 24 % y la mortalidad por ictus en un 42 %.

La hipertensión presenta diferencias entre hombres y mujeres. Los hombres antes de los sesenta años poseen mayor incidencia de hipertensión en comparación con las mujeres. El hecho de que las mujeres posean menor incidencia de hipertensión durante la edad fértil se ha relacionado con la

elevada concentración de estrógenos que poseen, que aumentan la liberación de NO endotelial, reduciendo así la resistencia periférica y la presión arterial. Sin embargo, tras la menopausia y la consiguiente disminución de los niveles plasmáticos de estrógenos, el riesgo de estas enfermedades es mayor en las mujeres que en los hombres de la misma edad.

En las enfermedades cardiovasculares, como la hipertensión, la disfunción vascular se produce debido a diversos mecanismos desencadenantes, entre ellos el estrés oxidativo y las vías relacionadas con el calcio. Una actividad elevada de los canales de calcio puede provocar una vasoconstricción excesiva e hipertensión. Los bloqueantes de los VGCCs de tipo L, como las DHP, se utilizan para tratar la hipertensión y constituyen un tratamiento efectivo, sin embargo, uno de los efectos secundarios principales es la generación de edema maleolar periférico, lo que obliga a muchos pacientes a interrumpir el tratamiento. El edema producido por los bloqueantes de los VGCCs tipo L se produce debido a la inhibición de la respuesta miogénica, que da lugar a una mayor dilatación de los vasos precapilares y por tanto a un aumento de la presión hidrostática del capilar. Ya que los VGCCs de tipo T tienen una función minoritaria en el tono miogénico, se esperaría que los bloqueantes de estos canales fueran buenos candidatos para tratar la hipertensión sin ocasionar edemas como efecto secundario. Un mejor conocimiento de la función de los VGCCs de tipo T en el músculo liso vascular y las células endoteliales, así como en otros órganos diana, constituye la base para el desarrollo racional de nuevos fármacos antihipertensivos con menos efectos secundarios. De hecho, diversos estudios clínicos ponen de manifiesto que el tratamiento combinado con bloqueantes

de los VGCCs de tipo L y T demuestra ser más eficaz que el uso de bloqueantes convencionales de tipo L por sí solos.

Por último, los estrógenos pueden inhibir los VGCCs de tipo L, por lo que no sería extraño que también pudieran tener algún efecto sobre los VGCCs de tipo T, hasta la fecha no descrito. Comprender el papel y la regulación de los VGCC de tipo T en los diferentes sexos podría conducir al desarrollo de nuevas terapias personalizadas para el tratamiento de la hipertensión u otras enfermedades cardiovasculares.

Hipótesis y objetivos

En condiciones fisiológicas, el NO podría modular a la baja la función de los VGCCs de tipo T. Por lo tanto, en presencia de disfunción endotelial, que cursa principalmente con un déficit de liberación de NO, estos canales podrían volverse más activos. Dado que nuestra hipótesis es que su función es principalmente vasoconstrictora, podrían empeorar el pronóstico de la hipertensión. Además, el papel de los VGCCs de tipo T podría variar en función del sexo, como se ha demostrado con los VGCC de tipo L.

El objetivo general de esta tesis es determinar la función vascular y la expresión de los VGCCs tipo T en condiciones fisiológicas y en la hipertensión, así como si el sexo puede modular esta función. Los objetivos específicos son: 1. Determinar la implicación de los VGCCs tipo T en la respuesta contráctil a la fenilefrina y a la angiotensina II en aorta y arteria renal de conejos sanos. Evaluar si la ausencia de NO influye en la respuesta α_1-adrenérgica. 2. Investigar el papel de los VGCCs de tipo T en la respuesta

relajante dependiente e independiente del endotelio en aorta y arteria renal de conejos sanos. 3. Analizar los niveles de expresión proteica de los VGCCs de tipo T en aorta y arteria renal de conejos sanos, y explorar la posible colocalización entre las proteínas de los VGCCs de tipo T y la eNOS. 4. Examinar si la función y la expresión de los VGCCs de tipo T están alteradas en un modelo de hipertensión y determinar si estas alteraciones están influidas por el sexo.

Material y métodos

Para conseguir la primera parte del objetivo general, es decir, determinar la función vascular y la expresión de los VGCCs tipo T en condiciones fisiológicas, se utilizaron conejos macho de 15 semanas de edad. Para estudiar el papel de los VGCCs tipo T en la hipertensión, se utilizó el modelo SHR y su control normotenso de ratas WKY. Para comprobar si el sexo afectaba la función de estos canales en la hipertensión, el estudio se realizó tanto en machos como en hembras.

Empleamos el sistema no invasivo NIBP CODA 8 para medir la tensión arterial en ratas. Para el estudio de la reactividad vascular, la aorta y la arteria renal de conejo se montaron en un baño de órganos, mientras que la arteria renal de rata se montó en un miógrafo de alambre. Se construyeron curvas concentración-respuesta para fenilefrina, angiotensina II, acetilcolina y nitroprusiato sódico. Para las dos últimas sustancias se realizó una precontracción de las arterias con noradrenalina. Se evaluó la implicación de los VGCCs de tipo T y del NO comparando las curvas sin incubar con las incubadas con cloruro de níquel, un bloqueante de los VGCCs de tipo T y con L-NAME, un inhibidor de la NOS. Para explorar el papel modulador del NO

sobre los VGCCs de tipo T se incubaron conjuntamente cloruro de níquel y L-NAME y se compararon las curvas de concentración-respuesta resultantes con las obtenidas en presencia de L-NAME.

Por otro lado, se analizó la expresión proteica por Western blot utilizando anticuerpos específicos para Cav3.1 y Cav3.2. La localización de estos dos subtipos en el endotelio, así como su posible colocalización con la eNOS se determinó mediante inmunohistoquímica en segmentos de arteria renal de conejo fijados, capturando las imágenes con un aumento digital de 2,5x y un seccionamiento óptico de 0,5 µm utilizando el software LAS X (Leica, Alemania).

Para los estudios de expresión génica, se utilizaron arterias intrarenales de machos y hembras WKY y SHR. Tras el aislamiento, las arterias se conservaron en solución de trizol. A continuación, se llevó a cabo un análisis RT-PCR utilizando ensayos de expresión génica TaqMan prediseñados para los genes diana *$Ca_V3.1$, $Ca_V3.2$* y *Nos3*, así como para el gen de referencia *Gapdh*. Para la RT-PCR se empleó el kit de transcripción inversa de ADNc de alta capacidad y el sistema de PCR en tiempo real QuantStudio 5.

Los experimentos de citometría de flujo se llevaron a cabo utilizando el citómetro FACSAria III de BD Biosciences, con adquisición y análisis de datos realizados mediante BD FACS Suite y el software FLOWJO V.10.1. Se emplearon los fluorocromos DAF-FM Diacetato, Dihidrorodamina 123 y Dihidroetidio.

Para determinar la concentración de nitratos y nitritos en el plasma de rata, se empleó un kit comercial de ensayo colorimétrico de nitratos/nitritos de Cayman Chemical, EE.UU.

Los análisis estadísticos se realizaron con Microsoft Excel (versión 2401) y GraphPad Prism 9.0.2 (GraphPad Software Inc.). Para la comparación de los distintos grupos y condiciones experimentales, se generaron valores *P* mediante análisis de la varianza (ANOVA) de una o dos vías o la prueba *t* de Student.

Resultados

Realizamos curvas concentración-respuesta a la fenilefrina en presencia de L-NAME para examinar si existía liberación de NO en respuesta a la estimulación del receptor α_1-adrenérgico en aorta y arteria renal de conejos sanos. L-NAME potenció la respuesta contráctil a la fenilefrina tanto en aorta como en arteria renal, aumentando la pCE_{50} y la Emax, lo que indica que el NO atenúa la contracción adrenérgica en estos dos lechos vasculares. Posteriormente, para analizar si existía participación de los VGCCs de tipo T en la respuesta contráctil a la fenilefrina y a la angiotensina II, realizamos curvas concentración-respuesta a estos agonistas en presencia de cloruro de níquel, bloqueante de estos canales. En ambos casos las curvas concentración-respuesta se desplazaron a la derecha, indicando que los VGCCs tipo T participan en la contracción inducida por estos agonistas. Además, para comprobar la hipótesis de que el NO podría modular la actividad de los VGCC de tipo T, se realizaron curvas concentración-respuesta a la fenilefrina en presencia L-NAME y cloruro de níquel. Los resultados mostraron que, en

ausencia de NO, la contribución de los VGCCs de tipo T en esta respuesta aumentaba significativamente sólo en arteria renal.

Además, se llevaron a cabo experimentos adicionales para investigar el papel de los VGCCs de tipo T en la relajación arterial, tanto dependiente como independiente del endotelio. En la aorta, el cloruro de níquel no tuvo ningún efecto sobre la relajación a la acetilcolina o al nitroprusiato sódico. Sin embargo, en la arteria renal, el cloruro de níquel redujo la respuesta a la acetilcolina, pero no al nitroprusiato sódico, lo que podría indicar la participación de los VGCCs de tipo T en la relajación dependiente del endotelio en este lecho vascular. Para estudiar si los VGCCs tipo T participaban en la relajación a la acetilcolina siguiendo una vía similar a la del NO, se realizaron los experimentos en presencia de L-NAME y de L-NAME más cloruro de níquel. Los resultados mostraron un bloqueo similar de la relajación a la acetilcolina al incubar con cloruro de níquel y con L-NAME. Además, la co-incubación de ambos bloqueantes fue semejante a la de cloruro de níquel y L-NAME por separado, lo que sugiere que la relajación mediada por los VGCCs tipo T podría compartir la misma vía vasodilatadora que el NO.

Mediante western blot, examinamos la expresión proteica de los subtipos $Ca_V3.1$ y $Ca_V3.2$ en aorta y arteria renal de conejos sanos. Nuestros resultados no revelaron diferencias significativas en la expresión proteica entre ambos vasos. Por otro lado, los resultados obtenidos mediante inmunohistoquímica indicaron que ambos subtipos se localizaban en las células endoteliales de arteria renal de conejo y que existía una colocalización entre $Ca_V3.1$ y eNOS en el citoplasma de estas células.

Basándonos en nuestros hallazgos en arterias de conejos sanos, en particular el aumento de la actividad de los VGCCs de tipo T y su modulación por el NO en la arteria renal, nos centramos en este lecho vascular para estudiar el papel de estos canales en la hipertensión. El estudio se realizó tanto en machos como en hembras del modelo SHR, tomando como control normotenso la cepa WKY.

Para comprobar los niveles de estrés oxidativo del modelo, medimos diferentes indicadores de éste en leucocitos circulantes de plasma de rata por citometría de flujo. Nuestros resultados mostraron que los machos del grupo SHR presentaban mayores indicadores de estrés oxidativo en células sanguíneas, en comparación con las hembras del grupo SHR. Estos resultados sugieren que el tejido vascular de los machos hipertensos estaría más expuesto al estrés oxidativo que las hembras del mismo grupo.

Para comprobar si la hipertensión provocaba disfunción vascular en el modelo SHR, se realizaron curvas concentración-respuesta a la acetilcolina y al nitroprusiato sódico en arteria renal de ratas macho y hembra WKY y SHR. Los resultados mostraron que la arteria renal procedente del modelo SHR presentaba disfunción endotelial, tanto en machos como en hembras, sin afectación de la capacidad vasodilatadora independiente de endotelio. Por otro lado, se realizaron curvas concentración-respuesta a la fenilefrina en los grupos de estudio. Los resultados mostraron que la hipertensión no modificó la respuesta contráctil a la fenilefrina en machos, pero sí en hembras, donde observamos una mayor sensibilidad en SHR. Para analizar si existía liberación de NO en respuesta a la fenilefrina, se realizaron las curvas en presencia de L-NAME. Los resultados mostraron que la producción de NO

en respuesta a este agonista era escasa en las ratas WKY macho, encontrando sólo diferencias significativas en un punto de la curva, mientras que en las ratas WKY hembras se observó un desplazamiento a la izquierda en presencia de L-NAME. La hipertensión redujo la liberación de NO en respuesta a la fenilefrina en ambos sexos.

Para estudiar la implicación de los VGCCs de tipo T en la respuesta a la fenilefrina en función del sexo y en la hipertensión, se realizaron curvas concentración-respuesta a este agonista en presencia de cloruro de níquel. Asimismo, para comprobar la hipótesis de que el NO podría modular la actividad de los VGCC de tipo T, se realizaron curvas concentración-respuesta a la fenilefrina en presencia L-NAME y cloruro de níquel en arteria renal de ratas macho y hembra WKY y SHR. Nuestros resultados mostraron que los VGCCs de tipo T contribuyen a la contracción inducida por fenilefrina en arteria renal de ratas tanto en macho como en hembra. La hipertensión aumentó la participación de los VGCCs de tipo T sólo en hembra. En ausencia de NO, la participación de los VGCCs de tipo T aumentó en hembras WKY. En el grupo SHR y en los machos WKY, la incubación con L-NAME no potenció el bloqueo por cloruro de níquel, en consonancia con la poca liberación de NO en respuesta a la fenilefrina en estos grupos.

Además, medimos la expresión génica de los subtipos predominantes en territorio vascular de los VGCCs de tipo T (*$Ca_V3.1$* y *$Ca_V3.2$*) y *Nos3* en arterias intrarrenales de rata de los grupos WKY y SHR, tanto machos como hembras, mediante RT-PCR. La expresión a nivel de ARNm tanto de *$Ca_V3.1$* como de *$Ca_V3.2$* fue significativamente mayor en los machos SHR comparado con las ratas WKY del mismo sexo, mientras que en hembras fue

significativamente menor en SHR comparado con las ratas WKY. Por otro lado, la expresión de *Nos3* fue significativamente mayor en los machos SHR comparado con las ratas WKY del mismo sexo. En hembras, no se observaron cambios en la expresión génica de *Nos3*. Por último, los resultaros mostraron una correlación positiva entre la expresión génica de $Ca_V3.1$ y $Ca_V3.2$ con la de *Nos3*.

En general, estos resultados indican un papel distinto para los VGCCs de tipo T dependiendo del sexo y una regulación en respuesta a la hipertensión también distinta entre machos y hembras.

Discusión

La regulación del tono vascular a través de los VGCCs de tipo T es compleja. Inicialmente se relacionó la función del subtipo $Ca_V3.1$ con la vasoconstricción y la del $Ca_V3.2$ con la vasodilatación. Sin embargo, modelos murinos deficientes en $Ca_V3.1$ o $Ca_V3.2$ han demostrado que ambos subtipos participarían tanto en la vasoconstricción como en la vasodilatación, dependiendo del lecho vascular.

Nuestros resultados ponen de manifiesto que los VGCCs de tipo T participan tanto en la vasoconstricción α_1-adrenérgica como en la respuesta a la angiotensina II en aorta y en arteria renal de conejo en condiciones fisiológicas. En ausencia de NO, la participación de los VGCCs de tipo T en respuesta a la estimulación α_1-adrenérgica aumenta significativamente en arteria renal, pero no en aorta. Además, estos canales también participan en la vasodilatación a la acetilcolina en arteria renal. Por tanto, podemos concluir que los VGCCs de tipo T poseen un efecto contráctil en aorta y arteria renal, pero, además, en esta última también modulan la relajación dependiente de

endotelio. Por otro lado, hemos comprobado por microscopía confocal que existe una colocalización endotelial entre $Ca_V3.1$ y eNOS en arteria renal de conejo, por lo que posiblemente la entrada de calcio a través de los $Ca_V3.1$ active la eNOS provocando la relajación del vaso. Asimismo, observamos que el bloqueo de la vasodilatación a la acetilcolina con L-NAME es similar al que se produce en presencia de cloruro de níquel, y que la co-incubación con ambos bloqueantes ofrece una respuesta semejante a la que obtenemos al incubar cada bloqueante por separado, lo cual afianza la hipótesis de que el NO y los VGCCs tipo T podrían compartir la misma vía para mediar la relajación. En este sentido, otros investigadores han indicado que los VGCCs de tipo T pueden desempeñar un papel importante en la vasodilatación mediada por NO, y su relación con éste parece variar en función del lecho vascular.

Nuestros resultados en conejos sanos sugieren que los VGCCs de tipo T desempeñan un papel contráctil en aorta y arteria renal, y en esta última, con un efecto que se hace más pronunciado en ausencia de NO. También son necesarios para la relajación inducida por la acetilcolina en la arteria renal. $Ca_V3.1$ y $Ca_V3.2$ están presentes en el territorio vascular y se expresan en el endotelio, donde $Ca_V3.1$ se colocaliza con eNOS. Debido a que la función de los VGCCs de tipo T parece ser más relevante en arteria renal, decidimos centrarnos en este lecho vascular para estudiar el papel de estos canales en la hipertensión en ambos sexos. Para ello, utilizamos el modelo de rata espontáneamente hipertensa (SHR) y realizamos el estudio tanto en machos como en hembras.

Nuestros resultados de citometría mostraron que los niveles de H_2O_2 y $ONOO^-$ en machos SHR se encontraban elevados, sin cambios en los niveles de O_2^- y NO, posiblemente debido a su consumo en la reacción para formar $ONOO^-$. En las hembras SHR, no encontramos cambios con respecto a las ratas WKY, lo que sugiere que el sexo femenino podría proporcionar protección frente al estrés oxidativo inducido por la hipertensión. Sin embargo, a nivel endotelial, la hipertensión causó disfunción en la arteria renal de ambos sexos, en línea con los resultados que presentan otros autores.

A través de los experimentos de reactividad vascular, observamos que la hipertensión aumentó la sensibilidad a la fenilefrina sólo en las hembras, lo que apunta a un papel crucial del NO en la contracción adrenérgica para las hembras WKY, que se pierde en las SHR. La hipertensión también volvió más activos los VGCCs de tipo T en las hembras, sin afectar a los machos. Cuando se bloqueó la síntesis de NO con L-NAME, la participación de los VGCCs de tipo T aumentó en las hembras WKY, sin embargo, este aumento no se observó en el modelo SHR, ya que la liberación de NO estaba reducida en este grupo. En general, estos resultados ponen de manifiesto que la hipertensión aumenta la participación de los VGCCs de tipo T en la contracción adrenérgica en hembras probablemente por presentar menos liberación de NO, que actuaría inhibiendo estos canales.

Por último, el aumento de estrés oxidativo que presentan los machos SHR también podría estar aumentando la expresión de *$Ca_V3.1$* y *$Ca_V3.2$*, tal y como describen otros autores. La expresión génica aumentada de *Nos3* en los machos hipertensos podría interpretarse como un intento de compensar la disminución en la biodisponibilidad de NO inducida por el estrés oxidativo

que sufre este grupo. Además, la correlación positiva entre la expresión génica de los dos subtipos de VGCCs de tipo T con la *Nos3* podría explicar la mayor expresión génica tanto de VGCCs de tipo T como de *Nos3* observada en los machos SHR. Paradójicamente esta sobreexpresión no se traduce en un aumento de participación vascular de los VGCCs de tipo T ni en un aumento de la liberación de NO.

Por otra parte, en las hembras, disminuye la expresión génica de los VGCCs de tipo T pese a la mayor participación de éstos en la respuesta adrenérgica. Precisamente, esta podría ser la causa de tal infraexpresión, es decir, el aumento de actividad de los VGCCs de tipo T en las hembras hipertensas ejercería un efecto inhibitorio sobre la expresión génica de los *Cav3.1* y *Cav3.2* que explicaría la infraexpresión que presenta este grupo. Por último, la hipertensión no cambia la expresión génica de *Nos3* en hembras, pese a la menor participación de NO. Este hallazgo indicaría la incapacidad en las hembras hipertensas para regular al alza la producción de NO endotelial que desembocaría en una disfunción endotelial y mayor sensibilidad a la fenilefrina.

La función y modulación de los VGCC de tipo T en condiciones fisiológicas y en la hipertensión, especialmente sus efectos específicos por sexo y su relación con el NO, se han explorado en esta tesis doctoral, aportando nuevos conocimientos sobre su papel en la regulación del tono vascular.

CONTENTS

Introduction……1
1. Vascular tone regulation 3
1.1. Endothelium-mediated regulation 4
1.2. Sympathetic regulation 8
2. Calcium and vascular homeostasis 9
2.1. Voltage-gated calcium channels 12
2.2. T-type voltage-gated calcium channels 15
3. Cardiovascular diseases 18
3.1. Arterial hypertension 19
3.2. T-type VGCCs in hypertension 24
Hypothesis and aims……..……...27
Hypothesis 29
Aims 29
Materials and Methods 31
1. Experimental animal models 33
2. Measurement of blood pressure in the tail of the rat 35
3. Study of vascular reactivity 36
3.1. Concentration-response curves 39
4. Study of protein expression 40
4.1. Incubation of samples 40
4.2. Sample processing 41
4.3. Separation and transfer of proteins 41
5. Immunohistochemistry 43
5.1. Immunostaining 43
5.2. Imaging of staining samples 45
6. Study of gene expression 45
6.1. Sample processing 45

6.2. Total RNA quality 47
6.3. Reverse transcription polymerase chain reaction (RT-PCR).... 47
7. Measurement of ROS production in leukocytes population by flow cytometry 49
8. Measurement of plasma levels of nitrates and nitrites 52
9. Statistics analysis 53
Results 55
1. Study of the physiological function of T-type VGCCs and their modulation by NO in healthy male rabbit vessels 57
1.1. Endothelial NO production in response to phenylephrine in the aorta and renal artery of healthy rabbits 57
1.2. Involvement of T-type VGCCs in the contractile response to phenylephrine in the aorta and renal artery of healthy rabbits in the absence and presence of NO 60
1.3. Involvement of T-type VGCCs in the contractile response to angiotensin II in the aorta and renal artery of healthy rabbits 64
1.4. Involvement of T-type VGCCs in the endothelium-dependent and independent relaxation in the aorta and renal artery of healthy rabbits 65
1.5. Protein expression of T-type VGCCs in the aorta and renal artery of healthy rabbits 69
1.6. Localisation of $Ca_V3.1$ and $Ca_V3.2$ in rabbit renal endothelial cells 70
2. Characterization of the SHR experimental model 74
2.1. Weight of animals and organs 74
2.2. Blood pressure 75
2.3. Oxidative stress in leukocytes 76
2.4. Plasma levels of nitrates and nitrites 78
2.5. Vasodilation in the renal artery of WKY and SHR groups 78
2.6. Vascular smooth muscle contractile response in the renal artery of WKY and SHR groups 81

2.7. Contractile response to phenylephrine in the renal artery of WKY and SHR groups 82

2.8. Endothelial NO release in response to phenylephrine in the renal artery of WKY and SHR groups. 83

3. Study of the function of T-type VGCCs in a model of hypertension. Differences between sexes 85

3.1. Involvement of T-type VGCCs in phenylephrine-induced contraction in the renal artery of WKY and SHR groups 85

3.2. Involvement of T-type VGCCs in phenylephrine-induced contraction in the renal artery of WKY and SHR groups in the absence of NO 89

3.3. Study of *$Ca_V3.1$*, *$Ca_V3.2$*, and *Nos3* gene expression in intrarenal arteries of WKY and SHR of both sexes. 95

Discussion 99

1. Advantages and limitations of the experimental procedure. 101

2. Role of T-type VGCCs in the aorta and renal artery of healthy male rabbits. 103

3. Involvement of T-type VGCCs in arterial hypertension. Differences by sex. 109

4. Final considerations. 113

Conclusions 115

Bibliography 119

Annexes 139

Abbreviations

AA: arachidonic acid

AC: adenylyl cyclase

ACh: acetylcholine

ADMA: NG, NG-dimethyl-L-arginine asymmetric

AngII: angiotensin II

ATP: adenosine triphosphate

AT1: angiotensin II receptor 1

BH_4: tetrahydrobiopterin

BK_{ca}: big-conductance calcium-activated potassium channels

Ca^{2+}: calcium ions

$CaCl_2$: calcium chloride

CaM: calmodulin

cAMP: cyclic adenosine monophosphate

Ca_V: voltage-activated calcium currents

cDNA: complementary deoxyribonucleic acid

cGMP: cyclic guanosine monophosphate

COX: cyclooxygenase

DAF-FM: diacetate (4-amino-5-methylamino)-2',7'-difluorofluorescein diacetate

DAG: diacylglycerol

DBP: diastolic blood pressure

DHE: dihydroethidium

DHPs: dihydropyridines

DHR 123: dihydrorhodamine 1,2,3

DNA: deoxyribonucleic acid

EDTA: ethylenediaminetetraacetic acid

eNOS: endothelial nitric oxide synthase

ET-1: endothelin-1

FAD: flavin adenine dinucleotide

FMN: flavin mononucleotide

GqPCR: G protein-coupled receptors

GTP: guanosine triphosphate

H_2O_2: hydrogen peroxide

HE: hydroethidine

iNOS: inducible nitric oxide synthase

IP_3: inositol-1,4,5-trisphosphate

IP_3R: inositol-1,4,5-trisphosphate receptor

Kca: calcium-activated potassium channels

KCl: potassium chloride

L-NAME: NG-nitro-L-arginine methyl ester

L-NMMA: NG-monomethyl-L-arginine

L-NOArg: NG-nitro-L-arginine

MAP: mean arterial pressure

$MgCl_2$: magnesium chloride

MLC: myosin light chain

MLCK: myosin light chain kinase

MLCP: myosin light chain phosphatase

MNCs: peripheral blood mononuclear cells

NaCl: sodium chloride

$NADP^+$: nicotinamide adenine dinucleotide phosphate

NADPH: nicotinamide adenine dinucleotide phosphate

$NaHCO_3$: sodium bicarbonate

nNOS: neuronal nitric oxide synthase

NO: nitric oxide

NOR-1: neuron-derived orphan receptor-1

Nos3: endothelial nitric oxide synthase coding gene

NOX: nicotinamide adenine dinucleotide phosphate oxidases

NPS: sodium nitroprusside

O_2^-: superoxide anion

OH^-: hydroxyl radical

$ONOO^-$: peroxynitrites

PBS: phosphate-buffered saline

PCR: polymerase chain reaction

PGH_2: prostaglandin H_2

PGI_2: prostacyclin

PHE: phenylephrine

PIP_2: phosphoinositide-4,5-bisphosphate

PKA: protein kinase A

PKC: protein kinase C

PKG: protein kinase G

PLA_2: phospholipase A_2

PLC: phospholipase C

pMLC: phosphorylated myosin light chain

PP: pulse pressure

RBC: red blood cell

RNA: ribonucleic acid

ROS: reactive oxygen species

RyRs: ryanodine receptors

SBP: systolic blood pressure

sGC: soluble guanylate cyclase

SHR: spontaneously hypertensive rat

SMC: smooth muscle cell

SOD: superoxide dismutase

SR: sarcoplasmic reticulum

t-BHP: tert-butyl hydroperoxide

TXA_2: thromboxane A_2

VGCCs: voltage-gated calcium channels

VPR: volume pressure recording

WHO: World Health Organization

Figures

Figure 1. Vascular wall structure…….……....3

Figure 2. The nitric oxide pathway in the vasculature……....6

Figure 3. Some of the vascular contraction and relaxation pathways that involve calcium…….....11

Figure 4. Instruments for the measurement of rat blood pressure by tail-cuff technique…….……..36

Figure 5. Organ bath scheme. Image of the equipment used for vascular reactivity assessment…….....37

Figure 6. Wire myograph system. Image of the equipment used for vascular reactivity assessment and image of a renal artery mounted on a wire myograph……..39

Figure 7. Nitrate and nitrite formation reactions…….....46

Figure 8. Colourimetric assay reaction resulting in the purple azo product that acts as a chromophore…...…….....53

Figure 9. Concentration-response curve to phenylephrine (PHE) in rabbit aorta and renal artery in the absence and presence of L-NAME (10^{-4} M)…….....58

Figure 10. Concentration-response curve to phenylephrine (PHE) in rabbit aorta in (A) absence (control) and presence of nickel chloride ($5x10^{-5}$ M); (B) presence of L-NAME (10^{-4} M), absence (control) and presence of nickel chloride ($5x10^{-5}$ M). (C) Participation of T-type VGCCs in the absence and presence of L-NAME (10^{-4} M) represented as AUC 1 and AUC 2 respectively…….....61

Figure 11. Concentration-response curve to phenylephrine (PHE) in rabbit renal artery in (A) absence (control) and presence of nickel chloride ($5x10^{-5}$ M); (B) presence of L-NAME (10^{-4} M), absence (control) and presence of nickel chloride ($5x10^{-5}$ M). (C) Participation of T-type VGCCs in the absence and presence of L-NAME (10^{-4} M) represented as AUC 1 and AUC 2 respectively…….....62

Figure 12. Concentration-response curve to angiotensin II in rabbit aorta and renal artery in the absence and presence of nickel chloride ($5x10^{-5}$M)……..64

Figure 13. Concentration-response curve (A) to acetylcholine (Ach) and (B) to sodium nitroprusside (NPS) in rabbit aorta in the absence and presence of nickel chloride ($5x10^{-5}$ M)…….....66

Figure 14. Concentration-response curve (A) to acetylcholine and (B) to sodium nitroprusside in rabbit renal artery in the absence and presence of nickel chloride ($5x10^{-5}$ M)…….....67

Figure 15. Concentration-response curve to acetylcholine in rabbit renal artery (A) in the absence (control) and presence of nickel chloride ($5x10^{-5}$ M) and L-NAME (10^{-4} M); (B) in the presence of nickel chloride ($5x10^{-5}$ M) and nickel chloride ($5x10^{-5}$ M) plus L-NAME (10^{-4} M)…….....68

Figure 16. Protein expression of $Ca_V3.1$ and $Ca_V3.2$ in the aorta and renal artery of healthy rabbits……69

Figure 17. Representative confocal microscopy images of rabbit renal endothelial cells stained for $Ca_V3.1$ (green) and $Ca_V3.2$ (red)……..71

Figure 18. Representative confocal laser-scanning microscopy image of rabbit renal endothelial cells stained for Cav3.1 (green) and eNOS (red). Nuclei were stained with Hoechst (blue). White arrows point to co-localization (yellow)…….....72

Figure 19. Systolic, diastolic, mean and pulse pressure (mmHg) values of male and female WKY and SHR groups……....75

Figure 20. Bar graphs summarising levels of reactive oxygen species (H_2O_2, $ONOO^-$ and O_2^-) as well as intracellular NO for white blood cells studied, measured by using the fluorescence markers DHR 123, DHE and DAF, respectively……...77

Figure 21. Concentration-response curve (A) to acetylcholine and (B) to sodium nitroprusside in renal artery of male WKY and SHR groups……...79

Figure 22. Concentration-response curve (A) to acetylcholine and (B) to sodium nitroprusside in renal artery of female WKY and SHR groups……..…….80

Figure 23. Contraction (mg) induced by KCl (60 mM) in the renal artery of male and female WKY and SHR groups……...81

Figure 24. Concentration-response curve to phenylephrine (PHE) in renal artery of (A) male and (B) female WKY and SHR……..…..82

Figure 25. Concentration-response curve to phenylephrine (PHE) in renal artery of male WKY and SHR (A and B respectively) and female WKY and SHR (C and D respectively) rats, in the absence and in the presence of L-NAME (10^{-4}M)……..84

Figure 26. Concentration-response curve to phenylephrine (PHE) in the renal artery of male (A) WKY and (B) SHR in the absence (control) and presence of nickel chloride ($5x10^{-5}$M). (C) The bar graph shows the ΔAUC from PHE curves indicating the involvement of T-type VGCCs in response to phenylephrine in male WKY and SHR groups……..86

Figure 27. Concentration-response curve to phenylephrine (PHE) in the renal artery of female (A) WKY and (B) SHR in the absence (control) and presence of nickel chloride ($5x10^{-5}$ M). (C) The bar graph shows the ΔAUC from PHE curves indicating the involvement of T-type VGCCs in response to phenylephrine in female WKY and SHR groups……..87

Figure 28. Concentration-response curve to phenylephrine (PHE) in the renal artery of male WKY rat in (A) absence (control) and presence of nickel chloride ($5x10^{-5}$ M); (B) in presence of L-NAME (10^{-4} M), absence (control) and presence of nickel chloride ($5x10^{-5}$M). (C) Participation of T-type VGCCs in the absence and presence of L-NAME (10^{-4} M) represented as bars……..…....90

Figure 29. Concentration-response curve to phenylephrine (PHE) in the renal artery of male SHR in (A) absence (control) and presence of nickel chloride ($5x10^{-5}$ M); (B) in the presence of L-NAME (10^{-4} M), absence (control) and presence of nickel chloride ($5x10^{-5}$M). (C) Participation of T-type VGCCs in the absence and presence of L-NAME (10^{-4} M) represented as bars……....91

Figure 30. Concentration-response curve to phenylephrine (PHE) in the renal artery of female WKY rat in (A) absence (control) and presence of nickel chloride ($5x10^{-5}$ M); (B) in the presence of L-NAME (10^{-4} M), absence (control) and presence of nickel chloride ($5x10^{-5}$M). (C) Participation of T-type VGCCs in the absence and presence of L-NAME (10^{-4} M) represented as bars……..…..92

Figure 31. Concentration-response curve to phenylephrine (PHE) in the renal artery of female SHR in (A) absence (control) and presence of nickel chloride ($5x10^{-5}$ M); (B) in the presence of L-NAME (10^{-4} M), absence (control) and presence of nickel chloride ($5x10^{-5}$M). (C) Participation of T-type VGCCs in the absence and presence of L-NAME (10^{-4} M) represented as bars……93

Figure 32. Relative mRNA expression of *$Ca_V3.1$* and *$Ca_V3.2$* genes in intrarenal arteries of male WKY and SHR groups…….……96

Figure 33. Relative mRNA expression of *$Ca_V3.1$* and *$Ca_V3.2$* genes in intrarenal arteries of female WKY and SHR groups…….……96

Figure 34. Relative mRNA expression of *Nos3* in intrarenal arteries of male and female WKY and SHR……..……..97

Figure 35. Correlation between Ct of T-type VGCCs subtypes (*$Ca_V3.1$* and *$Ca_V3.2$*) and Ct of *Nos3* in rat intrarenal arteries (male and female, WKY and SHR groups)…….…….....98

Supplementary Figure 1: Concentration-response curve to phenylephrine in the rabbit renal artery in the absence (control) and presence of nickel chloride ($5x10^{-5}$ M) and NNC 55-0396 (10^{-6} M)……...141

Supplementary Figure 2: Concentration-response curve to acetylcholine in the rabbit renal artery in the absence (control) and presence of nickel chloride ($5x10^{-5}$ M) and NNC 55-0396 (10^{-6} M)……..142

Tables

Table 1. Voltage-Gated Calcium Channels subtypes…….....13

Table 2. Primary antibodies used to detect each target protein……..…....43

Table 3. Primary and secondary antibodies used to detect each of the target proteins. Concentration and incubation conditions for each of them…….…….44

Table 4. Values of pEC_{50} ± standard error of the means (SEM) and Emax ± SEM of concentration-response curves to phenylephrine in rabbit aorta and renal artery in the absence and presence of L-NAME (10^{-4} M), nickel chloride ($NiCl_2$) ($5x10^{-5}$ M), or the combination of both…….59

Table 5. Values of the area under the curve (AUC) ± standard error of the means (SEM) of concentration-response curves to phenylephrine in rabbit aorta and renal artery…….63

Table 6. Mean weight of animals (g) ± standard error of the means (SEM) and mean weight of organs relative to animal weight (%) ± SEM…….....74

Table 7. Values of pEC_{50} ± standard error of the mean (SEM) and Emax ± SEM of concentration-response curves to phenylephrine in the renal artery of male and female WKY and SHR groups in the absence and presence of nickel chloride ($NiCl_2$) ($5x10^{-5}$ M)……..88

Table 8. Values of the area under the curve (AUC) ± standard error of the means (SEM) of the concentration-response curves to phenylephrine in the renal artery of male and female WKY and SHR groups……...94

INTRODUCTION

1. Vascular tone regulation

The vascular wall has three layers: the tunica intima, which consists of a monolayer of endothelial cells and an internal elastic lamina; the tunica media, formed by a smooth muscle cells layer and an external elastic lamina; and the tunica externa or adventitia, which contains perivascular adipose tissue cells, fibroblasts, collagen fibres, and nerve endings (see Figure 1).

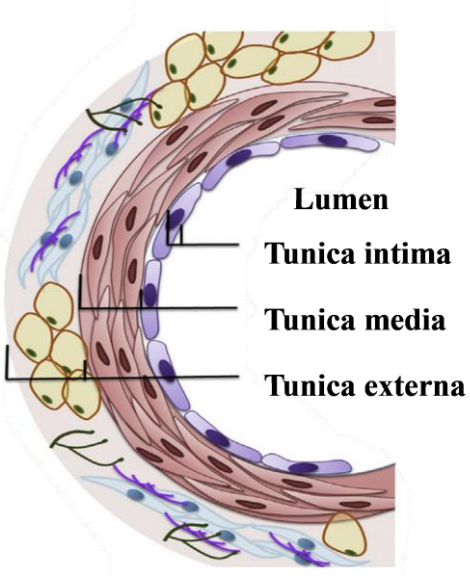

Figure 1. Vascular wall structure. Adapted from Zhao et al. (1).

The tunica media of the vascular wall, composed mainly of smooth muscle cells, acts as an effector system in regulating vascular tone, facilitating contraction and relaxation in response to different stimuli. An increase in the cytosolic calcium (Ca^{2+}) concentration initiates the contraction process. The Ca^{2+} binds to calmodulin to form the Ca^{2+}-Calmodulin complex (2) which

activates myosin light chain kinase (MLCK). Once activated, MLCK phosphorylates the 20 KDa myosin light chain, which forms a ring around the neck of the myosin heavy chain, allowing actin to interact with it. This activates the ATPase activity of myosin, which cleaves the high-energy phosphate bonds of ATP, providing the energy necessary to produce the sliding of the actin filaments over the myosin filaments and leading to muscle contraction (3).

The balance between the dilation and contraction of vascular smooth muscle determines the vascular tone. A combination of different substances, including hormones, platelet products, neurotransmitters, and endothelium-derived vasoactive substances regulates this balance.

1.1. Endothelium-mediated regulation

For many years, the endothelium has been considered a monolayer of cells that had only a support function. However, it is now known to be involved in numerous functions, such as the regulation of coagulation, the formation, repair, and remodelling of blood vessels, the inflammatory response and vascular homeostasis, participating, together with smooth muscle, in the regulation of vascular tone. The endothelium regulates vascular tone by producing and releasing vasoactive substances capable of contracting or relaxing adjacent smooth muscle cells. In 1980, Furchgott and Zawadki demonstrated that the administration of acetylcholine and other muscarinic agents only produced relaxation in rabbit aortas in those provided with endothelium (4). They explained that this relaxation resulted from the

synthesis and release of an endothelial substance, which Furchgott named endothelium-derived relaxing factor. It was later discovered that this substance was nitric oxide (NO) (5).

Likewise, the participation of the endothelium in the regulation of vascular tone is more complex than initially thought. Endothelial cells not only release vasodilator substances but also produce and release vasoconstrictor substances, known as endothelium-derived contractile factors, such as thromboxane A_2 (TXA_2), endothelin-1 (ET-1), angiotensin II (Ang II), and superoxide anion (O_2^-). All these substances are synthesised and released by the endothelium in response to different stimuli, and their balanced production maintains vascular tone. However, in cardiovascular diseases that involve endothelial dysfunction, there is an imbalance in these substances, which mainly implies a loss of vasodilatory capacity.

1.1.1. Nitric Oxide

NO acts as a platelet antiaggregant and antioxidant, significantly inhibiting adhesion molecule proliferation, and is responsible for most of the atheroprotective properties attributed to the endothelium (6). NO is a gaseous substance synthesised from L-arginine by the endothelial nitric oxide synthase (eNOS), a reaction producing L-citrulline. Due to its small size and high lipophilicity, NO diffuses into smooth muscle cell membranes and binds to the soluble guanylate cyclase (sGC) (7), forming a metal-nitrosyl adduct that catalyses the conversion of guanosine triphosphate (GTP) to cyclic guanosine monophosphate (cGMP). Increased intracellular concentrations of cGMP activate protein kinase G (PKG), leading to multiple phosphorylation

of cellular proteins and decreasing intracellular concentration of Ca^{2+}, causing vasodilation (see Figure 2) (8). The generation of NO by eNOS requires different cofactors, such as tetrahydrobiopterin (BH_4), flavin adenine dinucleotide (FAD), and flavin mononucleotide (FMN) (9).

Figure 2. The nitric oxide pathway in the vasculature. EC: endothelial cell; SMC: smooth

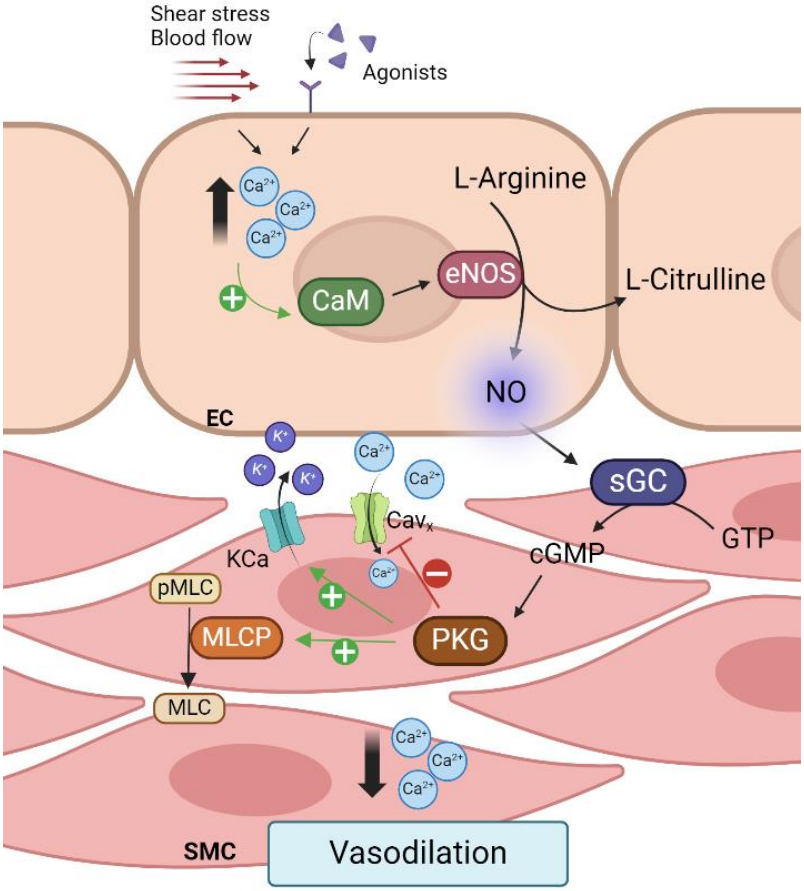

muscle cell; CaM: calmodulin; sGC: soluble guanylate cyclase; GTP: guanosine triphosphate; cGMP: cyclic guanosine monophosphate; PKG: protein kinase G; MLCP: Myosin light chain phosphatase; pMLC: phosphor-Myosin light chain; MLC: Myosin light chain. Adapted from Oliveira-Paula et al.(8). Created by BioRender.com.

There are three different isoforms of NOS: neuronal (nNOS or NOS1), inducible (iNOS or NOS2), and endothelial (eNOS or NOS3). eNOS and nNOS are enzymes that depend on the formation of the Ca^{2+}-Calmodulin complex for their activation. The formation of this complex is, in turn, dependent on an increase in intracellular Ca^{2+} concentration, which occurs in response to physical and chemical stimuli, such as shear stress, or the binding of agonists like acetylcholine or bradykinin to their corresponding receptors. On the other hand, iNOS is Ca^{2+} independent and is activated by proinflammatory cytokines and pathogen-related molecules (10). Although all three isoforms may be present in blood vessels, eNOS is the predominant enzyme in the endothelium. It is responsible for the production of most endothelium-derived NO under physiological conditions. For this reason, it plays a pivotal role in cardiovascular homeostasis (10). Multiple phosphorylation sites at tyrosine, serine, and threonine residues dynamically regulate eNOS activity (11). Phosphorylation of eNOS at Ser1177 leads to its activation at basal levels and in response to agonists (12).

The primary metabolic pathway for eliminating NO involves the reaction of NO with the hemo group of haemoglobin. NO can diffuse into erythrocytes, originating nitrates by reacting with oxyhaemoglobin. This reaction limits the half-life of NO to only 10 seconds (13). Inhibition of NO synthesis and release is achieved through NOS inhibitors and analogues of L-arginine. There are two known endogenous inhibitors: NG, NG-dimethyl-L-arginine asymmetric (ADMA), and NG-monomethyl-L-arginine (L-NMMA) (14). The most critical exogenous

inhibitors are NG-nitro-L-arginine methyl ester (L-NAME) and NG-nitro-L-arginine (L-NOArg) (15).

The production of NO occurs endogenously but can also be produced from several clinical compounds known as nitrovasodilators. These compounds, such as sodium nitroprusside, are clinically used in hypertensive crises, heart failure, or coronary ischemia, as well as to maintain hypotension during surgery. They exert their action by donating NO and causing relaxation of vascular smooth muscle (16).

1.2. Sympathetic regulation

Besides the endothelium, the function of vascular smooth muscle is also regulated by the sympathetic system, which innervates large arteries and arterioles (17) and plays a crucial role in the regulation of blood pressure and blood flow. External factors such as stress, trauma, bleeding, or pain can increase sympathetic activity and increase vascular resistance.

Norepinephrine, the primary sympathetic neurotransmitter, acts on different types of adrenergic receptors: α_1, α_2, β_1, and β_2 (18). The α_1-adrenergic receptors are in smooth muscle cells, and their activation contributes to an increase in intracellular Ca^{2+}, provoking a vasoconstrictor response. The α_2-adrenergic receptors are located presynaptically and postsynaptically at the sympathetic nerve. When activated at the presynaptic level, they increase the reuptake of noradrenaline released during sympathetic neurotransmission, reducing vasoconstriction (19). At the postsynaptic level, activation of α_2-adrenergic receptors in smooth muscle decreases adenylate cyclase activity and cAMP release, increasing intracellular Ca^{2+} and causing

vasoconstriction. Conversely, stimulation of endothelial α_2-adrenergic receptors reduces vasoconstriction by promoting NO release (20).

On the other hand, activation of the β_1 and β_2-adrenergic receptors activates adenylate cyclase, promoting cAMP production, thus leading to a decrease in intracellular Ca^{2+} and vasodilation (21).

2. Calcium and vascular homeostasis

Ca^{2+} is a highly versatile signalling molecule that influences various cellular processes. Many pathways are involved in the Ca^{2+} regulation at the vasculature. Various types of Ca^{2+} channels in cell membranes enable Ca^{2+} to enter and leave the cytoplasm. In addition, Ca^{2+} stores, such as the sarcoplasmic reticulum (SR) in muscle cells and the mitochondria, allow intracellular Ca^{2+} release and reuptake. The coordinated action of all these cellular mechanisms is essential for vascular homeostasis.

Endothelial vasodilation mostly depends on changes in intracellular Ca^{2+} concentration. For example, an increase in intracellular Ca^{2+} concentration can lead to: 1) binding of Ca^{2+}-Calmodulin complex with eNOS (22), 2) opening of Ca^{2+}-activated K^+ channels (K_{Ca}) (23) resulting in K^+ efflux and subsequent hyperpolarisation in vascular smooth muscle, and 3) release prostaglandin via phospholipase A_2-dependent cyclooxygenase pathway (24).

In smooth muscle cells, Ca^{2+} channels located in SR membranes play a crucial role in controlling vascular reactivity. These cellular structures are endowed with transmembrane ion channels, termed ryanodine receptors (RyRs) and inositol-1,4,5-trisphosphate (IP_3) receptors (IP_3Rs), which

mediate the release of Ca^{2+} into the cytosol (25). Vascular RyRs mediate Ca^{2+} release from the SR through Ca^{2+} sparks that activate big conductance K_{Ca} (BK_{Ca}), leading to hyperpolarisation of smooth muscle cells and, thus, vasodilation (26).

On the other hand, the activation of G protein-coupled receptors (GqPCR) is the canonical signalling pathway that stimulates phospholipase C (PLC), which hydrolyses membrane-associated phosphoinositide-4,5-bisphosphate (PIP_2) into IP_3 and diacylglycerol (DAG). Many vasoconstrictors, such as norepinephrine, Ang II, and ET-1, activate their respective GqPCRs on the membrane of vascular smooth muscle cells. Next, IP_3 binds to IP_3R and releases Ca^{2+} to the cytosol. Furthermore, DAG stimulates protein kinase C (PKC), opening Ca^{2+} channels, which increases intracellular Ca^{2+} levels. This increase facilitates the formation of the Ca^{2+}-calmodulin complex, promoting contraction by phosphorylating myosin light chain (MLC) through myosin light chain kinase (MLCK) (27) (see Figure 3).

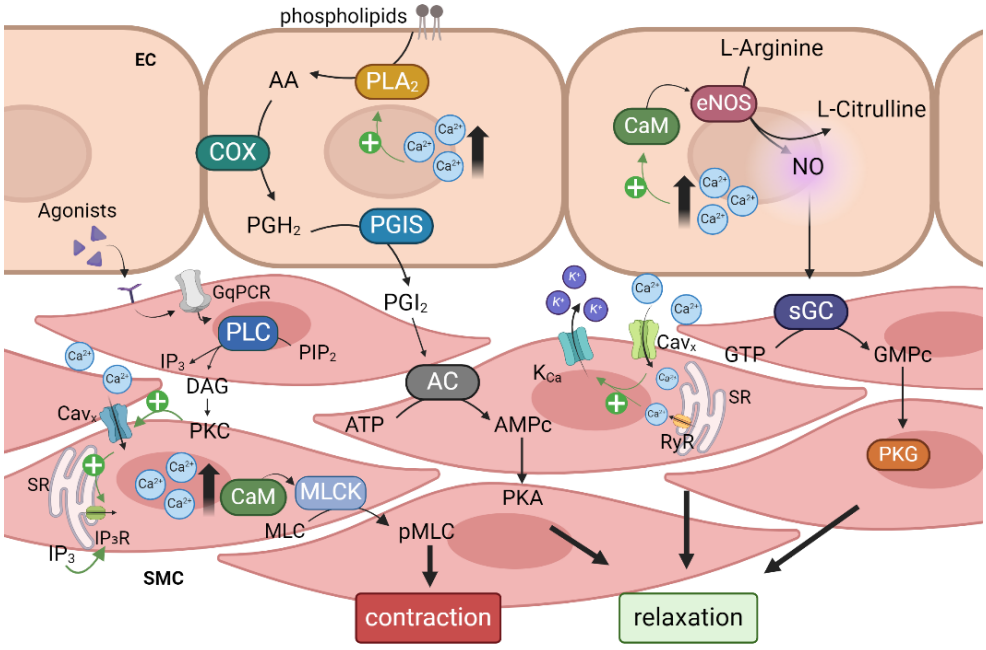

Figure 3. Some of the vascular contraction and relaxation pathways that involve calcium. EC: endothelial cell; SMC: smooth muscle cell; SR: sarcoplasmic reticulum; PLA_2: phospholipase A_2; AA: arachidonic acid; COX: cyclooxygenase; PGH_2: prostaglandin H_2; PGIS: prostacyclin synthase; PGI_2: Prostacyclin; AC: adenylyl cyclase; ATP: adenosine triphosphate; AMP_c: cyclic adenosine monophosphate; PKA: protein kinase A; GqPCR: G protein-coupled receptors; PLC: phospholipase C; PIP_2: phosphoinositide-4,5-bisphosphate; IP_3: inositol-1,4,5-trisphosphate; IP_3R: inositol-1,4,5-trisphosphate receptor; DAG: diacylglycerol; PKC: protein kinase C; CaM: calmodulin; MLCK: Myosin light chain kinase; MLC: Myosin light chain; pMLC: phosphor-Myosin light chain; eNOS: endothelial nitric oxide synthase; NO: nitric oxide; sGC: soluble guanylate cyclase; GTP: guanosine triphosphate; cGMP: cyclic guanosine monophosphate; PKG: protein kinase G; RyR: ryanodine receptor; Cav_x: voltage gated calcium channels; K_{Ca}: calcium-activated potassium channels. Created by BioRender.com.

2.1. Voltage-gated calcium channels

The main Ca^{2+} influx in vascular smooth muscle cells is via voltage-gated Ca^{2+} channels (VGCCs). These channels are transmembrane proteins located in the plasma membrane that open in response to membrane depolarisations, allowing the entry of Ca^{2+} in favour of their electrochemical gradient. This is an essential mechanism of myogenic vasoconstriction in resistance arteries. VGCCs are widely expressed among excitable cells and show a great diversity of electrophysiological properties, allowing them to influence many physiological functions (28).

Since their discovery in 1953, different subtypes of VGCCs have been characterised. Each subtype shares a common subunit composition consisting of a pore-forming subunit $Ca_V\alpha1$, plus auxiliary subunits $Ca_V\beta$, $Ca_V\alpha2\delta$ and, in some cases, $Ca_V\gamma$. The structure of the $Ca_V\alpha_1$ subunit includes four repeat domains (I-IV), each with six transmembrane segments. The domains are linked by intracellular loops subject to splicing and modulation by protein kinase A (PKA) and protein kinase C (PKC), which can phosphorylate the channel. Electrophysiological studies using vertebrate VGCCs have shown that the $Ca_V\alpha_1$ subunit largely determines the pharmacological and biophysical properties of Ca_V currents (29,30).

Molecular cloning studies have identified distinct genes encoding the channel pore-forming $Ca_V\alpha1$ subunit, assigned to three main families: Ca_V1, Ca_V2, and Ca_V3. These families are divided into two major groups: those activated by high voltage due to their activation at stronger depolarising voltages, which include L-, P/Q-, N-, and R-type VGCCs (Ca_V1 and Ca_V2, respectively) and activated by low voltage, due to their activation at more

hyperpolarised voltages, which include T-type VGCCs (Ca_V3) (28,31) (Table 1). The first gene sequenced was CACNA1S (S, for skeletal muscle); they were then named alphabetically according to their discovery. Currently, there is no evidence that Ca_V3 possesses auxiliary subunits in native systems (32). However, some studies suggest that auxiliary subunits of L-type VGCCs may modulate the functions of T-type VGCCs (33).

Table 1. Voltage-Gated Calcium Channels subtypes.

Voltage	Major Family	Family	Subtype	α_1 subunit	Gene
High-voltage activation	Ca_V1	L	$Ca_V1.1$	α_1S	*CACNA1S*
			$Ca_V1.2$	α_1C	*CACNA1C*
			$Ca_V1.3$	α_1D	*CACNA1D*
			$Ca_V1.4$	α_1F	*CACNA1F*
	Ca_V2	N, P/Q and R	$Ca_V2.1$	α_1A	*CACNA1A*
			$Ca_V2.2$	α_1B	*CACNA1B*
			$Ca_V2.3$	α_1E	*CACNA1E*
Low-voltage activation	Ca_V3	T	$Ca_V3.1$	α_1G	*CACNA1G*
			$Ca_V3.2$	α_1H	*CACNA1H*
			$Ca_V3.3$	α_1I	*CACNA1I*

Over the years, L-type VGCCs have been considered the main Ca^{2+} influx pathway into the vascular smooth muscle cell. In fact, Ca^{2+} influx through L-type VGCCs is the main mediator of the myogenic response, defined as the intrinsic ability of vascular smooth muscle to contract or relax

in response to changes in intraluminal pressure (34). Once the muscle cell depolarises, Ca^{2+} influx occurs mainly through L-type VGCCs, leading to vasoconstriction. Specifically, the $Ca_V1.2$ subtype is key in maintaining blood pressure (29).

As mentioned above, the $Ca_V\alpha1$ subunit, forming the channel pore, determines the properties of the different types of VGCCs. These properties have defined different current subtypes, depending on their activation at low or high voltages, their inactivation kinetics, which can be long or transient (L- or T-type), and their sensitivity to dihydropyridines (DHPs). DHPs block L-type VGCCs; therefore, these channels are known as DHP-sensitive channels, and their blockade with these drugs is currently an effective antihypertensive treatment. N-type VGCCs appear to be present only in neuronal cells, whereas the other VGCCs types have been identified in many cell types, including vascular smooth muscle and endothelial cells. In addition to $Ca_V1.2$, it has been suggested that P/Q- and T-type VGCCs are also involved in blood vessel contraction in both rodents and humans (35–38). The main VGCCs involved in Ca^{2+} influx in vascular smooth muscle cells are L- and T-type VGCCs. The greater or lesser abundance in the different populations of these channels varies along the vascular tree, with L-type VGCCs being predominant; however, T-type VGCCs are emerging as important contributors to myogenic tone (39).

2.2.T-type voltage-gated calcium channels

Numerous studies in the last decades describe the expression of T-type VGCCs in addition to L-type VGCCs in different vascular beds of various species (37,39–42). The activation of these channels occurs at lower depolarisation levels compared to L-type channels. They open between -70 and -60 mV, with a peak current between -30 and -10 mV, whereas the resting membrane potential of smooth muscle cells in most vascular beds during physiological pressures ranges between -60 mV and -35 mV. Currently, T-type VGCCs are classified into three subtypes: $Ca_V3.1$, $Ca_V3.2$, and $Ca_V3.3$. These channels exhibit faster activation and deactivation than L-type VGCCs and are relatively insensitive to DHP or other high-voltage currents (43). Among the three subtypes, the $Ca_V3.1$ has the fastest inactivation kinetics ($Ca_V3.1$ > $Ca_V3.2$ > $Ca_V3.3$) (44). The low activation threshold, not far from the resting potential of most excitable cells, and their fast kinetics, make T-type VGCCs key modulators of cellular excitability and pacemaking (45).

T-type VGCCs are mainly expressed in the central and peripheral nervous system, where they are required for repetitive firing of the action potential (43). They are also expressed in the heart and found in both the sinoatrial and atrioventricular nodes, suggesting that these channels play a role in pacemaking (46,47). At the molecular level, T-type VGCCs transcripts and proteins have been found in smooth muscle cells of various vascular beds and species, including humans (37,39–42). Several studies have also reported the expression T-type VGCCs in the endothelium of cerebral and mesenteric arteries and even in the pulmonary microvasculature (40,41,48). Particularly, $Ca_V3.1$ and $Ca_V3.2$ are the main subtypes of T-type VGCCs in the

cardiovascular system. Although $Ca_V3.3$ mRNA has been detected in vascular smooth muscle cells (49), this type is more enriched in the brain (50). It has been suggested that T-type VGCCs may have a more prominent contractile effect on smaller arterioles than larger arteries (51).

Emergent evidence points toward a contribution of T-type VGCCs in smooth muscle contractility and the maintenance of arterial tone (37,39,41). For instance, $Ca_V3.1$ currents are thought to be crucial in the constriction of cerebral and mesenteric vessels, as well as renal arterioles (40,41,52,53). In mesenteric arteries from $Ca_V3.1$ deficient mice ($Ca_V3.1^{-/-}$), myogenic tone was found to be decreased, particularly at lower intraluminal pressures (20 - 60 mm Hg), in which T-type VGCCs are known to be active (54). In fact, the lack of $Ca_V3.1$ coincided with a reduction in systolic blood pressure (SBP), diastolic blood pressure (DBP), and, therefore, mean arterial pressure (MAP) (54).

The myogenic response involves constriction and dilation of blood vessels in response to changes in intraluminal pressure, contributing to the mechanism of autoregulation of blood flow. Both L- and T-type VGCCs are involved in this response, with L-type playing a predominant role. In recent years, studies have increasingly demonstrated the involvement of T-type VGCCs in the myogenic response in some vascular beds, especially resistance vascular beds. Although the implication of T-type VGCCs on myogenic tone appears to be vascular bed-dependent, their contribution remains unclear (55). In specific vascular beds, such as the cerebral and mesenteric arteries, T-type VGCCs contribute to the regulation of myogenic tone at lower pressures (40 - 80 mmHg) (37,54,56,57). Overall, the

contribution of T-type VGCCs to the myogenic response appears to be minor compared to the participation of L-type VGCCs.

The contribution of T-type VGCCs in vascular tone regulation seems to increase especially in the absence of NO. It could, therefore, become a therapeutic target in cardiovascular diseases with endothelial dysfunction and NO deficiency. In this regard, previous studies in rodents have shown that NO deficiency engages T-type VGCCs (58,59), causing vasospasm (60,61). Therefore, blockade of T-type VGCCs may suppress vasospasm without affecting myogenic tone. The mechanism can imply NO-cGMP signalling pathway (60) or involve O_2^- (59,62). Therefore, in the absence of NO, levels of O_2^- would increase and activate T-type VGCCs, contributing to a hypertensive state. This vascular oxidative stress caused by increased O_2^- can lead to endothelial dysfunction, as has been previously demonstrated by our group (63). In fact, in an oxidative stress mice model, increased vascular tone was observed compared to non-hypertensive mice, which may be related to a higher expression and contribution of T-type VGCCs over L-type VGCCs (62).

On the other hand, recent research is focused on understanding the mechanisms that control T-type VGCCs activity in vasodilation. Chen *et al.* (64) reported the first evidence of vasodilation mediated by Ca_V currents since they observed abnormal relaxation in coronary arteries from $Ca_V3.2$ deficient ($Ca_V3.2^{-/-}$) mice when exposed to both independent and dependent endothelium vasodilator agents. From then on, other researchers have investigated the possible role of these channels in vasodilation. Some authors

have linked the $Ca_V3.2$ subtype to vasodilation mediated by BK_{ca} (65–67) or NO release (52,68).

In summary, T-type VGCCs play a complex and diversified role in the vascular system, contributing to myogenic tone, vasodilation, and vasoconstriction. Thus, a more complete knowledge of the role of these channels and their modulation in physiological and pathological conditions is the first step towards understanding the pharmacological application of T-type VGCCs blockers in the treatment of cardiovascular diseases.

3. Cardiovascular diseases

Cardiovascular diseases are a group of disorders that affect the heart and blood vessels. They are currently the leading cause of morbidity and mortality in developed societies and continue to be the leading cause of death worldwide. According to the World Health Organization (WHO), 20.5 million people died due to these diseases in 2021, representing for nearly 34 % of the deaths recorded worldwide (69). In Spain, around 120 thousand people died because of cardiovascular causes in 2020, accounting for almost 25 % of deaths in our country (70). The incidence of cardiovascular diseases is increasing, and it is predicted that there will be more than 23 million deaths due to this cause by 2030.

Moreover, cardiovascular diseases represent a significant economic impact on healthcare systems. In 2021, cardiovascular diseases cost the economy of the European Union 282 billion euros (71), while in Spain, the economic impact of these diseases increased by 20 % between 2014 and 2020, from 6.4 billion euros to 7.7 billion euros (72).

Arterial hypertension is a significant risk factor for global mortality and morbidity. It has been widely linked to cardiovascular diseases such as atherosclerosis, acute myocardial infarction, and cardiomyopathy (73,74). Blood pressure control rates are poor worldwide and remain far from satisfactory. As a result, hypertension continues to be the leading preventable cause of cardiovascular disease and all-cause mortality globally. Hypertension directly contributes to stroke, ischemic heart disease, and other cardiovascular diseases (73). Indeed, hypertension is considered, along with dyslipidaemia, smoking, poor eating habits, alcohol consumption, sedentary lifestyle, obesity, diabetes, advanced age, or family history, a risk factor for the development of cardiovascular disease.

3.1. Arterial hypertension

Blood pressure is defined as the pressure that blood exerts on the walls of the arteries. It is referred to as hypertension when this pressure exceeds normal limits, in which the heart may experience difficulties pumping blood (75). SBP normal values are equal to or less than 120 mm Hg. DBP normal values are equal to or less than 80 mm Hg (75). When SBP is 120 to 129 mm Hg and DBP between 80-90 mm Hg, the patient has high blood pressure, and increased values are classified as hypertension, which can be divided into (76):

- Grade 1 hypertension: SBP between 130-139 mm Hg and DBP between 80-89 mm Hg.
- Grade 2 hypertension: SBP is 140 mm Hg or higher, and DBP is 90 mm Hg or higher.

MAP and pulse pressure (PP) are two markers of cardiovascular risk when they are elevated (77). MAP is the average pressure in the arteries during a cardiac cycle and reflects the constant perfusion that the tissues receive. It is calculated by adding one-third of the pulse pressure to the diastolic pressure. PP is calculated as the difference between the SBP and DBP (78). Studies in the last decades have considered PP as an independent cardiovascular risk factor and suggest that values above 10 mm Hg over normal values (40 - 50 mm Hg) increase the risk of cardiovascular accidents by around 20 % (78). In addition, the relationship between elevated PP and endothelial dysfunction has been demonstrated (79), which constitutes the initial and essential step for the development of cardiovascular diseases and even some metabolic diseases, such as type II diabetes mellitus.

According to the WHO, hypertension causes 9 million deaths per year. It is a growing public health problem, with the number of cases increasing from 594 million people in 1975 to 1.13 billion in 2015. In 2021, an estimated 1.3 billion people around the world between the ages of 30 and 80 suffered from hypertension. One of the global targets for non-communicable diseases is precisely to reduce the prevalence of hypertension by 25 % by 2025 (compared with 2010) (75).

The prevalence of hypertension increases with age and causes secondary systemic involvement with renal, cerebrovascular, and cardiac effects (80). The recorded prevalence of hypertension stood at 16.5 % of the Spanish population in 2016, being higher in women (17.3 %) than in men (15.7 %) (81). However, a cross-sectional study conducted in Spain on the adult population estimated a prevalence of 42.6 %, higher in men (49.9 %)

than in women (37.1 %). Underdiagnosis is exceptionally high in age groups between 18 and 30 years of age, with 84.1 % of patients with undiagnosed hypertension (82). 88 % of patients with diagnosed hypertension were receiving pharmacological treatment, but only 30 % were well-controlled (82). It has been shown that correct control of hypertension reduces the rate of myocardial infarction by 24 % and mortality attributed to stroke by 42 % (83,84).

Hypertension indirectly aggravates heart failure and kidney dysfunction, with significant global differences between men and women (74). The prevalence, awareness, treatment, and control of hypertension vary significantly by gender. Men before the age of sixty have a higher incidence of hypertension compared to women (85). One of the reasons why women have a lower incidence of hypertension may be due to the high concentration of oestrogens which increase endothelial NO release, thereby reducing peripheral resistance and blood pressure (86). This effect is mainly attributed to oestradiol during the fertile age; however, after menopause and the subsequent decrease in plasma oestradiol levels, the risk of these diseases becomes higher in women than in men of the same age (87).

To get a better understanding of the vascular pathophysiological mechanisms that underlie hypertension, animal models such as the spontaneously hypertensive rat (SHR) are commonly used. The SHR model represents a well-studied animal model of hypertension. Unlike other models, these rats develop hypertension spontaneously and exhibit cardiovascular features specific to heart failure caused by hypertension, which is established

when the rats are between 9 and 12 weeks of age. After 16 months of age, the difference in blood pressure between sexes disappears (88).

Researchers at Kyoto University developed the SHR model in 1963 by selecting and crossbreeding Wistar strain rats with elevated blood pressure. The Wistar-Kyoto (WKY) strain of rats from which this model was developed was the normotensive control of SHR (89). In 1989, sex differences were identified in the development of blood pressure in this model (90). Similar to humans, males exhibit higher blood pressure than females. Mechanisms contributing to sex differences in blood pressure control range from adrenergic receptor regulation, which differs between males and females, to the renin-angiotensin system, oxidative stress, NO bioavailability, and immune cells (91).

Oxidative stress plays a crucial role in the pathogenesis of hypertension. It is involved in several chronic diseases, and its relationship with hypertension is bidirectional: it is both a cause and a consequence of this condition. Oxidative stress is associated with endothelial dysfunction, inflammation, cell migration, and angiogenesis, among other processes, which play an important role in vascular remodelling during hypertension (92). Reactive oxygen species (ROS) are a group of oxygen-derived molecules generated during the oxidative processes of normal metabolism in the mitochondria. The main molecules that form these species are O_2^- and its derivatives, hydrogen peroxide (H_2O_2) and hydroxyl radical (OH^-) (93). Under physiological conditions, O_2^- is removed by the enzyme superoxide dismutase (SOD), which converts O_2^- into H_2O_2, which is broken down into water and O_2 due to the action of antioxidant enzymes, such as catalase,

glutathione peroxidase or thioredoxin peroxidase (94). Oxidative stress occurs when an increase in ROS production generates an imbalance between the antioxidant and prooxidant systems (95). ROS originate from various enzymes, such as xanthine oxidase, cyclooxygenase, lipoxygenase, cytochrome P450 monooxygenase, as well as uncoupled eNOS or the mitochondrial electron transport chain. The primary source of O_2^- vascular is NADPH oxidase (NOX) (95). NOX is an enzyme that reduces oxygen to O_2^-, which reacts with NO to form peroxynitrites ($ONOO^-$), decreasing NO bioavailability and inducing endothelial dysfunction (94). It has also been shown that peroxynitrites can inactivate prostacyclin by nitration of tyrosine (96), leading to increased production of vasoconstrictor agents such as TXA_2 or prostaglandins, thus increasing vascular tone and favouring a hypertensive state. In addition, O_2^- can convert into OH^-, one of the most toxic ROS at the cellular level (94), and can catalyse the reaction of vasoconstrictor prostanoids (96).

In diseases such as hypertension, vascular dysfunction is present, and various mechanisms can trigger it. Not only is oxidative stress responsible for vascular alterations, but other mechanisms related to calcium can also be implicated. The role of calcium channels is essential to controlling vascular tone, and the elevated activity in these channels could lead to excessive vasoconstriction and, eventually, hypertension. Therefore, L-type VGCCs blockers, such as DHPs, constitute a pharmacological group commonly used in treating hypertension, either in monotherapy or combined with other antihypertensive drugs (97). However, one of the most common adverse effects is the production of peripheral malleolar oedema due to increased

transcapillary filtration. The most widespread theory is that a disproportionate decrease in arteriolar versus venular resistance would increase hydrostatic pressure in the capillary circulation and drive fluid displacement into the interstitial compartment. On numerous occasions, the appearance of this oedema leads to discontinuation or non-adherence to treatment (98).

A better understanding of the role of T-type VGCCs in vascular smooth muscle and endothelial cells, as well as in other target organs under pathophysiological conditions, forms the basis for the rational development of new, safer, and more effective antihypertensive drugs that block T-type VGCCs.

3.2. T-type VGCCs in hypertension

Numerous studies in recent years have pointed to T-type VGCCs as emergent contributors to the maintenance of myogenic tone and blood pressure in low ranges (40 to 80 mm Hg) (37,39,54). Despite their interest and potential clinical application, the function of T-type VGCCs is still unknown. Recent research suggests that T-type VGCCs blockers could be used as a pharmacological tool to reverse the vasoconstriction caused by endothelial dysfunction that underlies cardiovascular disease (60). The advantage of T-type over L-type VGCCs blockers is that the latter would influence basal myogenic tone, whereas T-type appears to be minority and activated under certain circumstances such as NO deficit. Consequently, since myogenic tone is mediated by L-type VGCCs involved in the autoregulation of blood flow to tissues, L-type VGCCs blockers cause complications such as

peripheral malleolar oedema. Hence, in the context of decreased NO bioavailability, a common feature of cardiovascular disease, blockade of T-type VGCCs may offer a new pathway that opposes vasospasm of small arteries. Furthermore, clinical trials have shown that targeting T-type VGCCs in addition to L-type VGCCs by using blockers such as benidipine and efonidipine is more effective than using only L-type VGCCs blockers like amlodipine for the treatment of hypertension. The combination of L- and T-type VGCCs blockers showed a reduction in blood pressure and an improvement in arterial stiffness and endothelial function, and appears to have a protective effect against hypertensive glomerular injury, in contrast to L-type VGCCs blockers (99–103). These studies are consistent with the idea that T-type VGCCs blockers have less capacity to cause peripheral oedema because they have a similar vasodilator effect on pre- and post-capillary vessels. In fact, in a study carried out in the SHR model, the authors demonstrate that, at antihypertensive doses, oedema formation is significantly lower in rats treated with mibefradil, an L- and T-type VGCCs blocker, than in rats treated with nifedipine, an L-type blocker (104).

As mentioned above, there are differences in the development and incidence of hypertension between men and women; however, there are currently no personalised treatments available based on sex. It has been proposed that oestrogens may down-regulate L-type VGCCs and thus prevent excess vasoconstriction through an endothelium-independent process (105). Specifically, 17β-oestradiol has been shown to exert vasorelaxant effects on the vascular smooth muscle cells from mesenteric arteries via inhibition of Ca^{2+} influx through L-type VGCCs (106). Furthermore, at the brain level, a

relationship between oestradiol and L-type VGCCs has been established (107). Based on this background, it is not unexpected that oestrogens may regulate T-type VGCCs activity and thus vascular tone, contributing to a lower risk of developing cardiovascular diseases. So far, little is known about whether the vascular role of T-type VGCCs is modulated by oestrogens, and more studies are needed in this field.

The role of T-type VGCCs in the vascular territory and the mechanisms by which the function of these channels is modulated are still unknown. Therefore, a detailed understanding of the mechanisms underlying blood pressure regulation may greatly facilitate the development of new therapies that lack or minimise the typical side effects of DHPs. To reach this point, it is first necessary to elucidate the physiological function of these channels in endothelial and smooth muscle cells, to know how their function is regulated, if it is altered in diseases such as hypertension, that cause endothelial dysfunction and low levels of NO, or if its function changes depending on sex. All of this is analysed in this doctoral thesis to shed light on the complex role of T-type VGCCs on vascular tone.

HYPOTHESIS AND AIMS

Hypothesis

Under physiological conditions, NO could act as a modulator of the function of T-type VGCCs. Therefore, in the presence of endothelial dysfunction due to NO deficiency, these channels could become more active and, since we hypothesise that their function is mainly vasoconstrictor, worsen the prognosis of hypertension. Moreover, the role of T-type VGCCs could vary depending on sex, as has been demonstrated for L-type VGCCs.

Aims

This thesis aims to determine the vascular function and expression of T-type VGCCs under physiological conditions and in hypertension, where we also study possible sex modulation.

Specific aims:

1. Determine the involvement of T-type VGCCs in the contractile response to phenylephrine and angiotensin II in the aorta and renal artery of healthy rabbits and assess whether the absence of NO influences the α_1-adrenergic response.

2. Investigate the role of T-type VGCCs in the endothelium-dependent and -independent relaxation responses in the aorta and renal artery of healthy rabbits.

3. Analyse the protein expression levels of T-type VGCCs in the aorta and renal artery of healthy rabbits, and explore potential colocalization between T-type VGCCs and eNOS.

4. Examine whether the function and expression of T-type VGCCs are altered in a model of hypertension, and determine if these alterations are influenced by sex.

MATERIALS AND METHODS

1. Experimental animal models

Since this thesis focuses on the vascular function of T-type VGCCs, we have used rabbits and rats as widely validated models for the study of cardiovascular disease. All animals were housed in the Central Research Unit of the Faculty of Medicine, University of Valencia and procedures were approved by the Institutional Animal Care and Use Committee of the University of Valencia in compliance with the European Union directive 2010/63 on protecting animals for scientific purposes.

The first procedure for rabbits was authorised under the designation 2020/VSC/PEA/0056 type 2, for the project entitled "Utility of intracellular calcium homeostasis stabilisation in the control of fibrillatory processes (Prometeo/2018/078)" developed by the Experimental Cardiac Electrophysiology group (GRELCA), Department of Physiology, University of Valencia. The second procedure for the SHR model was authorised under the designation 2021/VSC/VSC/PEA/0264 type 2, entitled “Vascular effect of T-type voltage-dependent calcium channels in a rat model of arterial hypertension” developed by the Vascular Function Research Group, INCLIVA and Department of Physiology, University of Valencia.

- Rabbits

To study the function and expression of T-type VGCCs ($Ca_V3.1$ and $Ca_V3.2$) at the vasculature under physiological conditions, we employed 15-week-old male White New Zealand rabbits (*Oryctolagus cuniculus*) with an average weight of 3.8 ± 0.2 kg. The rabbits were sourced from San Bernardo Laboratories S.L. (Navarra, Spain) and were housed in individual cages at a

stable temperature of 23 °C, with 12-h light-dark cycles, and were fed *ad libitum*. Rabbits were sacrificed by intravenous injection of sodium thiopental (60 mg/kg) with 800 IU of sodium heparin into the marginal vein of the ear. Removal of the abdominal aorta and renal artery was performed by abdominal laparotomy. Artery samples were used for vascular reactivity, immunohistochemistry and protein expression experiments.

- Rats

To elucidate whether T-type VGCCs function is altered at the vasculature with hypertension and whether sex can modulate this alteration, we used 16-week-old male and female SHR and their respective control WKY. The rats were obtained from Charles River Laboratories S.A. (Barcelona, Spain) and housed in groups of four rats per cage, separated by sex and experimental group. The animals remained at a stable temperature of 23 °C, with 12-h light-dark cycles, and were fed *ad libitum.* The rats were sacrificed by overdose of the halogenated anaesthetic isoflurane (IsofloR), which was administered by inhalation using a rodent induction chamber and having previously administered buprenorphine as an analgesic. Anaesthesia monitoring was based on verifying the absence or presence of the reflex response. Subsequently, blood was collected and placed in EDTA tubes for cytometry studies and quantifying plasma nitrates and nitrites. The aorta and renal arteries were dissected for vascular reactivity studies. Some samples were snap-frozen in liquid nitrogen and stored at -80°C until processing for gene expression experiments.

2. Measurement of blood pressure in the tail of the rat

To measure blood pressure in rats, a non-invasive system was used with the NIBP CODA 8 equipment (Kent Scientific Corporation), based on the tail-cuff technique originally described by Buñag (108). The indirect measurement of blood pressure in rats with this technique is similar to the measurement of blood pressure with a sphygmomanometer in humans. The device uses a volume pressure recording (VPR) sensor that allows continuous, real-time observation of the blood pressure of rats. The VPR sensor incorporates a differential pressure transducer specially designed to measure SBP and DBP, thus enabling the determination of the blood volume in the tail of rodents.

During blood pressure measurements, each rat was placed in a tube-shaped holder facing the open end, allowing it to enter freely. The holder was kept on a heating platform throughout the experiment to maintain the temperature at or above 32 ºC. The cuffs were placed by inserting the tail through the occlusion cuff and passing through the VPR-Cuff, the sensor that measures blood pressure (see Figure 4).

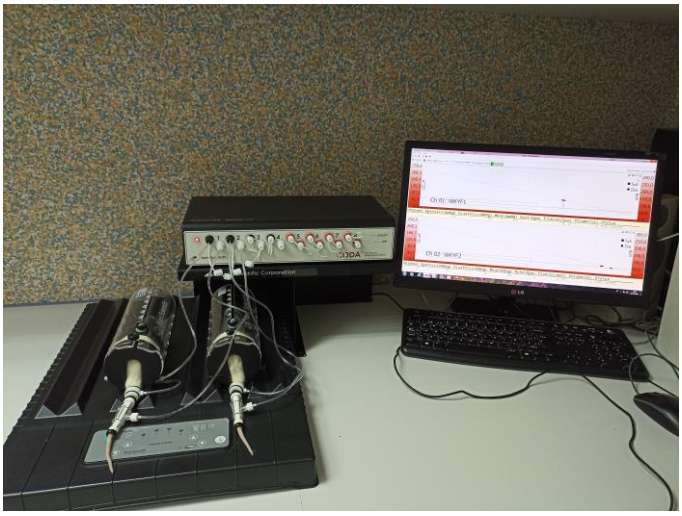

Figure 4. Instruments for the measurement of rat blood pressure by tail-cuff technique.

Upon completion of the measurement, the animals were placed back in their cages. Blood pressure readings were recorded five times daily for two weeks. To ensure the reliability of the data, the animals were acclimated to the process by being placed in the stand for at least 15 minutes a day, for a minimum of three consecutive days, prior to testing. The system provides SBP, DBP, and MAP values and we calculate PP.

3. Study of vascular reactivity

Dissected arteries were cleaned in a Petri dish with cold saline solution (NaCl 0.9 %) under microscopy, removing the perivascular adipose tissue. The aorta and renal artery from rabbit were cut into 3 mm rings and mounted in an organ bath system. Two stainless steel L-shaped pins (150 μm diameter) were introduced through the lumen of the ring. One pin was fixedly attached

to the wall of the organ bath, and the other was connected to a force transducer moving parallel to the first one (see Figure 5).

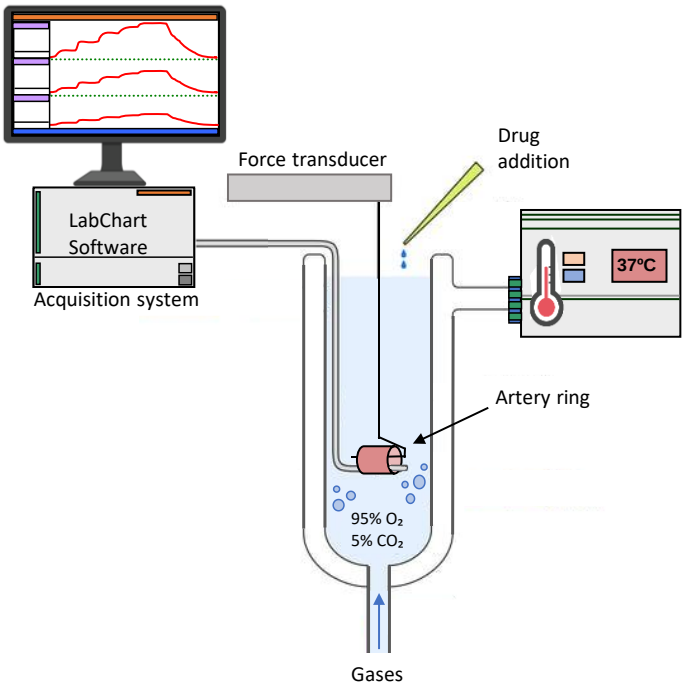

Figure 5. Organ bath scheme. Image of the equipment used for vascular reactivity assessment.

Each vascular segment was introduced into an organ bath containing 4 ml of physiological Krebs solution (NaCl 115 mM; KCl 4.6 mM; $MgCl_2 \cdot 6\ H_2O$ 1.2 mM; $CaCl_2$ 2.5 mM; $NaHCO_3$ 25 mM; glucose 11.1mM and EDTA disodium 0.01 mM) equilibrated with a gaseous mixture (95 % O_2 and 5 % CO_2) providing a pH between 7.3 - 7.4. A micrometre screw attached to the force transducer allows applying the appropriate passive tension to the vascular ring by pulling the pins apart. The temperature of the solution remained at 37 ºC during the experiment. Isometric tension changes were

recorded by a PowerLab 8/30 data acquisition system (AD Instruments) using LabChart 7 software.

Before analysing the response of the arterial rings to the different stimuli, a preliminary test was performed with rings of similar length and diameter to the experimental ones to determine the optimal basal tension for each type of artery. For this purpose, potassium chloride (KCl)-induced contraction (60 mM) was recorded after exposing the arterial rings to various basal tensions (1, 2, 3, and 4 g). The passive tension at which the highest contractile response to KCl was obtained was considered the optimal basal tension, which was 3 g for the rabbit aorta and 1 g for the renal artery.

Rat renal arteries were mounted on a wire myograph (620M DMT-Danis Myo Technologies) (see Figure 6), a technique that enables us to work with vessels of a calibre between 60 µm and 10 mm internal diameter. The arteries were cut into rings of 2 mm in length, and two wires of 40 µm diameter were introduced, attached to each of the platforms of the myograph. One platform was fixed and connected to an isometric tension transducer that records the changes in tension produced; the other one was attached to a micrometre screw, allowing modification of vessel stretching. Both were immersed in 5 mL of Krebs solution at 37 ºC, with carbogen mixture maintaining the pH at around 7.35. The transducer was connected to a PowerLab 8/35 data acquisition system (AD Instruments), and changes in tension were recorded with LabChart 7 software.

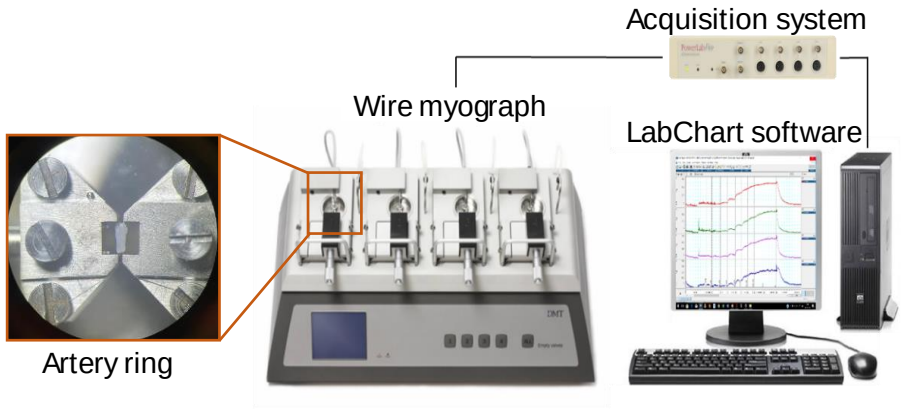

Figure 6. Wire myograph system. Image of the equipment used for vascular reactivity assessment and image of a renal artery mounted on a wire myograph.

The basal tension for each myograph-mounted ring was obtained through a normalization based on Laplace's Law, which was performed using MyoNORM software.

Before all experimental protocols, the functional integrity of the endothelium was tested by acetylcholine-induced relaxation (10^{-7} - 10^{-6} M) in rings previously contracted with noradrenaline (10^{-7} - $3x10^{-7}$ M). Rings that did not relax more than 40 % were not included in the study. The contractile capacity of vascular smooth muscle was tested by its response to KCl (60 mM).

3.1. Concentration-response curves

Concentration-response curves were constructed for phenylephrine (10^{-9} - $3x10^{-5}$ M), angiotensin II (10^{-11} - $3x10^{-7}$ M), acetylcholine (10^{-9} - 10^{-5} M),

and sodium nitroprusside (10^{-9} - $3x10^{-6}$ M). In the latter two cases, arteries were previously contracted with noradrenalin (10^{-7} - 10^{-6} M).

To evaluate the participation of T-type VGCCs, control curves were performed and incubated with nickel chloride ($5x10^{-5}$ M), a blocker of T-type VGCCs, specifically the $Ca_V3.2$ subtype (109). In addition, arteries were also incubated with L-NAME (10^{-4} M), a NOS inhibitor, and concentration-response curves were performed in the presence of L-NAME plus nickel chloride to study whether NO had a modulatory function on T-type VGCCs.

The curves performed in the presence of nickel chloride and L-NAME were performed after an incubation period with these drugs of 30 minutes.

4. Study of protein expression

For the study of protein expression, we performed the Western blot technique, which allows us to separate proteins based on the molecular weight and identify them with specific antibodies.

4.1. Incubation of samples

Rabbit aortic and renal segments, about 5 mm in length, were incubated in the organ baths for 30 minutes in the absence (control) and presence of nickel chloride ($5x10^{-5}$ M). Then, samples were snap-frozen in liquid nitrogen and stored at -80º C until further processing.

4.2. Sample processing

The arterial tissue (50 mg of rabbit arteries) was immersed in a 1.5 mL microtube with lysis buffer (0.125 M Tris-HCl, pH 6.8, 2 % SDS, 19 % glycerol and 1 % (v/v) proteases inhibitor) and homogenised by mechanical friction with sterile pistils. The homogenates were kept at -20 °C overnight and centrifuged the following day at 10,000 rpm for 20 minutes at 4 °C. Then, supernatant was collected, and protein concentration was determined by the bicinchoninic acid method using a bovine serum albumin (BSA) standard curve.

4.3. Separation and transfer of proteins

For each assay, samples (40-60 µg) were diluted with 4x Laemmli Sample buffer (Bio-Rad, USA) in a 3:1 ratio. 10 % β-mercaptoethanol (Sigma-Aldrich, USA) was previously added to the 4X Laemmli Sample buffer. Samples were heated by boiling the mixture at 70 °C in a heating block for 10 minutes to ensure proper denaturation.

Proteins were separated by denaturing SDS-PAGE (sodium dodecyl sulphate-polyacrylamide gel electrophoresis). For this purpose, the samples were loaded on Stain-Free gels (Bio-Rad, USA), prepared with a polyacrylamide gradient of 4-15 % or 7.5 %, depending on the molecular weight of the target protein. A protein standard (Precision Plus Protein Dual Colour, Bio-Rad, USA) was used for molecular weight estimation on SDS-PAGE gels and western blots. Electrophoresis was performed in the Mini-PROTEAN® Tetra Cell system (Bio-Rad, USA), which contained migration

buffer (25 mM Tris, 192 mM glycine and 0.1 % SDS, pH 8.3), and a constant voltage of 140 V was applied for 50 minutes.

After electrophoresis, the separated proteins in the gel were transferred to a polyvinylidene difluoride (PVDF) membrane (Bio-Rad, USA) previously activated with methanol. A transfer buffer (25 mM Tris, 192 mM Glycine and 5 % Methanol) was used, and a constant voltage of 100 V was applied for 40 minutes to ensure the transfer proteins larger than 200 KDa, and 70 V for 30 minutes for those with lower molecular weight. Throughout the transfer process, the system was maintained at 4 ºC.

To perform the immunodetection, the membranes were incubated with a blocking buffer to prevent nonspecific binding, composed of 5 % BSA or skimmed milk in TBS-Tween20 (Tris-Cl 20 mM, NaCl 150 mM, Tween20 0.1 %, pH 7.5). Blocking was performed under gentle agitation for 1 hour at room temperature. After blocking, the membranes were incubated with the primary antibodies at the concentrations and conditions described in Table 2. The following day, the membranes were washed with TBS-Tween20 (three times for 5 minutes), blocked for 10 minutes with blocking solution, and incubated for 1 hour at room temperature with proper secondary antibodies diluted in blocking buffer: IRDye Donkey anti-rabbit 680RD (1:10,000, cat #925-680731, LI-COR) and Donkey anti-mouse 800WC (1:10,000, cat #925-32212, LI-COR).-Finally, the membranes were washed with TBS-Tween20 (three times for 5 minutes) to remove excess secondary antibodies. Proteins were imaged through an Amersham ImageQuant 800 Fluor scanner (GE Healthcare) incorporating 700- 800 nm infrared emission filters. Each membrane was simultaneously imaged for both 680RD and 800WC fluorophores, and fluorescence was quantified using ImageJ software

(National Institutes of Health, Bethesda, MD, USA). In this thesis, the target protein was normalised to the total protein using Stain-Free imaging technology, which utilises a polyacrylamide gel containing a proprietary trihalo compound to make proteins fluorescent directly in the gel, allowing immediate visualisation during electrophoresis and western blotting. Normalisation to total protein has less variability and a greater normalisation range (110).

Table 2. Primary antibodies used to detect each target protein.

Primary antibody	Reference	Company	Conditions
$Ca_V3.1$ anti-rabbit	PA599755	Invitrogen	1:250 in TBST- 5 % skimmed milk, 4 ºC, O/N.
$Ca_V3.2$ anti-mouse	MA5-45397	Invitrogen	1:250 in TBST- 5 % skimmed milk, 4 ºC, O/N.

O/N: Overnight; RTº: room temperature.

5. Immunohistochemistry

5.1. Immunostaining

For the localization of T-type VGCCs in endothelium, immunohistochemistry was used, whereby arterial segments were fixed and stained to detect the protein of interest. Arterial segments were fixed in 4 % paraformaldehyde for 1 hour at RTº. Subsequently, the paraformaldehyde was

removed, and the segments were washed with phosphate-buffered saline (PBS, P4417-50TAB, MERCK, Germany) three times for 5 minutes. Then, the segments were cut, obtaining 2 strips for each arterial segment. The strips were stored at 4 ºC in PBS in a 96-well plate until use.

Strips were then incubated in blocking buffer (BB) containing 1 % bovine serum albumin (A3059, Sigma), 0.05 % Tween20 (Sigma, P2287) and 0.5 % Triton X-100 (T8532, Sigma) diluted in PBS for 2 hours at room temperature. Then, they were incubated with the primary antibodies at concentrations and conditions described in Table 3. After incubation, the strips were washed with PBS and incubated with secondary antibodies at concentrations and conditions described in Table 3. In addition, Hoechst 33342 (1:1,000, H3570, Invitrogen) was added for staining of cell nuclei. After incubation, strips were washed with PBS (three times for 5 minutes) and kept in PBS until slide preparation.

Table 3. Primary and secondary antibodies used to detect each of the target proteins. Concentration and incubation conditions for each of them.

Target protein	Primary antibody	Secondary antibody
Cav3.1	$Ca_V3.1$ anti-rabbit PA599755 (Invitrogen), 1:200 in BB, 4ºC, 24 h.	AF-488 Goat anti-rabbit, A11008 (Invitrogen), 1:1,000 in BB, RTº, 2 h.
Cav3.2	$Ca_V3.2$ anti-mouse MA5-45397 (Invitrogen), 1:200 in BB, 4 ºC, 24 h.	AF-647 Goat anti-mouse, A21235 (Invitrogen), 1:1,000 in BB, RTº, 2 h.
eNOS	eNOS anti-mouse, ab76198 (Abcam), 1:200 in BB, 4 ºC, 24 h.	AF-647 Goat anti-mouse, A21235 (Invitrogen), 1:1,000 in BB, RTº, 2 h.

RTº: room temperature; BB: blocking buffer.

For mounting strips, a drop of mounting medium (SlowFade™ Glass Soft-set, S36917, Invitrogen) was placed in the centre of a slide (25 x 70 mm). The strip was dipped into the mounting medium and flattened with the help of forceps, leaving the endothelial monolayer on top of the strip. Finally, a coverslip (22 x 22 mm) was placed over the immersed sample by pressing gently, and the edges were sealed with nail polish. The slides were stored at 4 ºC until analysis under confocal microscopy.

5.2. Imaging of staining samples

Slides were excited at 405 nm, 488 nm and 683 nm, and the emitted fluorescence was acquired through an oil immersion objective (40×/1.30 objective; working distance 0.24 mm; Leica, Germany) using a line scanning confocal microscope (TCS-SP8 Leica, Germany). The images were captured using digital magnification at 2.5x and optical sectioning in 0.5 µm increments. This was accomplished using LAS X software (Leica, Germany), and reconstruction of the images was performed using ImageJ software.

6. Study of gene expression

6.1. Sample processing

Intrarenal arteries from both male and female WKY and SHR groups were used for gene expression experiments. After isolation and removal of renal tissue and perivascular fat with RNase-free surgical tools (treated with

RNaseZap®, Ambion), the arteries were immersed in microtubes containing 300 µL of Trizol solution to preserve the messenger RNA (mRNA) present in the tissues. They were then snap-frozen and stored at -80 ºC until use.

The total RNA extraction protocol followed the method described by Chomczynski and Sacchi (111). Vascular tissue was homogenised using sterile RNaseZap-treated pestles® for mechanical friction. After homogenisation, microtubes were centrifuged at 3,000 rpm for 5 minutes at 4 °C, and the supernatant was collected and placed in another sterile microtube. Then, chloroform was added (in a ratio of 200 µL chloroform: 1mL Trizol) and thoroughly mixed by gentle shaking. Centrifugation was repeated at 13,000 rpm for 15 minutes at 4 °C, to separate the mixture into a lower phenol-chloroform, an interphase and a colourless upper aqueous phase. The upper aqueous phase containing the RNA was transferred to a new sterile microtube.

To precipitate RNA, 150 µL of isopropanol and 2 µL of glycogen were added to each microtube, mixed by pipetting, and incubated overnight at -20 ºC. The following day, samples were centrifuged at 13,000 rpm for 15 minutes at 4 °C, the supernatant was discarded, and the pellet was washed with 300 µL of 75 % ethanol. Samples were briefly vortexed to separate the pellet from the microtube wall and centrifuged again at 13,000 rpm for 15 minutes at 4 ºC. Finally, the supernatant was removed, and the pellet was resuspended with PCR-grade water.

6.2. Total RNA quality

The quality of total RNA was evaluated by examining concentration and purity using the NanoDrop spectrophotometer. 1 µL of the sample was added to obtain its absorbance, from which the system automatically estimates the RNA concentration from the included data. The absorbance is measured at 260 nm, the wavelength that nucleic acids absorb most intensely. The amount of light absorbed is proportional to the amount of nucleic acids in the sample.

This technique provides information about the total RNA concentration of the sample as well as two ratios, 260/280 and 260/230. The 260/280 ratio reflects the RNA purity, with the recommended range being between 1.8 and 2.1. A lower ratio may indicate the presence of proteins or other contaminants that absorb at 280 nm. The 260/230 ratio serves as a secondary measure of nucleic acid purity. While nucleic acids are measured at 260 nm, contaminants introduced during isolation are measured at 230 nm. Ideally, the 260/230 ratio should fall between 2.0 and 2.2. A lower ratio may suggest the presence of contaminants that absorb at 230 nm, such as phenols.

6.3. Reverse transcription polymerase chain reaction (RT-PCR)

The first step for RT-PCR was the acquisition of complementary DNA (cDNA) from total RNA in a reverse transcription process that requires the use of specific DNA polymerases. We used the "High-Capacity cDNA Reverse Transcription Kit" manufactured by Thermo Fisher Scientific, following the reverse transcription method. The amplification and detection

of the PCR product was performed in a Bio-Rad T100 Thermal Cycler™. The reaction was carried out under the following conditions:

1. 10 minutes at 25 ºC
2. 120 minutes at 37 ºC
3. 10 minutes at 85 ºC
4. ∞ at 4 ºC

The synthesised cDNA was stored at -20 °C.

Once the cDNA was generated, specific DNA sequences were selectively amplified by real-time polymerase chain reaction (RT-PCR) using TaqMan® Gene Expression Assays probes (Applied Biosystems®, Foster City, CA) according to the manufacturer's recommendations.

Predesigned TaqMan gene expression assays from ThermoFisher Scientific were used for the quantification of selected target genes: *$Ca_V3.1$, $Ca_V3.2$*, and *Nos3* (Rn01299126_m1, Rn01460348_m1, and Rn07312037_g1, respectively) and endogenous housekeeping gene glyceraldehyde-3-phosphate dehydrogenase (*Gapdh*) (Rn01775763_g1). RT-PCR was carried out using the High Capacity cDNA Reverse Transcription Kit (ref. 4368814, Applied Biosystems) and the QuantStudio 5 Real-Time PCR System (Thermo Fisher Scientific) with the following conditions:

1. 2 minutes at 50 ºC
2. 2 minutes at 95 ºC
3. PCR (x 40):
    a. 1 second at 95 ºC
    b. 20 seconds at 60 ºC

Samples were run in triplicate, and fold changes were generated for each sample by calculating $2^{-\Delta\Delta Ct}$ (112).

Relative expression: $2^{-\Delta\Delta Ct}$

ΔΔCt: [Ct of X studied gene -Ct *Gapdh*] - [Ct X control -Ct *Gapdh*], in our case X is *Ca_V3.1, Ca_V3.2*, and *Nos3.*

Ct comparison equation was applied to calculate the gene expression difference between male and female WKY and SHR groups. The control group (male WKY rats) takes the value of $2^{-\Delta\Delta Ct}$ as 1.

7. Measurement of ROS production in leukocyte population by flow cytometry

Cytometry is a multiparametric cell analysis method that allows the measurement of certain physical and chemical characteristics of cells or particles suspended in a fluid. Our flow cytometry assays were conducted using the FACSAria III cytometer (BD Biosciences). The data acquisition on the cytometer was facilitated through the use of BD FACS Suite software, while the subsequent off-line data analysis was performed with FLOWJO V.10.1 software.

We used different fluorochromes to measure intracellular ROS levels in leukocytes, which can reflect cardiovascular oxidative stress.

The fluorochromes used in this thesis were:

1. DAF-FM Diacetate (4-amino-5-methylamino)-2',7'-difluorofluorescein diacetate) is a reagent used to detect and quantify low concentrations of NO. It does not fluoresce until it reacts with NO, forming a fluorescent benzotriazole, which gives this probe specificity for detecting NO levels in the cells under study (113,114).

2. DHR 123 (Dihydrorhodamine 1,2,3) is an uncharged, non-fluorescent ROS indicator, which can passively diffuse across membranes. There, it is oxidised to cationic rhodamine 1,2,3, emitting green fluorescence. It is activated by several reactive oxygen species, which include H_2O_2 and $ONOO^-$ (115,116).
3. O_2^- is specifically detected with DHE (dihydroethidium) also called hydroethidine (HE). This fluorescent probe shows blue fluorescence in the cytosol until it is selectively oxidised and hydroxylated by O_2^- to 2-OH-ethidium, emitting red fluorescence when it intercalates into the DNA of the cell nucleus (117).

During the cytometry experiments, blue (488 nm), violet (405 nm), and red (635 nm) lasers were used. DAF and DHR 123 fluorescence were collected on a 530/30 505LP filter and DHE fluorescence on a 700/54 665LP filter.

Whole blood was extracted from the rats by cannulation of the portal vein and introduced into a tube with EDTA. The tubes were transported to the

cytometry service of the Central Research Unit of the University of Valencia, where the experimental protocol was followed:

1. For each marker, as well as for its positive and negative controls, 50 µL of whole blood was separated into separate 12x75 mm cytometry tubes, which were treated with 2 µL of Brilliant Violet 421™ anti-rat CD45 conjugate (BD Biosciences) and incubated 15 minutes at RT and in the dark, with the aim of performing leukocyte labelling.

2. On the other hand, to obtain peripheral blood mononuclear cells (MNCs), the red blood cell (RBC) lysis separation method was employed using eBioscience™ 10x erythrocyte lysis buffer (Invitrogen, Thermo Fisher Scientific). This buffer was added to each of the tubes with the CD45-labeled blood in a total volume of 5 mL. Once the blood was lysed, 300 µL of it was added to each cytometry tube.

3. DAF-FM DA (1 µM), DHR 123 (100 µM), or DHE (2.5 µg/mL) diluted in DMSO was added to each tube. Samples were incubated at 37 °C for 30 minutes in the dark with the corresponding fluorochrome. For each experimental group, the mean ± SEM of four replicates was determined.

Before starting the experiments, the fluorochromes were tested using both positive and negative controls. Negative controls did not include any fluorochrome to eliminate the possibility of autofluorescence. For positive controls, tubes were pre-treated with inducers for 30 minutes. The inducers used were NOR-1 (16 µg/mL), a NO generator; tert-butyl hydroperoxide

(t-BHP) (100 µM), an H_2O_2 generator; and plumbagin (Pb) (2.4 µg/mL) to induce an increase in O_2^-.

The events acquired per sample were 10,500 cells as a stop condition, with a slow flow rate to avoid the occurrence of doublets.

8. Measurement of plasma levels of nitrates and nitrites

NO is synthesised in biological systems by the NOS enzyme complex, which acts on molecular oxygen, arginine, and NADPH to produce, in addition to NO, citrulline and $NADP^+$. The measurement of plasma nitrate and nitrite concentrations has been shown to reflect NO synthesis (118) (see Figure 7).

$$NO + O_2^- \longrightarrow ONO_2^- + H^+ \longrightarrow NO_3^- + H^+$$

$$2NO + O_2 \longrightarrow N_2O_4 + H_2O \longrightarrow NO_2^- + NO_3^-$$

$$NO + NO_2 \longrightarrow N_2O_3 + H_2O \longrightarrow 2NO_2^-$$

Figure 7. Nitrate and nitrite formation reactions.

To determine the concentration of nitrate and nitrite in rat plasma, we used a commercially available Nitrate/Nitrite Colourimetric Assay Kit (#780001, Cayman Chemical, USA). This kit offers a two-step method that ensures precise measurement of total nitrate and nitrite concentration in the sample. The first step is the conversion of the nitrate in the sample to nitrite by the addition of the enzyme nitrate reductase. In the second step, Griess reagent is

added to convert nitrites into a purple azo compound acting as a chromophore, whose absorbance is measured to determine the concentration (see Figure 8).

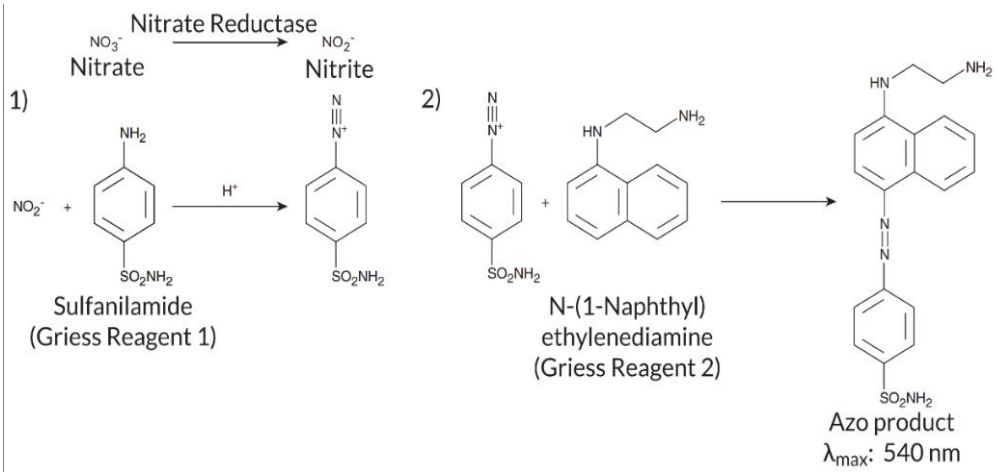

Figure 8. Colourimetric assay reaction resulting in the purple azo product that acts as a chromophore.

9. Statistics analysis

The results for blood pressure and levels of ROS in circulating leukocytes are presented as the mean ± standard error of the means (SEM). The results of flow cytometry experiments are expressed as fluorescent arbitrary units (f.a.u.). Protein expression results are normalised to total protein and expressed in absolute fluorescence units. The results for protein expression experiments and measurements of plasmatic nitrates and nitrites are presented as the mean ± standard deviation (SD).

For vascular reactivity experiments, the results are presented as the mean ± SEM. Vasodilation is expressed as a percentage of relaxation (%) relative

to noradrenaline-induced contraction. Vasoconstriction is expressed as a percentage of contraction (%) relative to the value of maximal contraction to KCl (60 mM) for each vascular segment. The pEC_{50} (-logarithm of the molar concentration at which half of the maximum effect occurs) was determined by nonlinear regression analysis from each concentration-response curve. The area under the curve (AUC) was calculated for each concentration-response curve to phenylephrine performed in the absence and presence of L-NAME, nickel chloride, and the combination of both, and expressed as arbitrary units (a.u.).

Statistical analyses were conducted using Microsoft Excel (version 2401) and GraphPad Prism 9.0.2 (GraphPad Software Inc.). For multiple comparisons between the different groups and experimental conditions *P* value was analysed by using one-way or two-way analysis of variance (ANOVA) or Student's *t*-test, where $P<0.05$ was considered statistically significant. Statistically significant differences were indicated in the graphs with asterisks by using * for $P<0.05$, ** for $P<0.01$, *** for $P<0.001$, and **** for $P<0.0001$.

RESULTS

1. Study of the physiological function of T-type VGCCs and their modulation by NO in healthy male rabbit vessels

1.1. Endothelial NO production in response to phenylephrine in the aorta and renal artery of healthy rabbits

Concentration-response curves to phenylephrine (10^{-9} - $3x10^{-5}$ M) in the absence and presence of L-NAME (10^{-4} M) were performed to evaluate NO production in response to α_1-adrenergic receptor stimulation in the aorta and renal artery. In both arteries, L-NAME potentiated contractile response to phenylephrine, increasing pEC_{50} and Emax (see Figure 9 and Table 4). These results indicated that endothelium modulates the contractile response to phenylephrine through NO release in the two vascular beds studied.

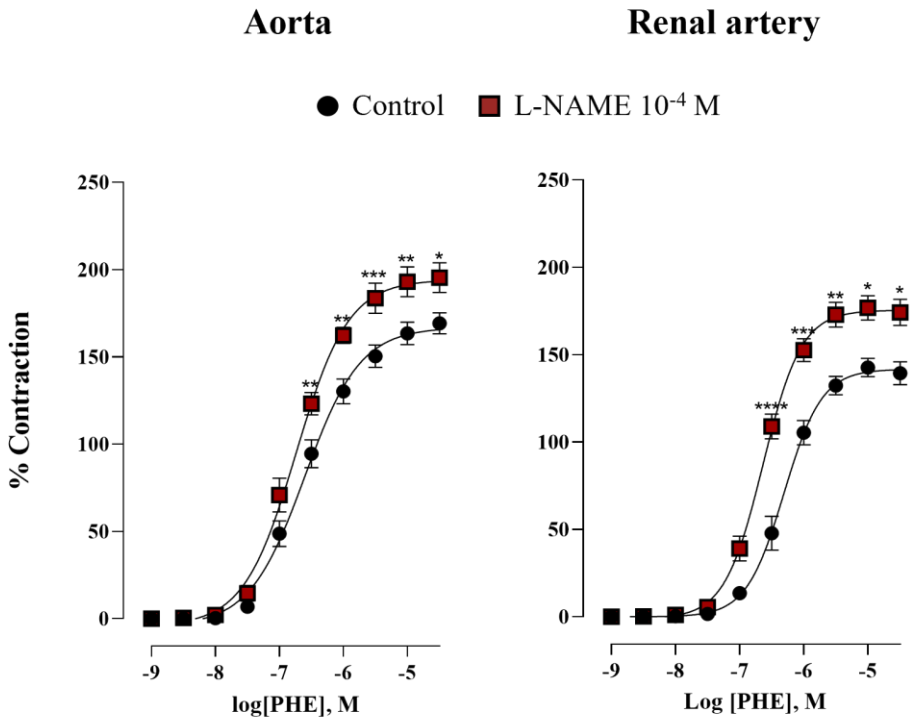

*Figure 9. Concentration-response curve to phenylephrine (PHE) in rabbit aorta and renal artery in the absence (control) and presence of L-NAME (10^{-4} M). n=9-12. *P<0.05; **P<0.01; ***P<0.001; ****P<0.0001 compared to control at the same concentration. Data are means ± SEM.*

Table 4. Values of pEC_{50} ± standard error of the means (SEM) and Emax ± SEM of concentration-response curves to phenylephrine in rabbit aorta and renal artery in the absence (control) and presence of L-NAME (10^{-4} M), nickel chloride ($NiCl_2$) ($5x10^{-5}$ M), or the combination of both.

Phenylephrine	**n**	**pEC_{50} ± SEM**	**Emax ± SEM**
Aorta			
Control	12	6.55 ± 0.08	162.25 ± 8.90
L-NAME 10^{-4} M	9	6.82 ± 0.09*	196.56 ± 9.13*
$NiCl_2$ $5x10^{-5}$ M	7	6.20 ± 0.07*	135.14 ± 7.20**
L-NAME 10^{-4} M + $NiCl_2$ $5x10^{-5}$ M	7	6.29 ± 0.13#	154.00 ± 5.37#
Renal artery			
Control	12	6.34 ± 0.08	145.08 ± 5.49
L-NAME 10^{-4} M	12	6.64 ± 0.06*	176.08 ± 7.59*
$NiCl_2$ $5x10^{-5}$ M	8	5.56 ± 0.14*	125.13 ± 15.04
L-NAME 10^{-4} M + $NiCl_2$ $5x10^{-5}$ M	7	5.40 ± 0.06#	96.71 ± 23.25#

*n= number of animals. *P<0.05; **P<0.01 compared to control. #P<0.05 compared to L-NAME 10^{-4} M.*

1.2. Involvement of T-type VGCCs in the contractile response to phenylephrine in the aorta and renal artery of healthy rabbits in the absence and presence of NO

In order to evaluate the involvement of T-type VGCCs, concentration-response curves to phenylephrine (10^{-9} - $3x10^{-5}$ M) were performed in the absence and presence of nickel chloride ($5x10^{-5}$ M), a T-type VGCCs blocker. Contractile response curves to phenylephrine were significantly right-shifted in the presence of this blocker, indicating that calcium influx through T-type VGCCs contributes to the contraction induced by phenylephrine in the two vascular beds studied (see Figures 10A and 11A and Table 4 in section 1.1).

In addition, to study whether NO modulates the activity of these channels, concentration-response curves to phenylephrine (10^{-9} - $3x10^{-5}$ M) were performed in the presence of L-NAME (10^{-4} M) and the combination of L-NAME plus nickel chloride ($5x10^{-5}$ M) (see Figures 10B and 11B, and Table 4 in section 1.1). To quantify this effect, i.e., whether nickel chloride-induced blockade was greater in the absence of NO, the area under the curve (AUC) was calculated from each individual concentration-response curve to phenylephrine. Then, the ΔAUC was determined by subtracting the AUC of the control phenylephrine curve from the phenylephrine curve incubated with nickel chloride (AUC 1). This value indicated the involvement of T-type VGCCs in the presence of NO. Next, the ΔAUC between phenylephrine curves in the presence of L-NAME and the additional presence of nickel chloride (AUC 2) was also calculated to indicate the involvement of T-type VGCCs in the absence of NO. The AUC 1 and AUC 2 values were then

compared and plotted as a bar graph to evaluate the participation of T-type VGCCs in each experimental condition (see Figures 10 and 11, and Table 5).

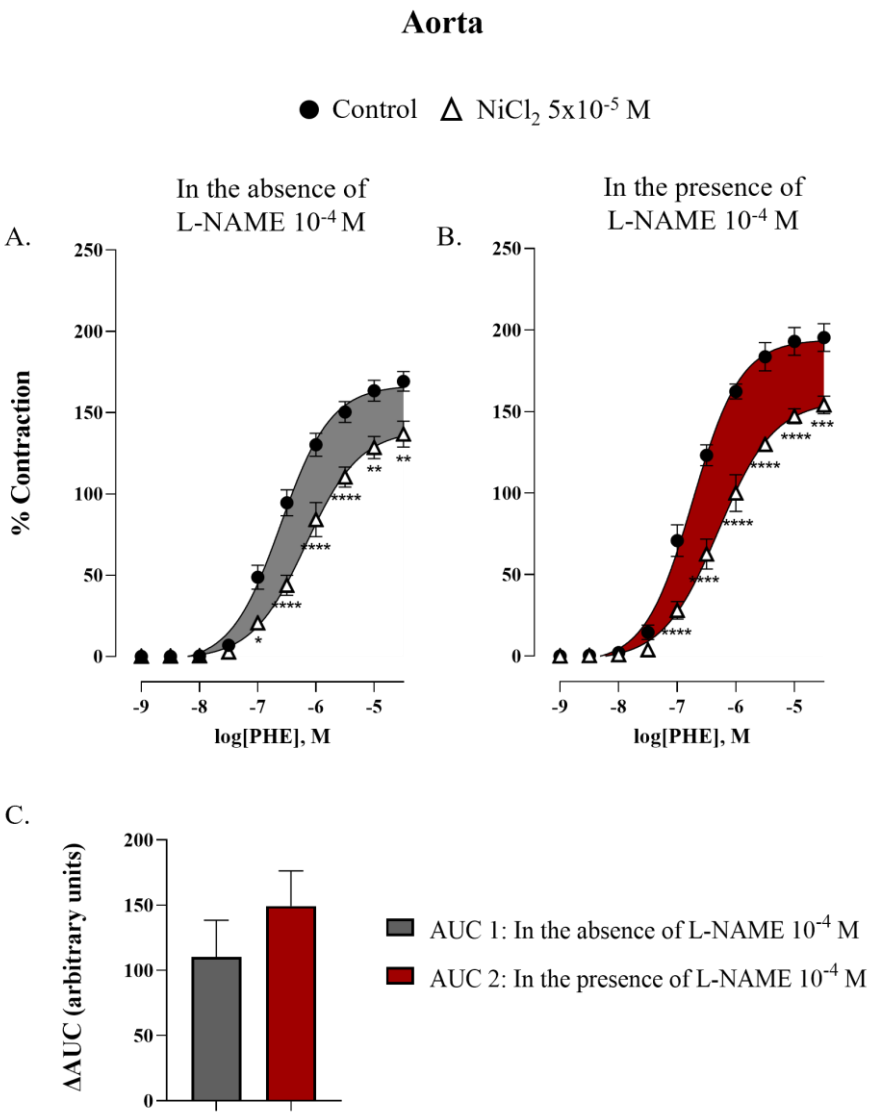

*Figure 10. Concentration-response curve to phenylephrine (PHE) in rabbit aorta in (A) absence (control) and presence of nickel chloride (5x10^{-5} M); (B) presence of L-NAME (10^{-4} M), absence (control) and presence of nickel chloride ($NiCl_2$) (5x10^{-5} M). (C) Participation of T-type VGCCs in the response to PHE in the absence and presence of L-NAME (10^{-4} M) represented as AUC 1 and AUC 2 respectively. n=7-12. *P<0.05; **P<0.01; ***P<0.001; ****P<0.0001 compared to control curve. Data are means ± SEM.*

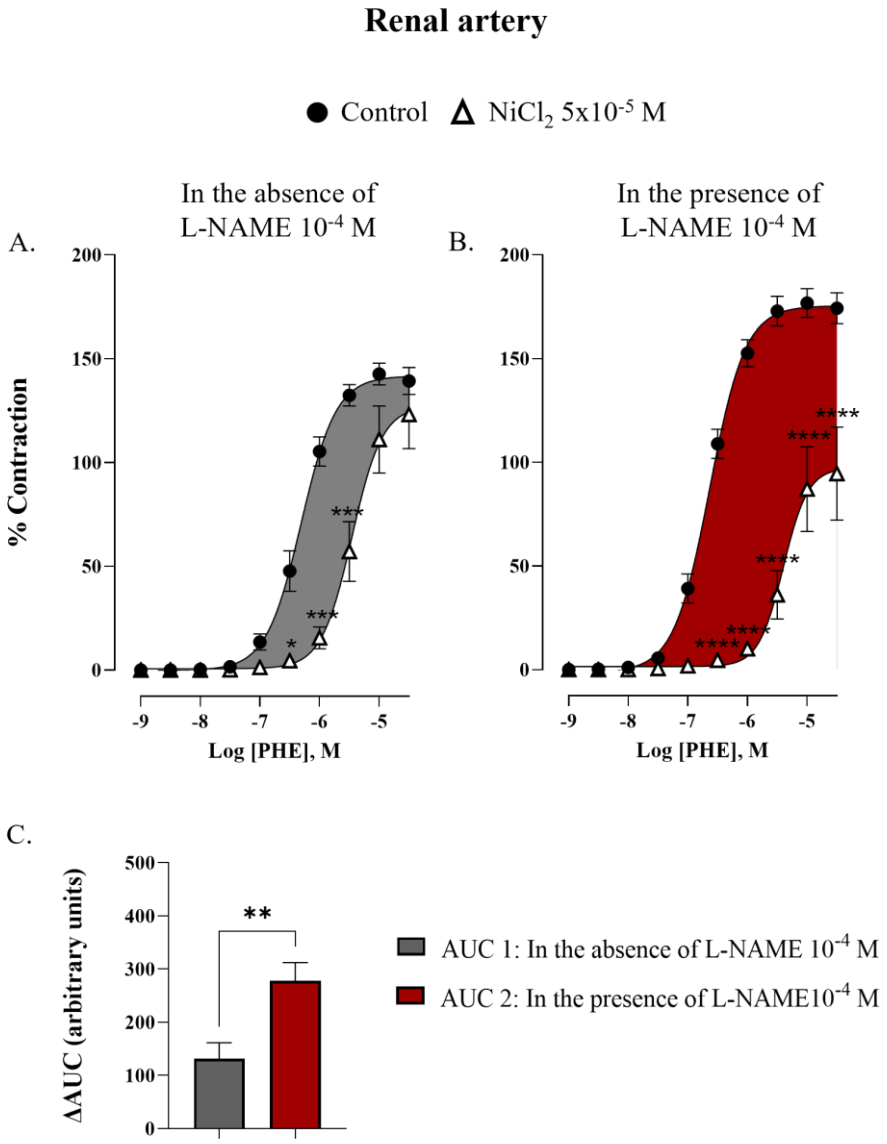

*Figure 11. Concentration-response curve to phenylephrine (PHE) in rabbit renal artery in (A) absence (control) and presence of nickel chloride ($5x10^{-5}$ M); (B) presence of L-NAME (10^{-4} M), absence (control) and presence of nickel chloride ($5x10^{-5}$ M). (C) Participation of T-type VGCCs in the response to PHE in the absence and presence of L-NAME (10^{-4} M) represented as AUC 1 and AUC 2 respectively. n=7-12. *P<0.05; **P<0.01; ***P<0.001; ****P<0.0001 compared to control curve. Data are means ± SEM.*

Table 5. Values of the area under the curve (AUC) ± standard error of the means (SEM) of concentration-response curves to phenylephrine in rabbit aorta and renal artery.

Phenylephrine	AUC ± SEM
Aorta	
AUC 1	110.20 ± 28.22
AUC 2	149.20 ± 27.02
Renal artery	
AUC 1	131.00 ± 30.56
AUC 2	278.3 ± 33.8*

*AUC 1: Difference between AUCs of phenylephrine control curve and phenylephrine curve with nickel chloride ($5x10^{-5}$M); AUC 2: difference between AUCs of phenylephrine curve with L-NAME (10^{-4} M) and phenylephrine curve with L-NAME (10^{-4} M) plus nickel chloride ($5x10^{-5}$ M). *P<0.05 compared to AUC 1.*

The results showed a slight non-significant increase in AUC 2 compared to AUC 1 in the aorta. However, in the renal artery, there was a significant increase in AUC 2 compared to AUC 1, indicating that in the absence of NO, the participation of T-type VGCCs increased.

1.3. Involvement of T-type VGCCs in the contractile response to angiotensin II in the aorta and renal artery of healthy rabbits

To evaluate the involvement of T-type VGCCs, concentration-response curves to angiotensin II (10^{-11} - $3x10^{-7}$ M) were performed in the absence and presence of nickel chloride ($5x10^{-5}$ M). Contractile response curves to angiotensin II were significantly right-shifted in the presence of this blocker, practically abolishing the contraction, indicating that calcium influx through T-type VGCCs contributes to the contraction induced by angiotensin II in both the aorta and the renal artery of healthy rabbits (see Figure 12).

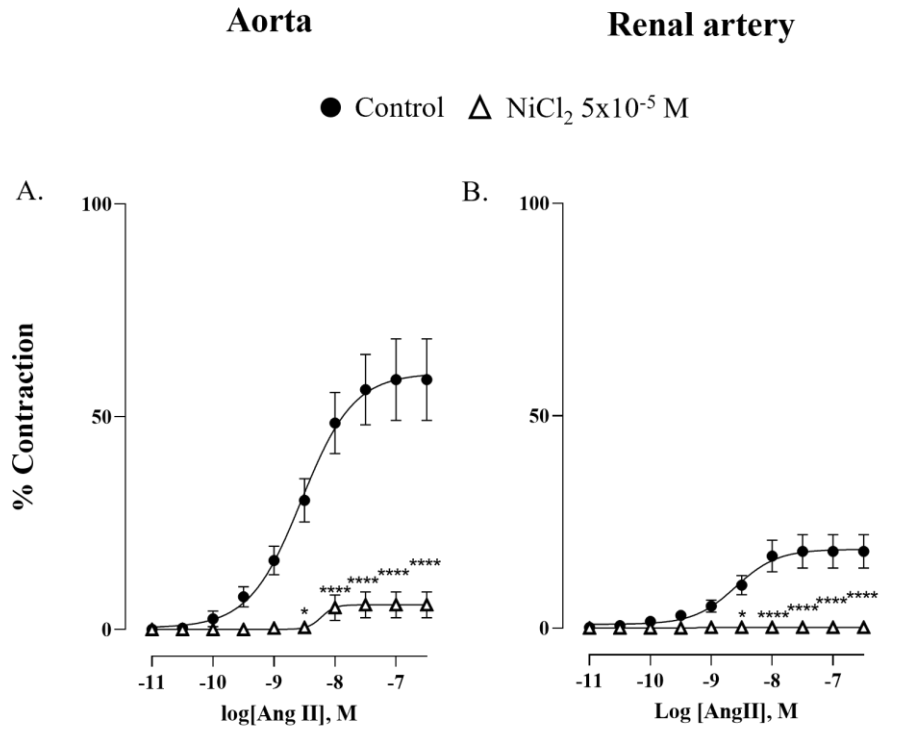

*Figure 12. Concentration-response curve to angiotensin II in rabbit aorta and renal artery in the absence (control) and presence of nickel chloride ($5x10^{-5}$ M). n=6-12. *P<0.05; ****P<0.0001 compared to control at the same concentration. Data are means ± SEM.*

1.4. Involvement of T-type VGCCs in the endothelium-dependent and independent relaxation in the aorta and renal artery of healthy rabbits

To study the involvement of T-type VGCCs in endothelium-dependent and -independent relaxation, concentration-response curves to acetylcholine (10^{-9} - $3x10^{-5}$ M) and sodium nitroprusside (10^{-11} - 10^{-5} M) were performed in the absence and presence of nickel chloride ($5x10^{-5}$ M), in arterial rings precontracted with noradrenaline (10^{-7} M).

Results in the aorta showed that the addition of nickel chloride did not affect the response to acetylcholine and sodium nitroprusside (see Figure 13). However, in the renal artery, nickel chloride attenuated the relaxant response to acetylcholine but not to sodium nitroprusside (see Figure 14), indicating that calcium influx through T-type VGCCs is probably required to activate eNOS and cause endothelium-dependent relaxation.

On the other hand, to test whether T-type-mediated relaxation follows the NO pathway, we performed concentration-response curves to acetylcholine (10^{-9} - $3x10^{-5}$ M) in the presence of L-NAME (10^{-4} M) to block NO synthesis. The results show that in the presence of L-NAME (10^{-4} M), the block of relaxation to acetylcholine is similar to that with nickel chloride ($5x10^{-5}$ M). Moreover, blocking the acetylcholine-dependent relaxation with L-NAME (10^{-4} M) plus nickel chloride ($5x10^{-5}$ M) yields the same blocking effect as with L-NAME (10^{-4} M) or with nickel chloride ($5x10^{-5}$ M) alone (see Figure 15), which may indicate that T type-mediated relaxation to acetylcholine may follow the same pathway as that mediated by NO.

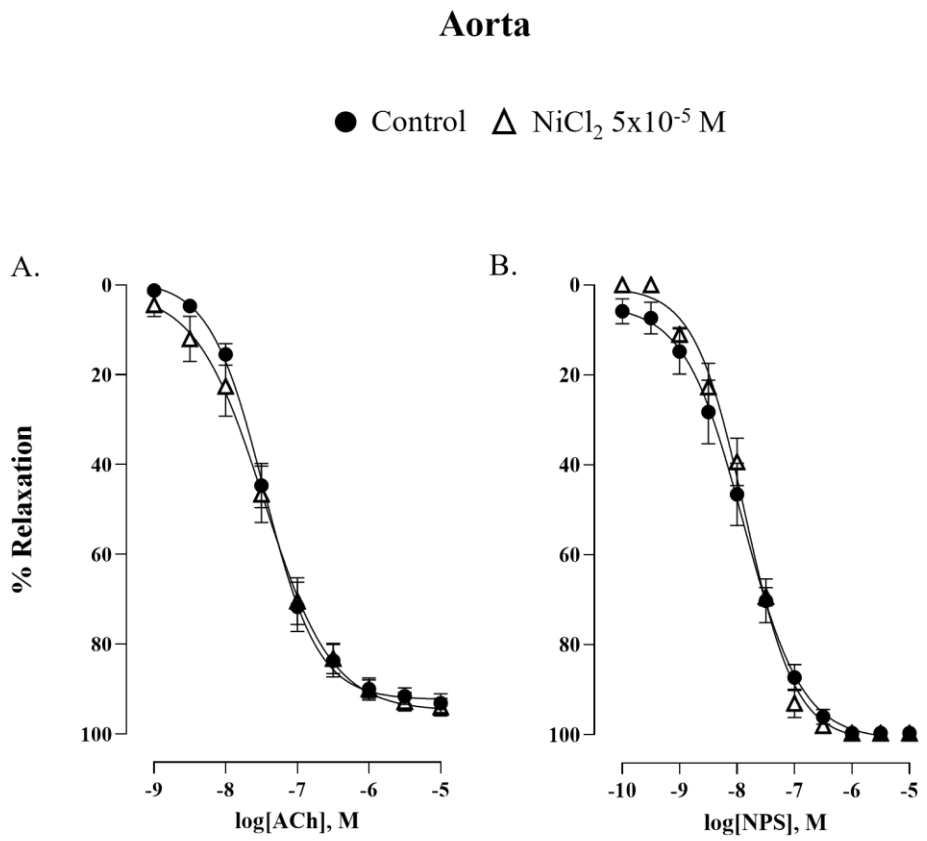

*Figure 13. Concentration-response curve (A) to acetylcholine (ACh) and (B) to sodium nitroprusside (NPS) in rabbit aorta in the absence (control) and presence of nickel chloride ($5x10^{-5}$ M). n=5-9. *P<0.05; **P<0.01; ***P<0.001; ****P<0.0001 compared to control at the same concentration Data are means ± SEM.*

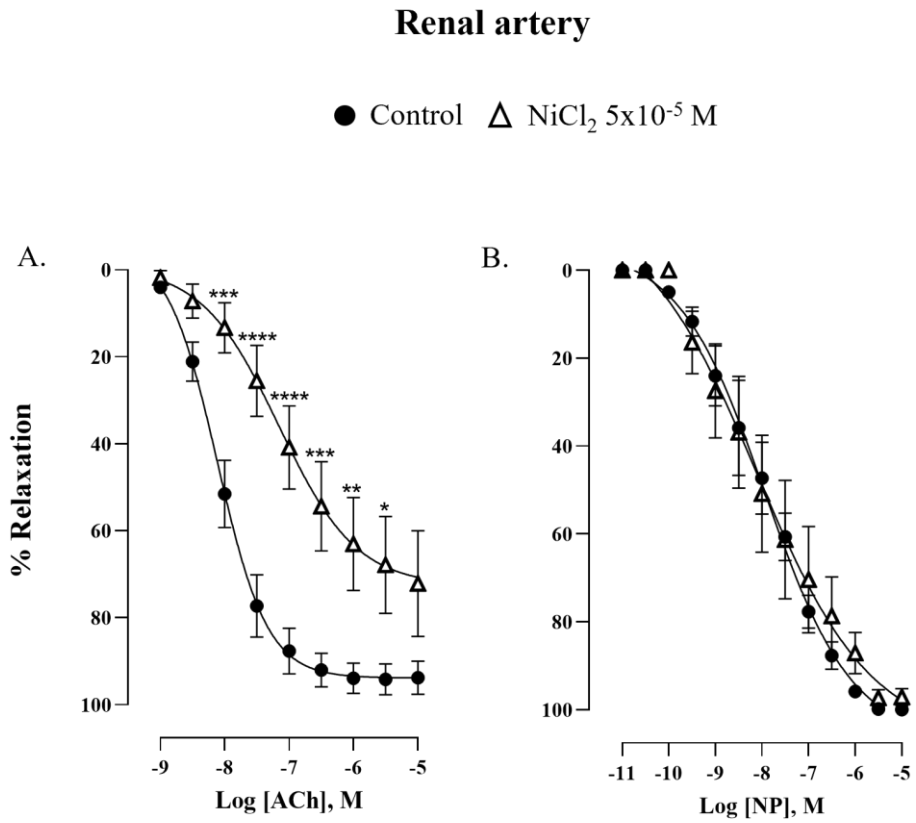

*Figure 14. Concentration-response curve (A) to acetylcholine (Ach) and (B) to sodium nitroprusside (NPS) in rabbit renal artery in the absence (control) and presence of nickel chloride ($5x10^{-5}$ M). n=5-8. *P<0.05; **P<0.01; ***P<0.001; ****P<0.0001 compared to control at the same concentration. Data are means ± SEM.*

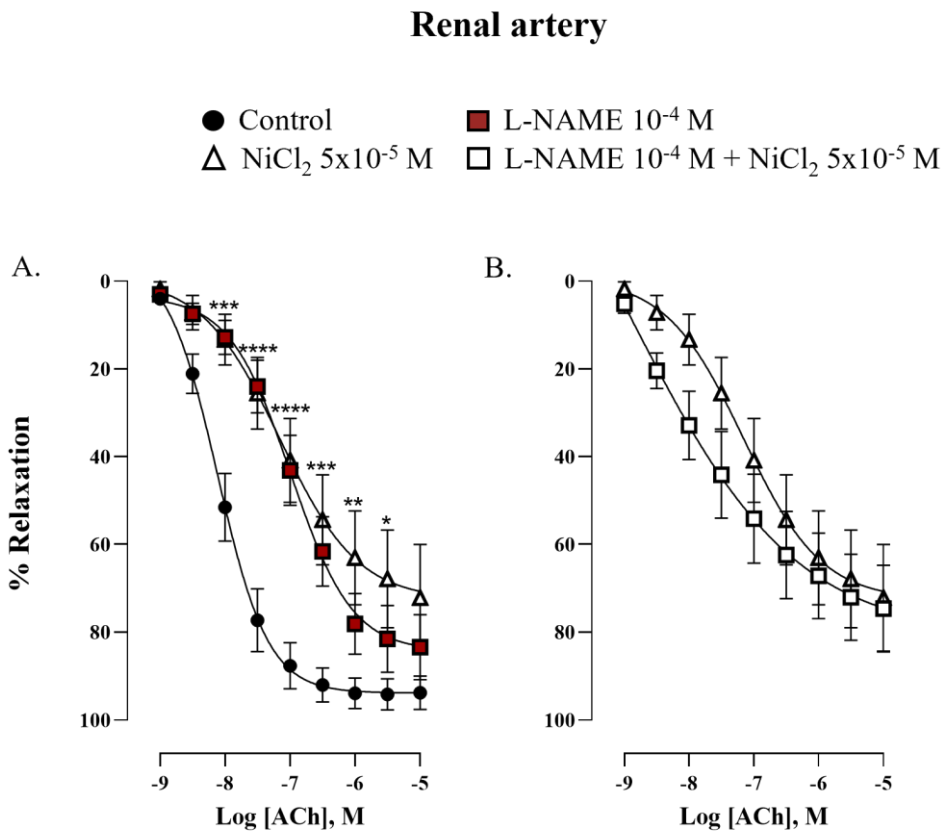

*Figure 15. Concentration-response curve to acetylcholine (Ach) in rabbit renal artery (A) in the absence (control) and presence of nickel chloride ($5x10^{-5}$ M) and L-NAME (10^{-4} M); (B) in the presence of nickel chloride ($5x10^{-5}$ M) and nickel chloride ($5x10^{-5}$ M) plus L-NAME (10^{-4} M). n=6-8. *P<0.05; **P<0.01; ***P<0.001; ****P<0.0001 compared to control at the same concentration. Data are means ± SEM.*

1.5. Protein expression of T-type VGCCs in the aorta and renal artery of healthy rabbits

We measured the protein expression of the two main subtypes of T-type VGCCs at the vasculature ($Ca_V3.1$ and $Ca_V3.2$) by Western Blot in the aorta and renal artery of rabbits. Our results showed no significant differences in the protein expression of both subtypes of T-type VGCCs between these vessels (see Figure 16).

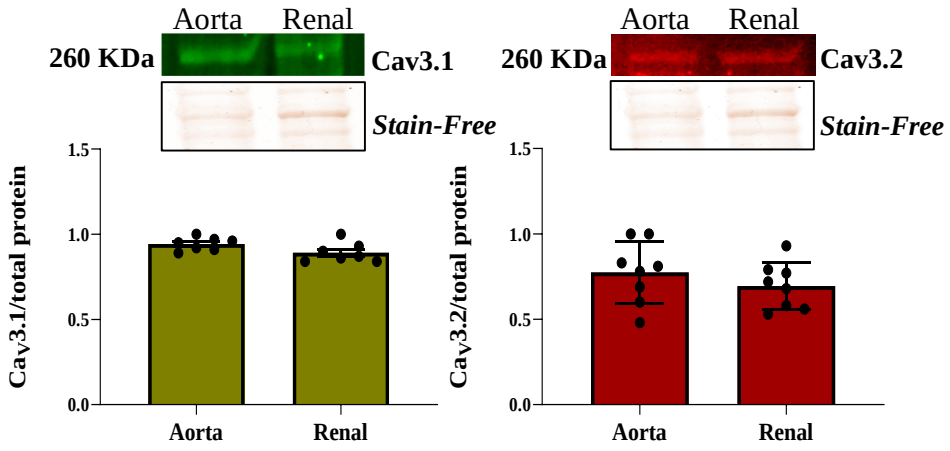

Figure 16. Protein expression of $Ca_V3.1$ and $Ca_V3.2$ in the aorta and renal artery of healthy rabbits. n=5-7 Results normalised to total protein and expressed in absolute fluorescence units.

1.6. Localisation of $Ca_V3.1$ and $Ca_V3.2$ in rabbit renal endothelial cells

In endothelium-dependent vasodilation experiments, it was observed that T-type VGCCs showed higher involvement in the renal artery compared to the aorta. Therefore, we aimed to use immunohistochemistry to demonstrate the localisation of T-type VGCC subtypes $Ca_V3.1$ and $Ca_V3.2$ in the endothelium of the renal artery. Additionally, we sought to establish whether either of these subtypes colocalised with eNOS.

Confocal laser-scanning microscopy showed clear and punctate expression of both subtypes in the cytoplasm of endothelial cells, with $Ca_V3.2$ also expressed in the nucleus (see Figure 17).

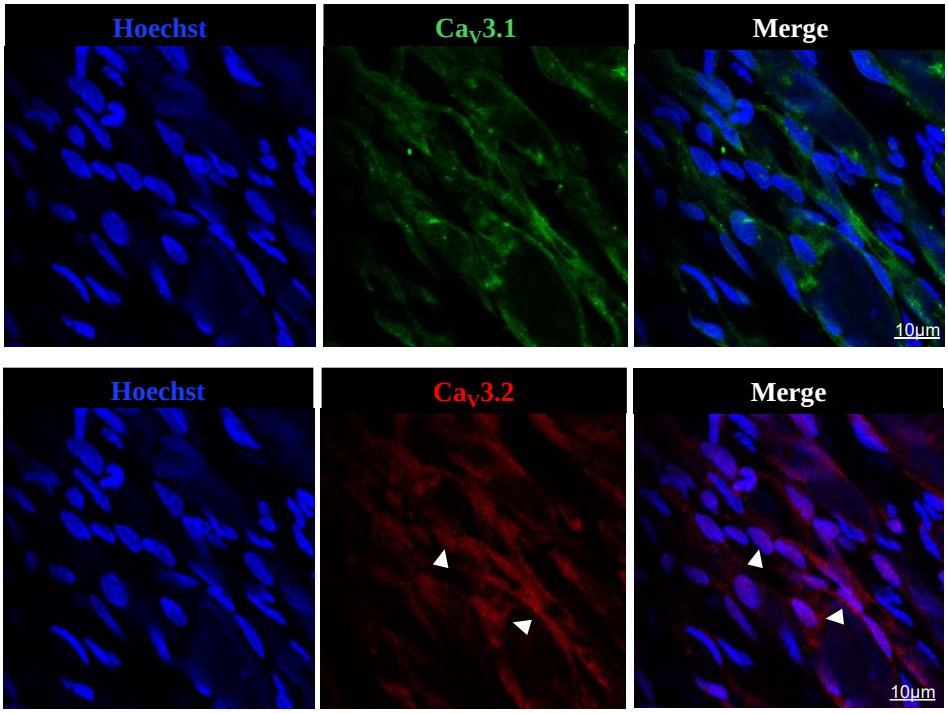

Figure 17: Representative confocal microscopy images of rabbit renal endothelial cells stained for $Ca_V3.1$ (green) and $Ca_V3.2$ (red). Nuclei was staining with Hoechst (blue). White arrows indicate expression of Cav3.2 in the cell nucleus. Images are representative of 3 independent experiments. Scale bar 10 µm.

Interestingly, co-localization of eNOS and $Ca_V3.1$ was confirmed in endothelial cells (see Figure 18). However, co-localization of eNOS and $Ca_V3.2$ was not observed (data not shown). This observation may reflect the physiological role of $Ca_V3.1$ in eNOS activation in the renal artery.

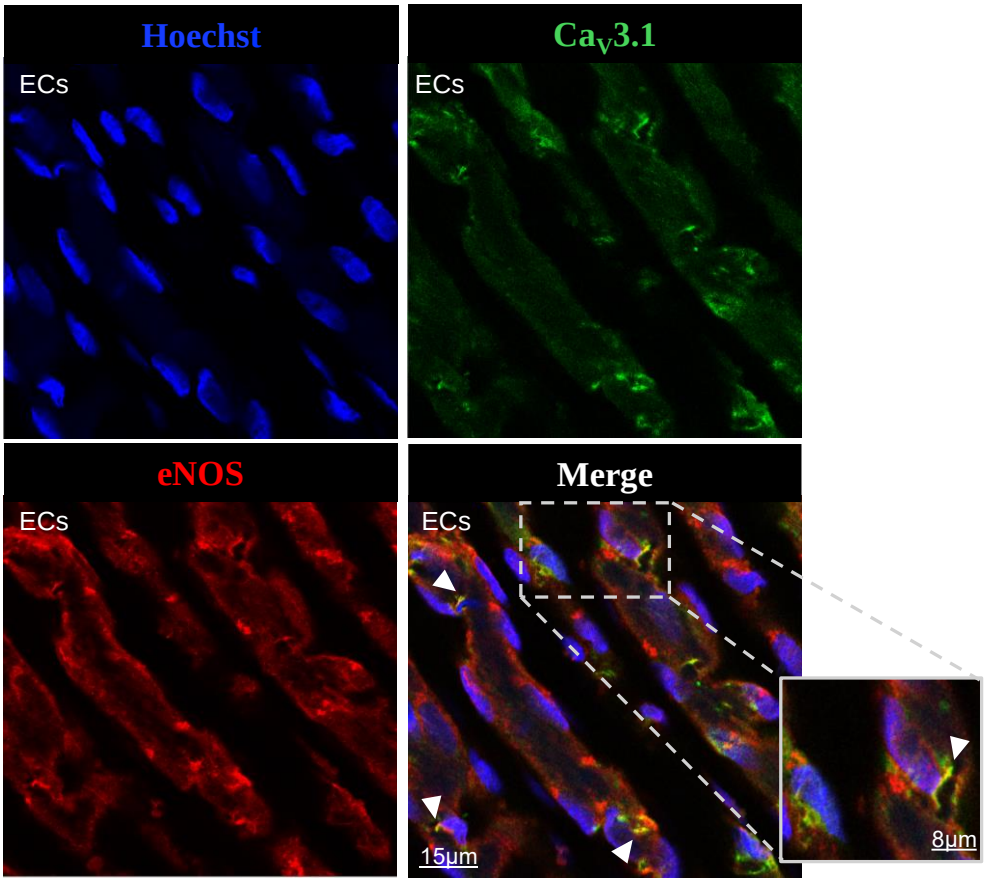

Figure 18. Representative confocal laser-scanning microscopy image *of rabbit renal endothelial cells stained for Cav3.1 (green) and eNOS (red). Nuclei were stained with* Hoechst *(blue). White arrows point to co-localization (yellow). Images are representative of 3 independent experiments. Scale bar 15 µm and 8 µm for zoom image.*

Based on the findings from healthy rabbit arteries, which highlighted the increased activity of T-type VGCCs and their possible modulation by NO in the renal artery, we decided to focus on this vascular bed and study the role of these channels in hypertension. Thus, we chose the SHR model and, as a control, the normotensive WKY rats. In addition, the sex variable was introduced, and therefore, the results are presented in both males and females.

2. Characterization of the SHR experimental model

2.1. Weight of animals and organs

Data on organ weights are expressed in relation to the body weight of the animal (see Table 6). No significant differences were found in the organ weights among the different study groups.

Table 6. Mean weight of animals (g) ± standard error of the means (SEM) and mean weight of organs relative to animal weight (%) ± SEM. n= 8 animals per group.

Group	Rat weight	Liver	Heart	Right kidney	Left kidney
Male WKY	316.625 ± 4.33	3.76 ± 0.17	0.44 ± 0.03	0.39 ± 0.01	0.39 ± 0.01
Male SHR	314.125 ± 4.34	4.02 ± 0.10	0.45 ± 0.01	0.38 ± 0.01	0.38 ± 0.01
Female WKY	207.25 ± 2.23	3.93 ± 0.53	0.52 ± 0.05	0.31 ± 0.04	0.37 ± 0.01
Female SHR	182.875 ± 1.09	4.82 ± 0.17*	0.56 ± 0.01	0.37 ± 0.01	0.38 ± 0.01

**P<0.05 compared to male SHR.*

2.2. Blood pressure

Both male and female SHR showed higher values of SBP, DBP, and MAP than WKY, with no significant differences in pulse pressure (see Figure 19).

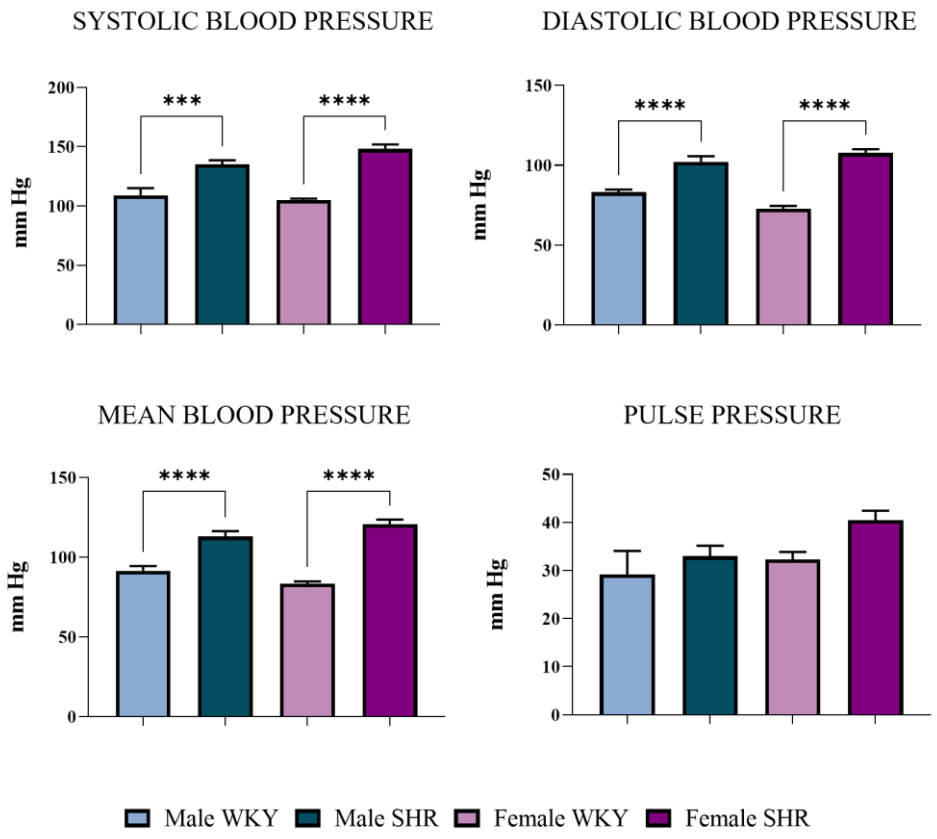

*Figure 19. Systolic, diastolic, mean and pulse pressure (mmHg) values of male and female WKY and SHR groups. n= 8 per group. Bars represent mean ± SEM. *P<0.05 compared to male WKY; ***P<0.001; ****P<0.0001 compared to WKY of the same sex.*

2.3. Oxidative stress in leukocytes

To test whether the vascular tissue of the SHR model might be more exposed to oxidative stress than that of WKY rats, we measured basal intracellular levels of ROS in circulating white blood cells (leukocytes, neutrophils, lymphocytes and monocytes) by flow cytometry.

DHR123 fluorochromes were used to quantify $ONOO^-$ and H_2O_2, DHE to quantify O_2^- production and DAF to quantify NO.

Our results indicated that in male SHR, there was an increased production of H_2O_2 and $ONOO^-$ in both leukocytes and neutrophils (see Figure 20). Together these results indicate that the vascular tissue of male SHR would be more exposed to oxidative stress than that of WKY and female SHR.

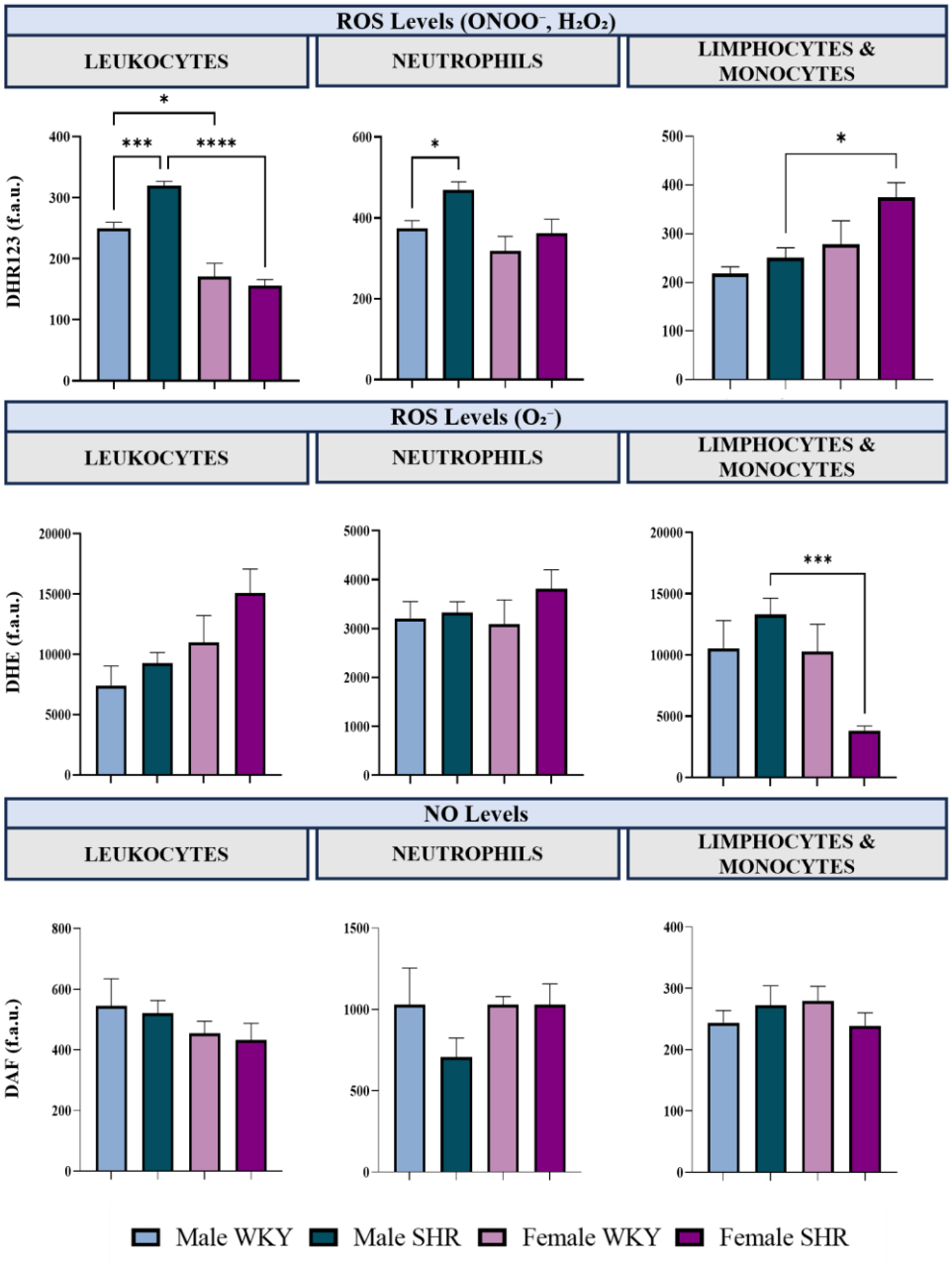

*Figure 20. Bar graphs summarising levels of H_2O_2, $ONOO^-$ and O_2^- as well as intracellular NO for white blood cells studied, measured by using the fluorescence markers DHR 123, DHE and DAF, respectively. n= 6-8 per group. Bars represent mean ± SEM. *P<0.05; ***P<0.005; ****P<0.001.*

2.4. Plasma levels of nitrates and nitrites

The results obtained in the quantification of nitrates and nitrites in rat plasma showed no significant differences between WKY and SHR groups (153.50 ± 11.50 for male WKY; 159.27 ± 37.78 for male SHR; 148.48 ± 30.22 for female WKY and 126.83 ± 9.36 for female SHR). These results indicate that hypertension did not alter plasma NO levels.

2.5. Vasodilation in the renal artery of WKY and SHR groups

To study endothelium-dependent and -independent relaxant capacity, concentration-response curves to acetylcholine (10^{-9} - 10^{-5} M) and sodium nitroprusside (10^{-9} - 10^{-5} M) were performed in renal artery segments precontracted with noradrenaline (10^{-7} M).

The results showed less relaxation to acetylcholine in the SHR model compared to WKY rats, both in females and males, with no change in nitroprusside-induced relaxation. These results indicate that the SHR model at 16 weeks of age exhibited endothelial dysfunction, whereas the capacity of smooth muscle to dilate was not affected (see Figures 21 and 22).

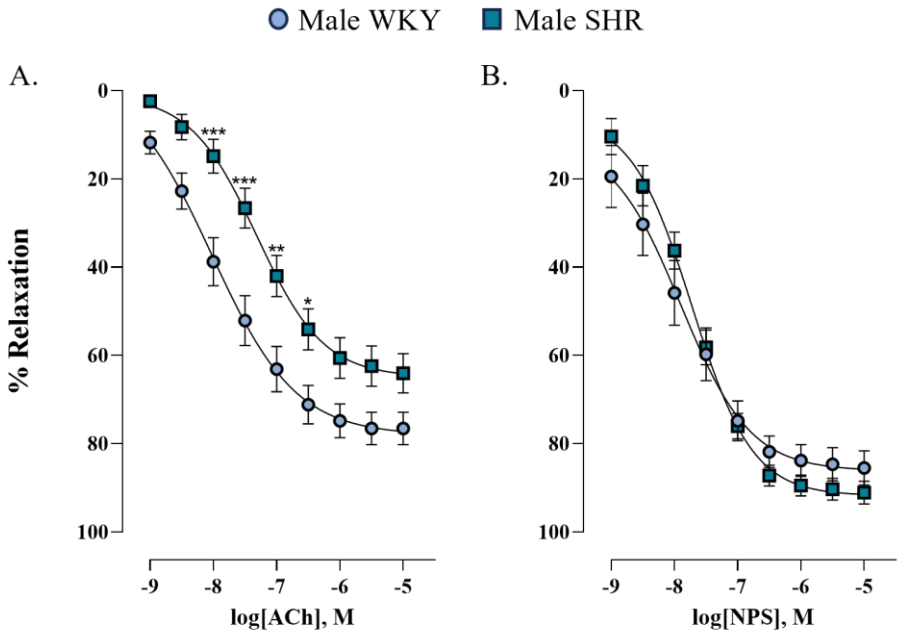

*Figure 21. Concentration-response curve (A) to acetylcholine (Ach) and (B) to sodium nitroprusside (NPS) in renal artery of male WKY and SHR groups. n=8. *P<0.05; **P<0.01; ***P<0.001 compared to male WKY. Data are shown as mean ± SEM.*

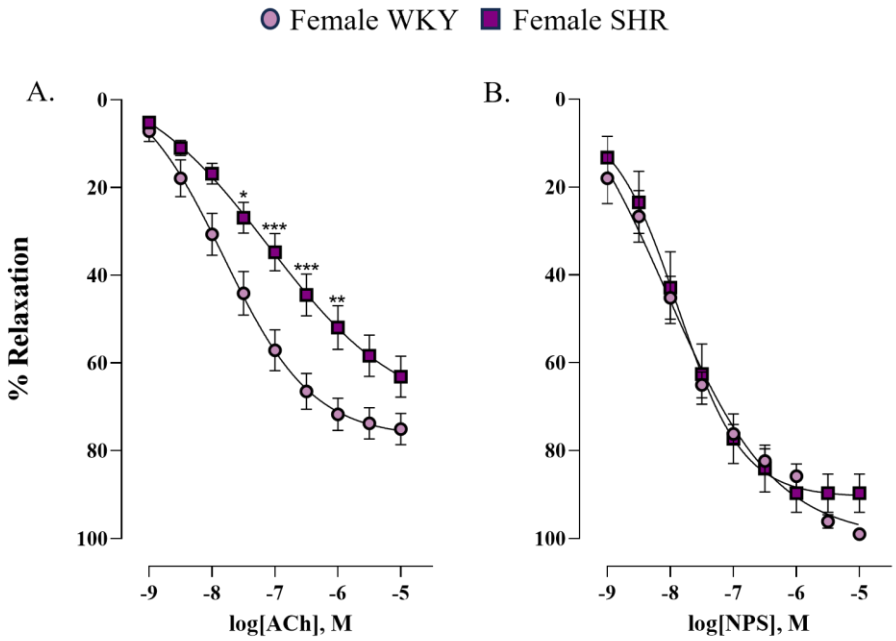

*Figure 22. Concentration-response curve (A) to acetylcholine Ach) and (B) to sodium nitroprusside (NPS) in renal artery of female WKY and SHR groups. n=8. *P<0.05; **P<0.01; ***P<0.001 compared to male WKY. Data are shown as mean ± SEM.*

2.6. Vascular smooth muscle contractile response in the renal artery of WKY and SHR groups

To study whether hypertension affected the contractile capacity of vascular smooth muscle, the response to KCl (60 mM), a nonspecific contractile agent that produces depolarisation of the muscle cell with consequent calcium influx and contraction, was measured. The results showed that hypertension did not affect this response (see Figure 23). In addition, female rats showed a lower response to KCl-induced contraction compared to male rats.

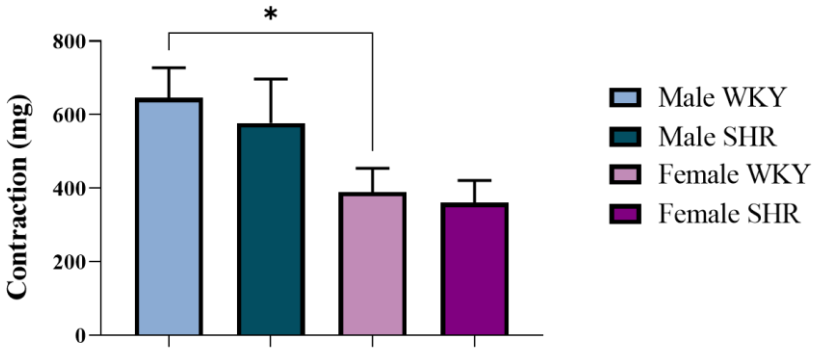

*Figure 23. Contraction (mg) induced by KCl (60 mM) in the renal artery of male and female WKY and SHR groups. n=8 per group. Data are shown as mean ± SEM. *P<0.05 compared to male WKY.*

2.7. Contractile response to phenylephrine in the renal artery of WKY and SHR groups

Concentration-response curves to phenylephrine (10^{-9}- $3x10^{-5}$ M) were performed to evaluate whether hypertension increases α_1-adrenergic contraction. The results showed a greater response in the SHR model compared with the WKY group, only in female rats, with no significant differences between WKY and SHR in males (see Figure 24).

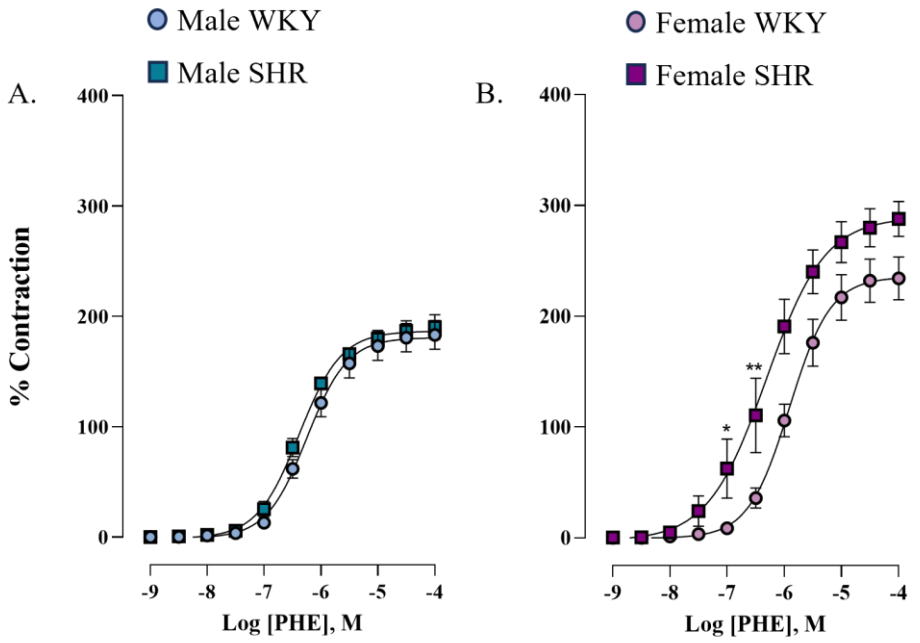

*Figure 24. Concentration-response curve to phenylephrine (PHE) in renal artery of (A) male and (B) female WKY and SHR. n=8. Data are shown as mean ± SEM. *P<0.05; **P<0.01 compared to female WKY.*

2.8. Endothelial NO release in response to phenylephrine in the renal artery of WKY and SHR groups.

Concentration-response curves to phenylephrine (10^{-9} - 10^{-4} M) in the absence and presence of L-NAME (10^{-4} M) were performed to evaluate NO release by α_1-adrenergic stimulation.

In male WKY, L-NAME potentiated only at 10^{-7} M, whereas, in female WKY, a significant left-shift in the contractile response to phenylephrine was found, indicating NO release in response to this agonist. In the SHR, this increase did not occur, indicating that the SHR model decreases NO production in response to phenylephrine (see Figure 25).

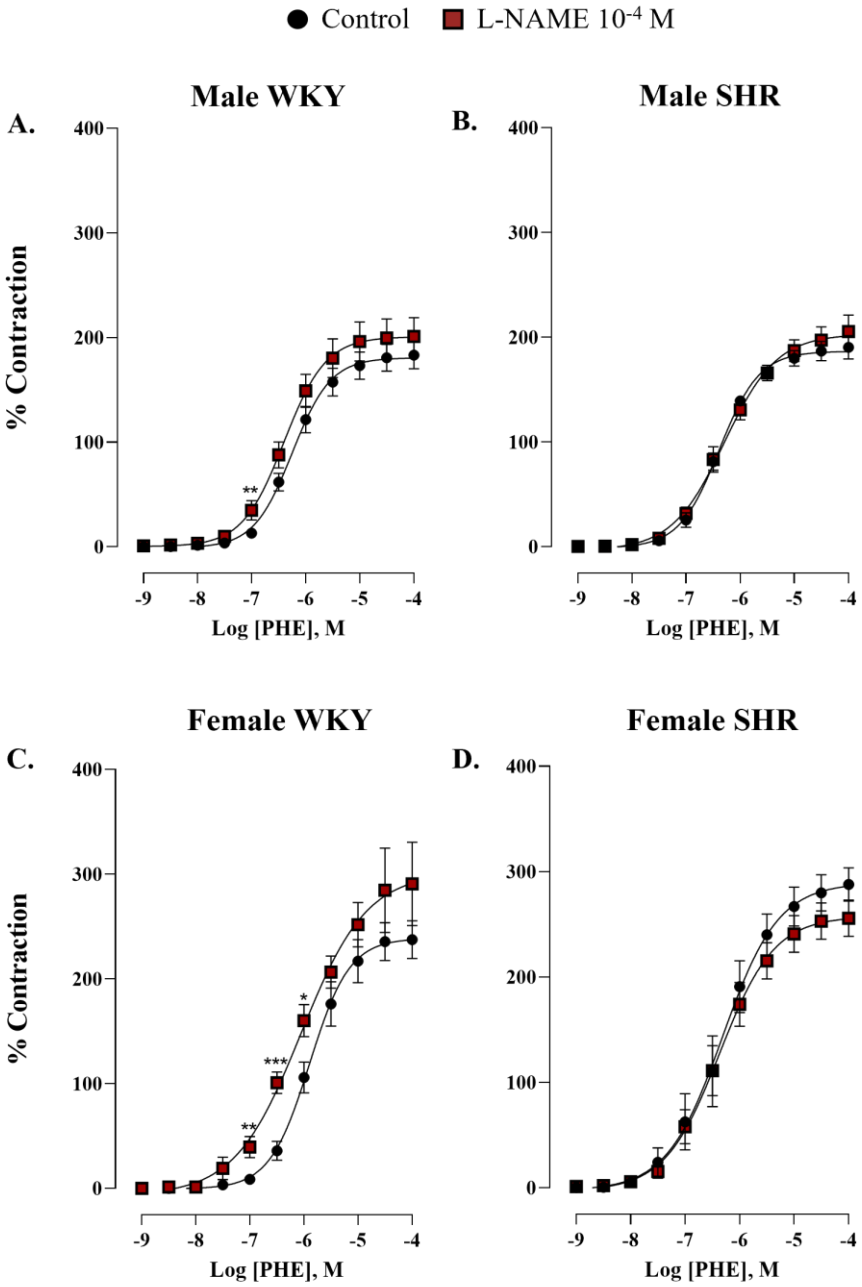

*Figure 25. Concentration-response curve to phenylephrine (PHE) in renal artery of male WKY and SHR (A and B respectively) and female WKY and SHR (C and D respectively) rats, in the absence (control) and in the presence of L-NAME (10^{-4}M). n=7-8. Data are shown as mean ± SEM. *P<0.05; **P<0.01; ***P<0.001 compared to the control curve.*

3. Study of the function of T-type VGCCs in a model of hypertension. Differences between sexes

3.1. Involvement of T-type VGCCs in phenylephrine-induced contraction in the renal artery of WKY and SHR groups

To study whether T-type VGCCs participated in phenylephrine-induced contraction in the rat renal artery, concentration-response curves to this agonist (10^{-9} - 10^{-4} M) were performed in the absence and presence of nickel chloride ($5x10^{-5}$ M) in arteries of WKY and SHR groups, both male and female.

Contractile response curves to phenylephrine were significantly right-shifted in the presence of this blocker, indicating that there is a calcium influx through T-type VGCCs contributing to contraction in response to phenylephrine in the rat renal artery of WKY and SHR in both sexes (See Figures 26 and 27, and Table 7).

In order to assess whether the involvement of these channels was greater in hypertension, the AUC from the phenylephrine control curve and phenylephrine with nickel chloride curve were calculated for both the WKY and SHR groups. AUC tended to be higher in male SHR than in male WKY (AUC = 285.1 ± 44.95 a.u. for WKY vs AUC = 371.70 ± 30.69 a.u. for the SHR, P=0.1142). Despite finding an increased, no significant differences were found, indicating that hypertension does not increase the participation of T-type VGCCs in male rats (Figure 26). However, in females, the results obtained showed a significant increase in the participation of T-type VGCCs

in hypertension (AUC = 314.10 ± 84.23 a.u. for WKY vs AUC = 556.70 ± 75.51 a.u. for the SHR, *P*=0.0336) (see Figure 27).

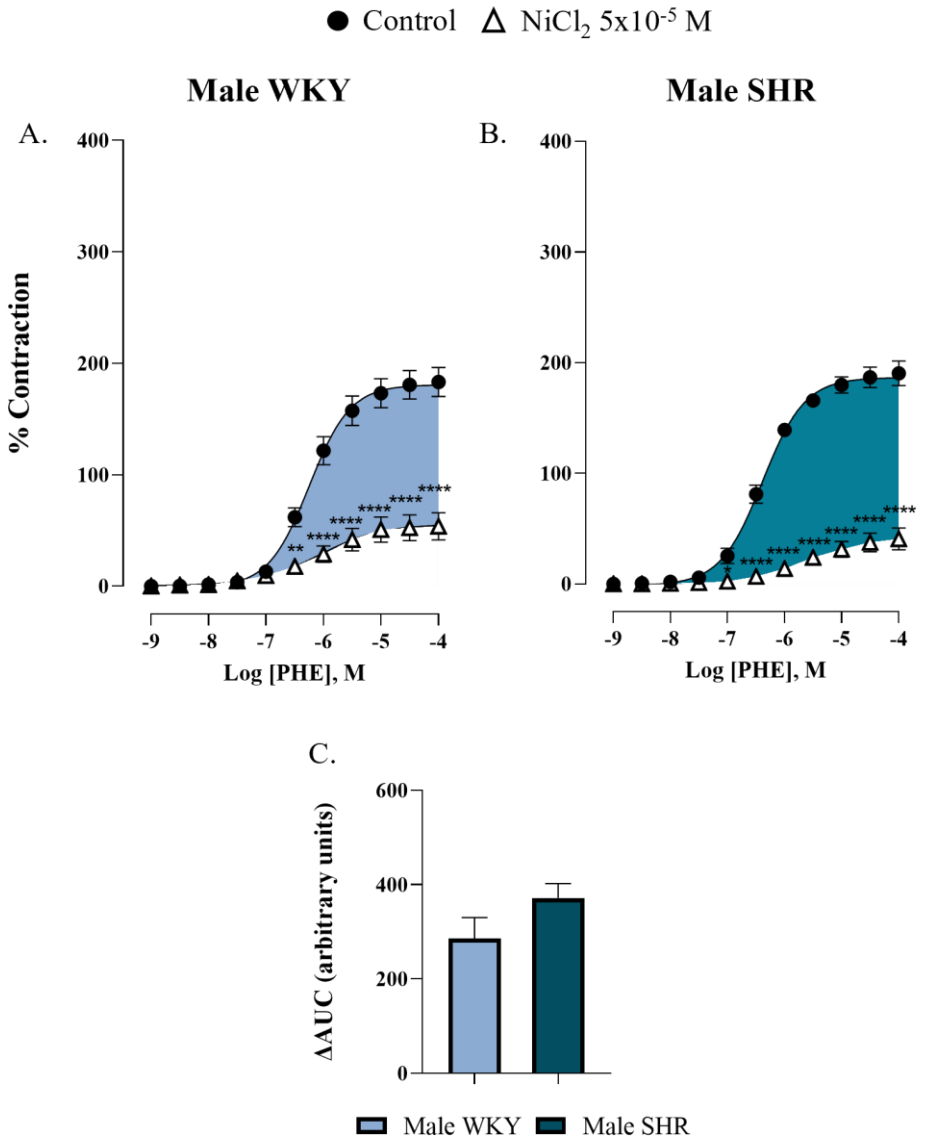

*Figure 26. Concentration-response curve to phenylephrine (PHE) in the renal artery of male (A) WKY and (B) SHR in the absence (control) and presence of nickel chloride ($5x10^{-5}$M). (C) The bar graph shows the ΔAUC from PHE curves indicating the involvement of T-type VGCCs in response to phenylephrine in male WKY and SHR groups. n=8. **P<0.01 ****P<0.0001 compared to the control curve.*

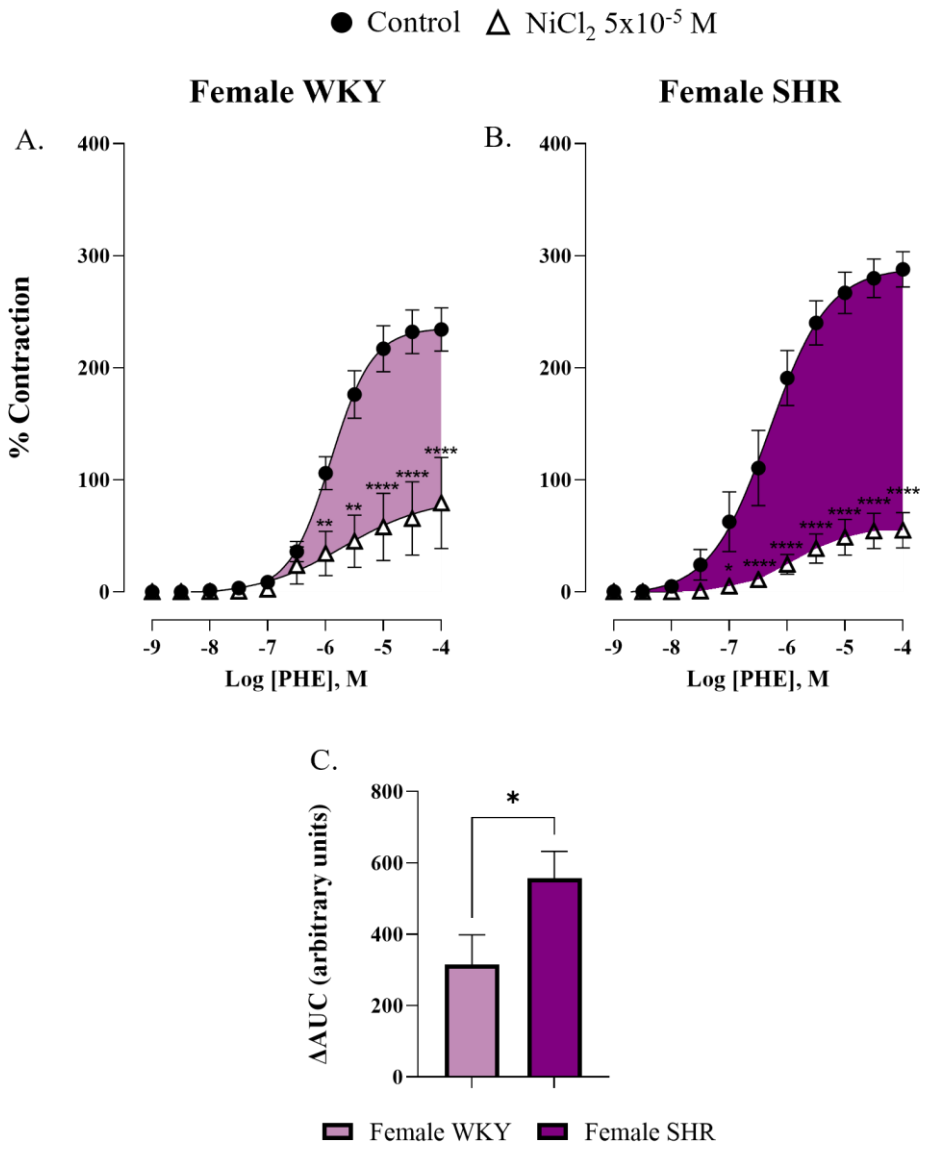

*Figure 27. Concentration-response curve to phenylephrine (PHE) in the renal artery of female (A) WKY and (B) SHR in the absence (control) and presence of nickel chloride ($5x10^{-5}$ M). (C) The bar graph shows the ΔAUC from PHE curves indicating the involvement of T-type VGCCs in response to phenylephrine in female WKY and SHR groups. n=7-8. *P<0.05; **P<0.01 ****P<0.0001 compared to the control curve.*

Table 7. Values of pEC_{50} ± standard error of the mean (SEM) and Emax ± SEM of concentration-response curves to phenylephrine in the renal artery of male and female WKY and SHR groups in the absence and presence of nickel chloride ($NiCl_2$) ($5x10^{-5}$ M).

Phenylephrine	n	pEC_{50} ± SEM	Emax ± SEM
Male WKY			
Control	8	6.34 ± 0.08	185.20 ± 14.50
$NiCl_2$ $5x10^{-5}$ M	8	6.02 ± 0.12*	65.90 ± 28.18*
Male SHR			
Control	8	6.43 ± 0.07	190.33 ± 11.03
$NiCl_2$ $5x10^{-5}$ M	8	5.73 ± 0.12*	45.02 ± 19.46*
Female WKY			
Control	8	5.84 ± 0.08	234.14 ± 19.34
$NiCl_2$ $5x10^{-5}$ M	8	5.91 ± 0.24	79.25 ± 40.70*
Female SHR			
Control	7	6.11 ± 0.15	278.29 ± 25.09
$NiCl_2$ $5x10^{-5}$ M	7	5.66 ± 0.17*	74.25 ± 16.15*

*n= number of animals. *P<0.05 compared to control of the same group.*

These results indicate that, as previously observed in the aorta and renal artery of healthy male rabbits, T-type VGCCs participate in α_1-adrenergic contractions in rat renal arteries of both sexes. Moreover, hypertension significantly increases the involvement of T-type VGCCs in response to phenylephrine only in females, probably because the decrease in NO release induced by hypertension was more intense in female than in male.

3.2. Involvement of T-type VGCCs in phenylephrine-induced contraction in the renal artery of WKY and SHR groups in the absence of NO.

Our results in healthy rabbit renal arteries showed that in the absence of NO, these channels became more active, increasing calcium influx for phenylephrine-induced contraction. To test whether this was reproduced in the rat renal artery and whether it was affected by sex or hypertension, concentration-response curves were performed for phenylephrine (10^{-9} - $3x10^{-5}$ M) in the presence of L-NAME (10^{-4} M) plus nickel chloride ($5x10^{-9}$ M). ΔAUCs were calculated as described above (see section 1.2). The values are shown in Figures 28, 29, 30 and 31, and in Table 8.

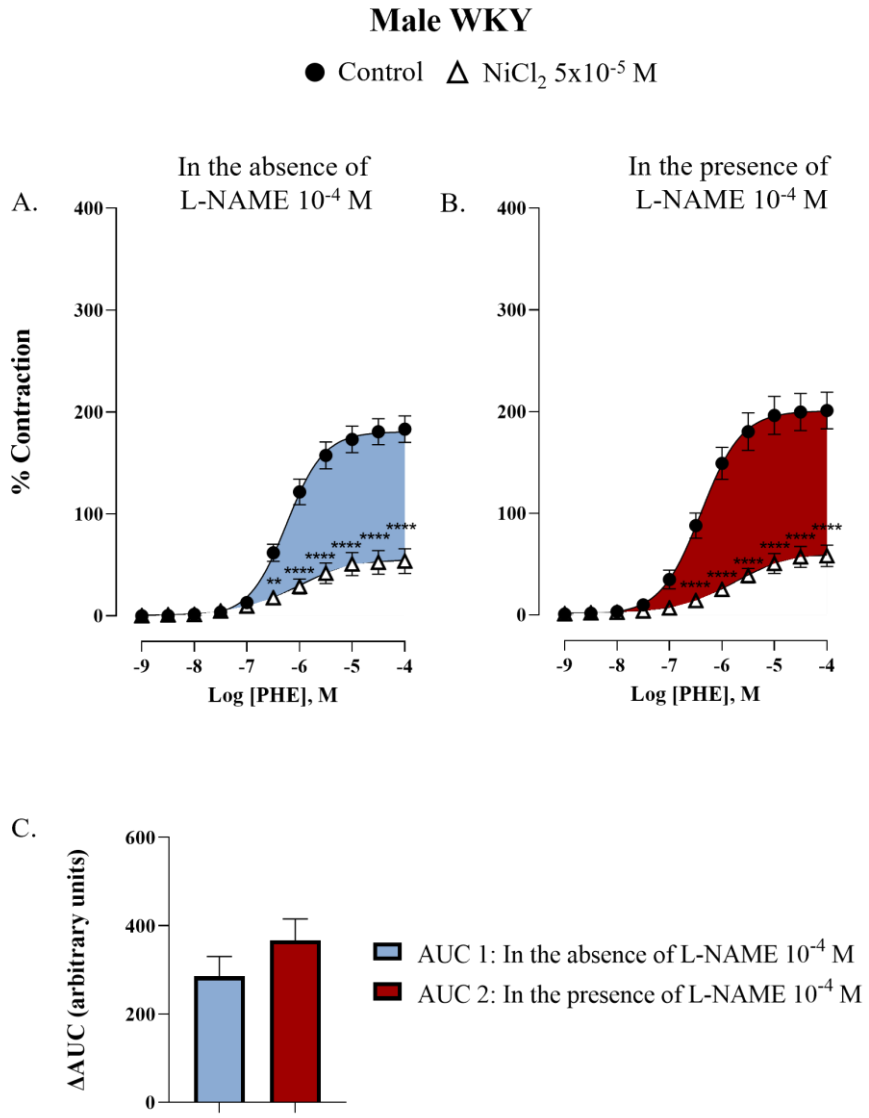

*Figure 28. Concentration-response curve to phenylephrine (PHE) in the renal artery of male WKY rat in (A) absence (control) and presence of nickel chloride ($5x10^{-5}$ M); (B) in presence of L-NAME (10^{-4} M), absence (control) and presence of nickel chloride ($5x10^{-5}$M). (C) Participation of T-type VGCCs in the response to PHE in the absence and presence of L-NAME (10^{-4} M) represented as bars. n=8. Data are shown as mean ± SEM. **P<0.01; ****P<0.0001 compared to control curve of the same group.*

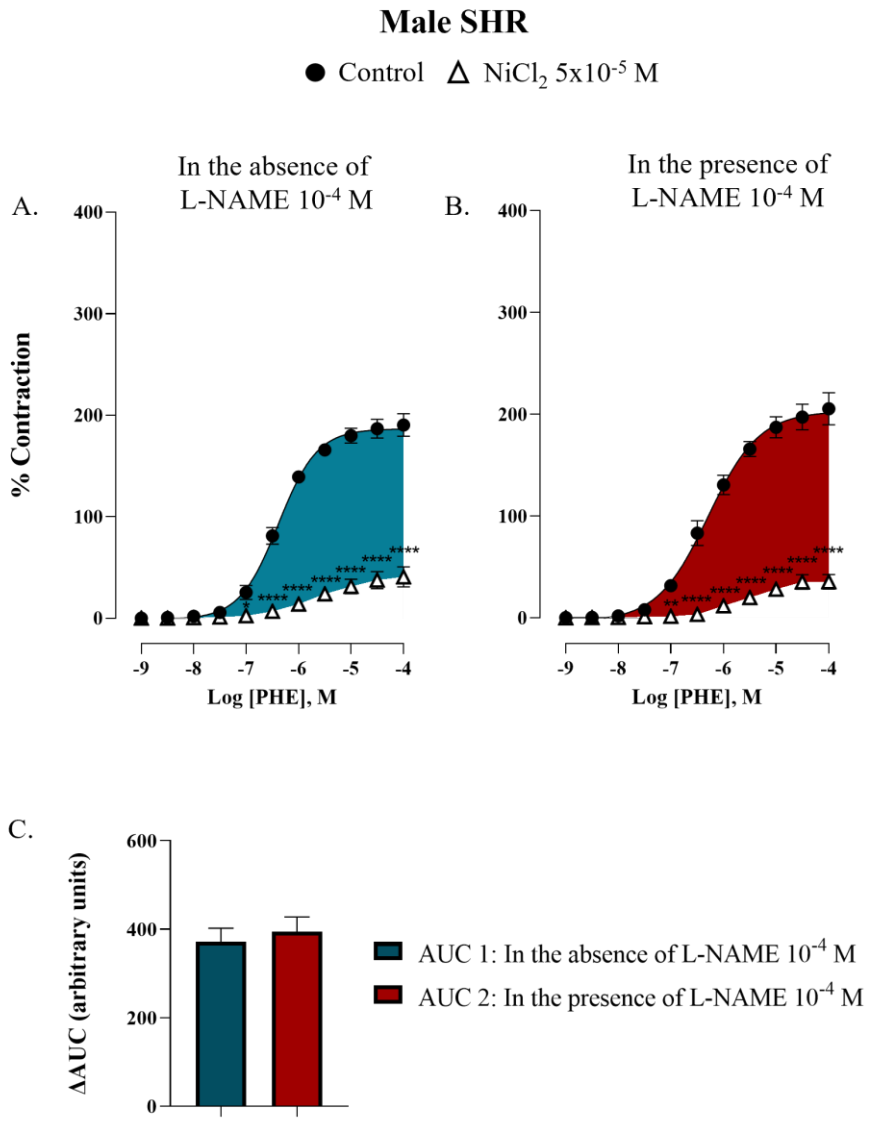

*Figure 29. Concentration-response curve to phenylephrine (PHE) in the renal artery of male SHR in (A) absence (control) and presence of nickel chloride ($5x10^{-5}$ M); (B) in the presence of L-NAME (10^{-4} M), absence (control) and presence of nickel chloride ($5x10^{-5}$M). (C) Participation of T-type VGCCs in the response to PHE in the absence and presence of L-NAME (10^{-4} M) represented as bars. n=8. Data are shown as mean ± SEM. **P<0.01; ****P<0.0001 compared to control curve of the same group.*

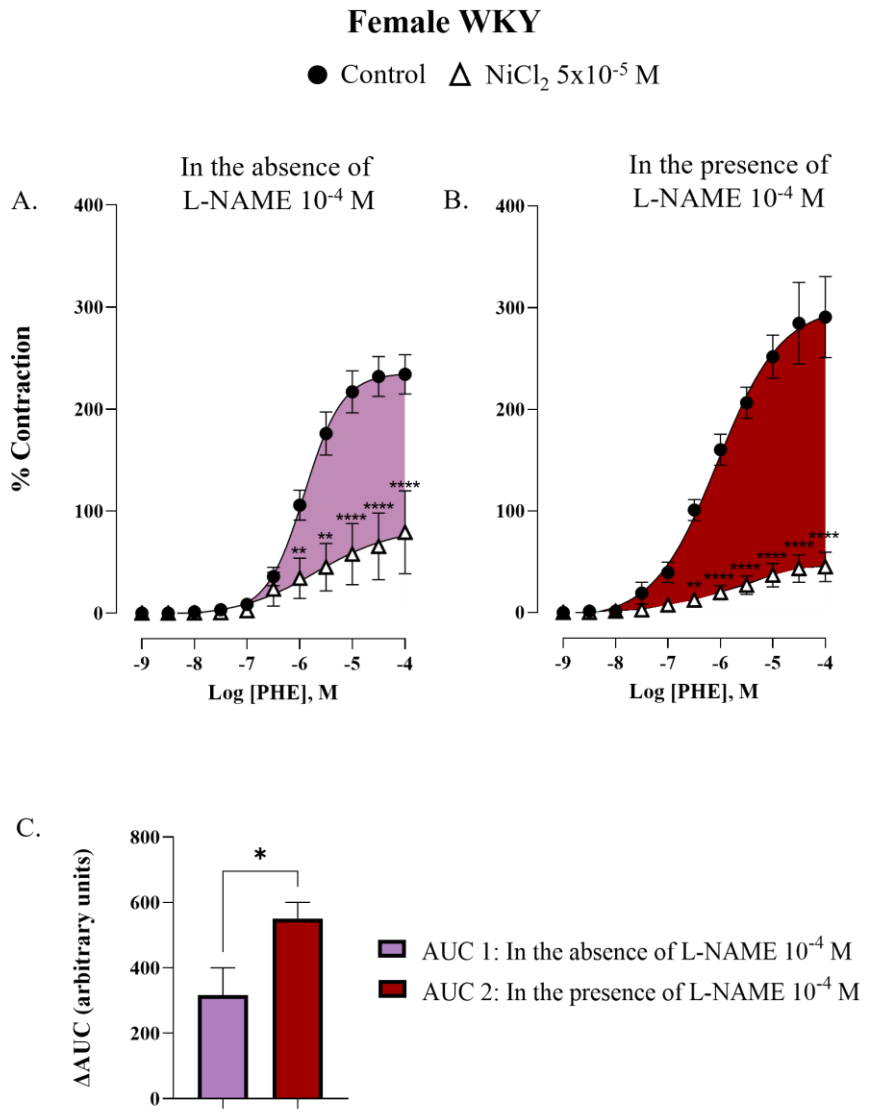

*Figure 30. Concentration-response curve to phenylephrine (PHE) in the renal artery of female WKY rat in (A) absence (control) and presence of nickel chloride ($5x10^{-5}$ M); (B) in the presence of L-NAME (10^{-4} M), absence (control) and presence of nickel chloride ($5x10^{-5}$ M). (C) Participation of T-type VGCCs in the response to PHE in the absence and presence of L-NAME (10^{-4} M) represented as bars. n=8. Data are shown as mean ± SEM. **P<0.01; ****P<0.0001 compared to the control curve of the same group. *P<0.05 compared to WKY in the absence of L-NAME (10^{-4} M).*

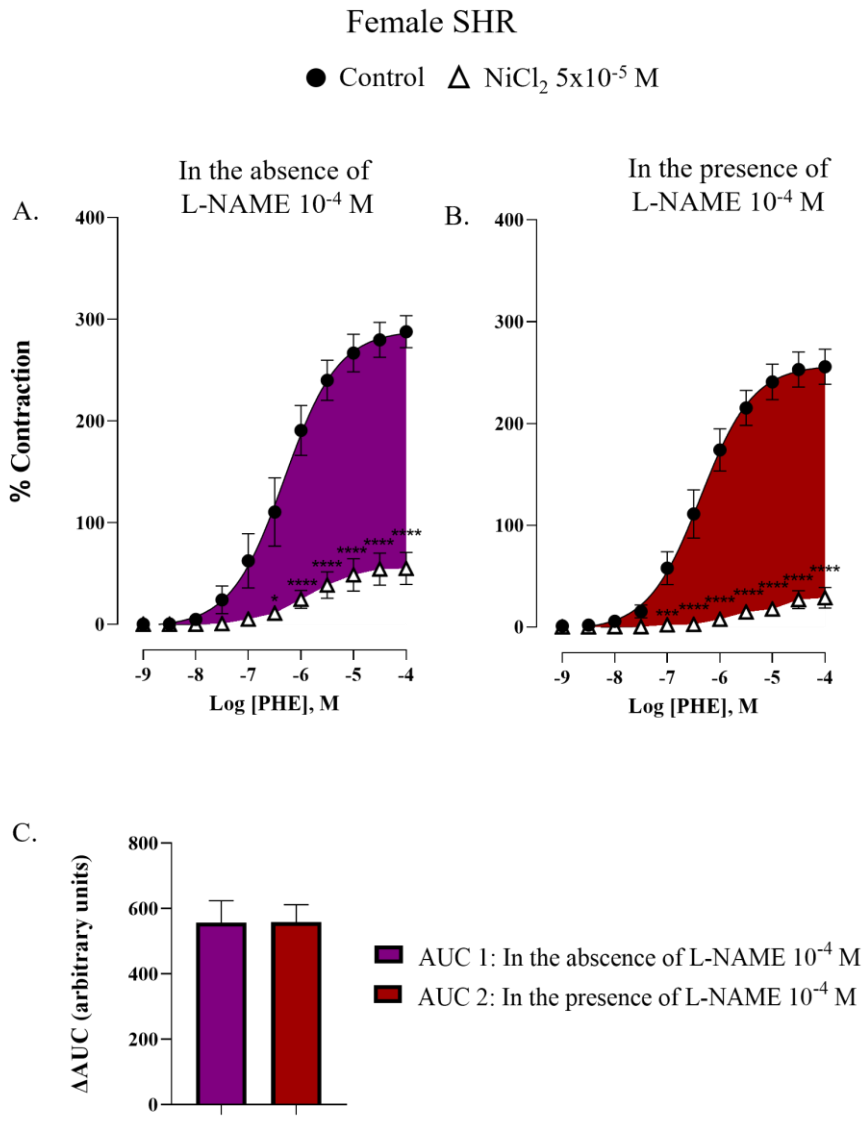

*Figure 31. Concentration-response curve to phenylephrine (PHE) in the renal artery of female SHR in (A) absence (control) and presence of nickel chloride ($5x10^{-5}$ M); (B) in the presence of L-NAME (10^{-4} M), absence (control) and presence of nickel chloride ($5x10^{-5}$M). (C) Participation of T-type VGCCs in the response to PHE in the absence and presence of L-NAME (10^{-4} M) represented as bars. n=7. Data are shown as mean ± SEM. **P<0.01; ***P<0.001; ****P<0.0001 compared to control curve of the same group.*

Table 8. Values of the area under the curve (AUC) ± standard error of the means (SEM) of the concentration-response curves to phenylephrine in the renal artery of male and female WKY and SHR groups.

Phenylephrine	AUC ± SEM
Male WKY	
AUC 1	285.10 ± 45.00
AUC 2	366.90 ± 48.70
Male SHR	
AUC 1	371.70 ± 30.70
AUC 2	394.50 ± 33.08
Female WKY	
AUC 1	316.80 ± 83.41
AUC 2	551.10 ± 49.41*
Female SHR	
AUC 1	556.70 ± 75.51
AUC 2	516.10 ± 62.90

*AUC 1: the difference between AUCs of phenylephrine control curve and phenylephrine curve with nickel chloride ($5x10^{-5}$ M); AUC 2: the difference between AUCs of phenylephrine curve with L-NAME (10^{-4} M) and phenylephrine curve with L-NAME (10^{-4} M) plus nickel chloride ($5x10^{-5}$ M). *P<0.05 compared to AUC 1.*

Our results indicated that, in the absence of NO, there was a slight trend to increase the T-type VGCCs participation in male WKY. This trend became significant in female WKY (P=0.017). The presence of L-NAME did not affect the nickel chloride blockade in SHR groups of both sexes. This was expected because the renal artery of the SHR group did not show NO release in response to phenylephrine, as indicated in Figure 25 (see section 2.8).

3.3. Study of *$Ca_V3.1$*, *$Ca_V3.2$*, and *Nos3* gene expression in intrarenal arteries of WKY and SHR of both sexes.

We measured the gene expression of the two main subtypes of T-type VGCCs at the vasculature (*$Ca_V3.1$* and *$Ca_V3.2$*) and *Nos3* by RT-PCR in rat intrarenal arteries of male and female, WKY and SHR groups.

Relative mRNA expression of both $Ca_V3.1$ and $Ca_V3.2$ was significantly higher in arteries of male SHR compared with WKY (P=0.009 and P=0.029 for $Ca_V3.1$ and $Ca_V3.2$, respectively) (see Figure 32). In contrast, in females, the results showed a significant decrease in the expression of both *$Ca_V3.1$* and *$Ca_V3.2$* in SHR compared to WKY (P=0.044 and P=0.023, for $Ca_V3.1$ and $Ca_V3.2$, respectively) (see Figure 33).

Regarding *Nos3* gene expression, the results showed a significant increase in the intrarenal arteries of male SHR compared to WKY (P=0.0013). However, this increase was not observed in females (see Figure 34).

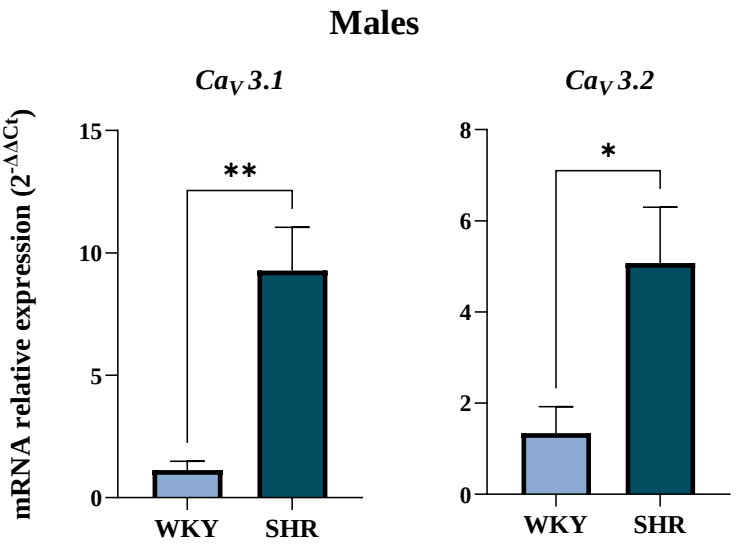

*Figure 32. Relative mRNA expression of $Ca_V3.1$ and $Ca_V3.2$ genes in intrarenal arteries of male WKY and SHR groups. n=6-8. Data are shown as mean ± SEM. *P<0.05; **P<0.005 compared to WKY.*

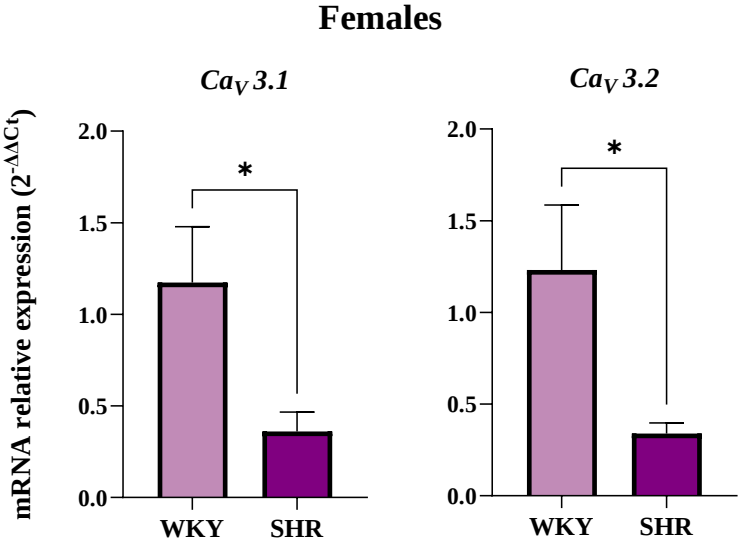

*Figure 33. Relative mRNA expression of $Ca_V3.1$ and $Ca_V3.2$ genes in intrarenal arteries of female WKY and SHR groups. n=6-8. Data are shown as mean ± SEM. *P<0.05 compared to WKY.*

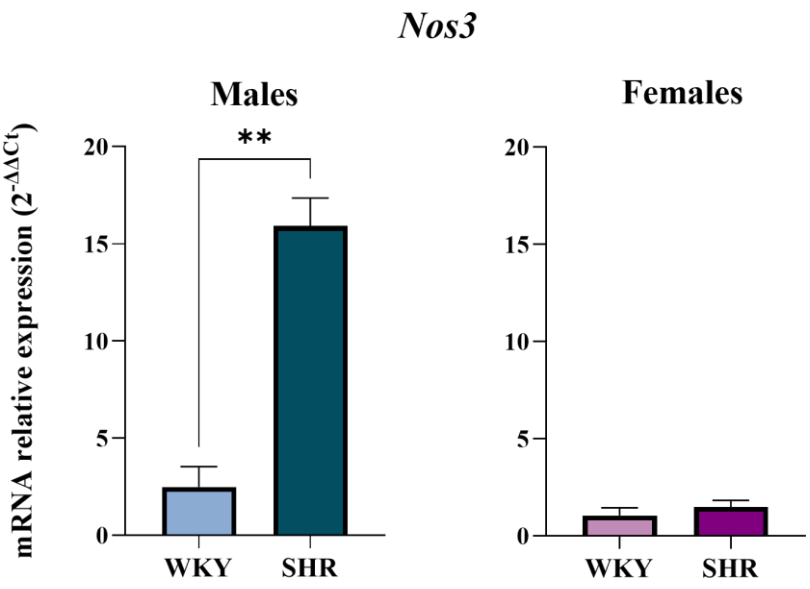

*Figure 34. Relative mRNA expression of Nos3 in intrarenal arteries of male and female WKY and SHR. n=6-8. Data are shown as mean ± SEM. **P<0.005 compared to WKY.*

Furthermore, we found a positive correlation between the Ct values of the two subtypes of T-type VGCCs (*$Ca_V3.1$* and *$Ca_V3.2$*) and the Ct of *Nos3* (see Figure 35).

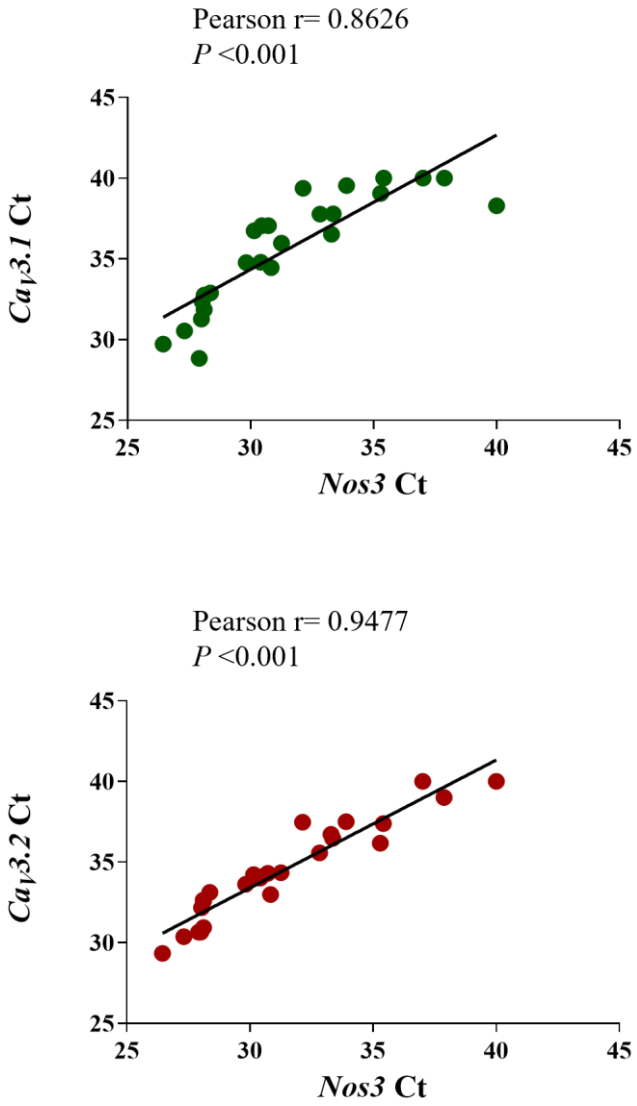

Figure 35. Correlation between Ct of T-type VGCCs subtypes ($Ca_V3.1$ and $Ca_V3.2$) and Ct of Nos3 in rat intrarenal arteries (male and female, WKY and SHR groups). n=8 per group.

Taken together, these findings indicate different vascular mechanisms of sex-specific adaptation in response to hypertension.

DISCUSSION

1. Advantages and limitations of the experimental procedure.

The present thesis explores the role of T-type VGCCs in vascular tone, mainly by studying vascular reactivity using organ baths and wire myography. Both techniques allow to measure the isometric response of isolated vessels to different pharmacological agents to understand the signalling pathways controlling vascular tone. Also, these techniques maintain the integrity of the isolated vessel for an extended period of time by providing the desired physiological conditions while measuring the response. In general, multiple rings of the same vessel can be prepared and studied simultaneously, and results can be obtained in real time. Furthermore, isolating the vessel from the living organism means that vascular function can be assessed independently of systemic influences, such as mechanical loading from blood pressure or neurohumoral regulation. However, functional results need to be interpreted carefully as the isolated vessel does not necessarily reflect the in vivo situation precisely because of the absence of the aforementioned systemic influences.

Regarding the animals used in this thesis, it should be noted that both the rabbit (under physiological conditions) and the SHR (under pathological conditions) are models that have been widely validated in cardiovascular research (119–122). For instance, SHR mimics essential features of human hypertension and suffers complications arising from the hypertensive state, such as endothelial dysfunction, hypertrophy, and heart failure, as they appear in humans (123,124). However, animal models generally have limitations, such as genetic variability, differences in response to agonists, or exact replication of human conditions. Although the SHR model offers insights into

essential hypertension mechanisms, it may not fully represent all forms of hypertension observed in humans.

Finally, it is important to bear in mind that the use of nickel chloride as a tool to investigate T-type VGCCs function offers several advantages over other blockers of these channels, such as its availability and cost-effectiveness. Nickel chloride is considered a selective blocker of T-type VGCCs (109,125). Nevertheless, the compound has limitations due to its heavy metal nature, so it can be toxic to cells and, in addition to blocking T-type VGCCs, it could react with other channels or receptors, complicating the interpretation of the experimental results. In this sense, previous experiments performed by our group showed that the blockade with nickel chloride ($5x10^{-5}$ M) is similar and comparable to NNC 55-0396 (10^{-6} M), a selective blocker of T-type VGCCs (126) (see thesis annexes), so we can assume that the effects observed in our experiments with nickel chloride can be attributed to the function of T-type VGCCs.

2. Role of T-type VGCCs in the aorta and renal artery of healthy male rabbits.

The regulation of vascular tone by T-type VGCCs is complex. It was initially hypothesised that the $Ca_V3.1$ subtype might mediate vasoconstriction (52,127), whereas the $Ca_V3.2$ subtype might be involved in vasodilation (64,67). Upon reviewing the literature, it is apparent that the statement mentioned above may not be entirely accurate, and further evidence is necessary to deepen our comprehension of the vascular function of these channels.

It has been shown that the blockade of T-type VGCCs with nickel chloride reduces the angiotensin II-induced increase in intracellular Ca^{2+} and its contraction via AT1 receptors in human subcutaneous arteries (128). Other authors also described that angiotensin II mediated its contractile effect by increasing the activity of Ca_V3 currents in rat renal efferent and afferent arterioles (129). Furthermore, it has been described that the application of mibefradil, a T-type VGCC blocker, abolishes vasoconstriction after stimulation with high potassium concentrations and significantly inhibits contraction of U46619, the thromboxane A_2 analogue, in mouse renal efferent arterioles (52). In this regard, other researchers described that mibefradil, as well as pimozide, both blockers of T-type VGCCs, inhibited vasoconstriction induced by high potassium concentrations in afferent arterioles expressing both L-type and T-type VGCCs, and also in efferent arterioles, which expressed exclusively T-type VGCCs (101). Consequently, based on these studies, we could suggest that the role of T-type VGCCs is vasoconstrictor.

Murine models deficient in $Ca_V3.1$ or $Ca_V3.2$ offer controversial results. In this regard, Hansen *et al*. (38) showed that the maximum contraction induced by phenylephrine was lower in mesenteric arteries of $Ca_V3.1^{-/-}$ mice compared to WT, both groups having similar responses to high potassium concentrations, which would suggest a vasoconstrictor role of these channels. However, another study conducted by El-Lakany *et al.* (54) concludes that the deletion of the $Ca_V3.1$ gene does not affect phenylephrine-induced contraction in the mesenteric artery. These differences could be due to the type of experimental technique, as Hansen *et al.* (38) used a perfusion set-up to measure changes in luminal diameter and a wire myograph to measure the isometric contraction, whereas El-Lakany *et al*. (54) used a pressure myograph. In other vascular beds, such as in the intrarenal arteries of mice, it has been described that phenylephrine produces a greater contraction in $Ca_V3.1^{-/-}$ mice compared to WT (38). This suggests that calcium entry through $Ca_V3.1$ may be associated with vasodilation in intrarenal arteries. Similarly, in the mesenteric artery of $Ca_V3.1^{-/-}$ mice, norepinephrine produced a greater contraction compared to WT (39). Therefore, depending on the vascular bed, $Ca_V3.1$ could be involved in both vasocontraction and vasodilation.

Regarding murine models deficient in $Ca_V3.2$, Thuesen *et al.* (127) showed that $Ca_V3.2$ was involved in the dilatation of renal postglomerular blood vessels since the contractile response induced by potassium chloride was significantly increased in the efferent arterioles of $Ca_V3.2^{-/-}$ mice without differences in the response of afferent arterioles. No differences were found in the contraction in either efferent or afferent arterioles of $Ca_V3.1^{-/-}$ mice compared with WT. These results support the idea that $Ca_V3.1$ and $Ca_V3.2$ may have different roles in the regulation of vascular reactivity.

The first report of Ca_V3 current-mediated vasodilation came from Chen *et al.* (64), who demonstrated that, in the coronary artery of $Ca_V3.2^{-/-}$ mice with unaltered vasoconstrictor responses, the response to acetylcholine produced contraction rather than relaxation and the response to sodium nitroprusside was reduced, similarly to incubation with nickel chloride in arteries of WT mice. The authors proposed that this relaxation mechanism involves BK_{Ca} channels. According to this hypothesis, other studies in rat cerebral and mouse mesenteric arteries propose that $Ca_V3.2$ could induce Ca^{2+} sparks through the RyRs, leading to the activation of BK_{Ca} and promoting vasodilation (65,67,130,131).

With this thesis, we demonstrated that T-type VGCCs have a dual role, vasoconstrictor and vasodilator, depending on the vascular bed. Phenylephrine exerts its effect by activating α_1-adrenergic receptors (132), while angiotensin II activates AT1 receptors (133), both mainly found in vascular smooth muscle cells. Incubation with nickel chloride reduced phenylephrine-induced contraction, indicating that T-type VGCCs participate in Ca^{2+} entry responsible for α_1-adrenergic contraction in the aorta and renal artery. Similarly, nickel chloride reduced angiotensin II-induced contraction, indicating that these channels are also involved in the AT1 stimulation and contraction in both the aorta and renal artery. This blockade, in the case of angiotensin II, practically abolishes the contractile response. For this reason, we continued the experimental protocol only with phenylephrine.

It is also important to consider here that the release of NO impacts the function of T-type VGCCs. In this regard, Howitt *et al.* (59) described that acute and chronic NO inhibition by L-NAME increased the contribution of

T-type VGCCs to vascular tone in mouse arteries. Hence, a decrease in NO bioavailability, as occurs during cardiovascular diseases, would lead to an increase in the contribution of T-type VGCCs, which, considering their vasoconstrictor function, could increase peripheral resistances and have an impact on blood pressure and cardiac output. Therefore, one of the objectives of this thesis was to study whether T-type VGCCs became more active in the absence of NO. To that end, we first verified that there was indeed NO release in response to phenylephrine, as occurs in most vascular beds (134–136). As expected, both the aorta and renal artery increased α_1-adrenergic response in the presence of L-NAME, indicating that NO attenuates the contraction of phenylephrine in these vascular beds.

Blockade of T-type VGCCs with nickel chloride in the presence of L-NAME was used to test the function of these channels in the absence of NO. Interestingly, our results indicate a higher involvement of T-type VGCCs in the absence of NO in the rabbit renal artery but not in the aorta. An increasing number of studies support the idea that T-type VGCCs are responsible for maintaining tone in smaller calibre vessels (37,41,53,59,137,138). Therefore, this regulatory mechanism seems to become more important as the vessel diameter decreases, which would explain why we did not observe differences in the aorta. Thus, here, we demonstrate for the first time that, even in a non-resistance vessel, such as the renal artery, T-type VGCCs significantly contribute to the response to α_1-adrenergic stimulation, which is further potentiated in the absence of NO.

As well as vasoconstriction, T-type VGCCs have been shown to contribute to vasodilation. Therefore, to study the involvement of T-type

VGCCs in vasodilation, we performed concentration-response curves to endothelium-dependent and -independent agonists. We used acetylcholine, which activates muscarinic receptors located on endothelial cells, producing vasodilation (4), and sodium nitroprusside, a NO donor, that induces endothelium-independent vasodilation, indicating the relaxant capacity of smooth muscle (139)**.** Based on our results, T-type VGCCs are not involved in vasodilation in the rabbit aorta. In contrast, they are required for endothelium-dependent vasodilation in the rabbit renal artery, probably by mediating the Ca^{2+} influx necessary to activate eNOS. In order to test this hypothesis, we conducted experiments using L-NAME, and the blockade of the acetylcholine-induced vasodilation was similar to that obtained with nickel chloride. Moreover, the co-incubation with both L-NAME and nickel chloride did not show a greater inhibition than when each one was applied separately. This suggests that both L-NAME and nickel chloride reduce acetylcholine-induced vasodilation by affecting the same pathway. As a result, it is plausible that the influx of Ca^{2+} necessary to activate eNOS in the rat renal artery occurs through T-type VGCCs. In this sense, it has been proposed that the opening of $Ca_V3.1$ triggers an increase in intracellular Ca^{2+} concentration in the vicinity of eNOS, which could activate the enzyme and promote vasodilation (68). Indeed, our results showed that $Ca_V3.1$ and eNOS are colocalised.

Given that in the renal artery, T-type VGCCs seem to have a more important modulatory role than in the aorta, we wanted to demonstrate the expression of T-type VGCCs subtypes ($Ca_V3.1$ and $Ca_V3.2$) in the renal artery endothelial cells by immunohistochemistry, finding that $Ca_V3.1$ was located in the cytoplasm and $Ca_V3.2$ is predominantly expressed in the nucleus of

endothelial cells. Other studies have also described the expression of T-type VGCC in the endothelium of other vascular beds (40,41,48,131).

As we demonstrated in this thesis, previous studies have reported that $Ca_V3.1$ colocalises with eNOS in the endothelium of mouse mesenteric arteries, and that could modulate endothelium-dependent vasodilation (68). Furthermore, evidence in humans shows that blocking T-type VGCCs improves endothelial function through a NO-related mechanism (140). The results of this randomised controlled trial indicate a significant increase in endothelium-dependent dilation, while dilation in response to a NO donor remained unchanged.

In summary, T-type VGCCs participate in the α_1-adrenergic response of the aorta and renal artery of healthy rabbits, having a vasoconstrictor role that is enhanced in the absence of NO only in the renal artery. Moreover, endothelium-dependent-vasodilation requires activation of eNOS by Ca^{2+} through T-type VGCCs in the renal artery. Even though the renal artery is not a resistance vessel, $Ca_V3.1$ and $Ca_V3.2$ are expressed in the endothelium, where $Ca_V3.1$ colocalises with eNOS underlying the disruption of healthy vasodilation observed when T-type VGCCs are blocked.

3. Involvement of T-type VGCCs in arterial hypertension. Differences by sex.

To determine whether the function and expression of T-type VGCCs were modified by hypertension and whether sex could vary this function, we decided to focus on the renal artery based on our findings in rabbit arteries. The SHR model serves as a valuable experimental approach in studies exploring the pathophysiologic mechanisms of hypertension (141). We used male and female SHR and normotensive WKY rats at 16 weeks of age. At this age, hypertension is already established in the SHR model (142). Our results confirmed a significant increase in SBP, DBP, and MAP of both male and female SHR, compared with WKY rats of the same sex, as previously described (143–145). We also noticed a trend towards increased PP in female SHR. Hypertension can increase plasma NO levels (146,147), which may be due to inflammation linked to an increased iNOS; however, we did not find differences in plasma NO levels between WKY and SHR groups.

On the other hand, we set out to measure basal intracellular levels of ROS and NO in circulating leukocytes by flow cytometry. Our results showed that H_2O_2 and $ONOO^-$ production was increased in male SHR in both leukocytes and neutrophils. It is likely that no changes in O_2^- and NO levels were observed due to their consumption in the reaction to form $ONOO^-$.

Several authors describe an increase in the oxidative environment of the SHR model compared to WKY in other tissues such as bone marrow (148), aorta (149–151), mesenteric artery, and kidney (152), among others. In addition, it has been described that the O_2^- increases vasoconstriction by releasing IP_3, which is enhanced in the SHR model (153). Thus, hypertension

could increase vascular sensitivity to oxidative stress, contributing to disease progression. In females, no significant differences in oxidative stress were observed between the SHR model and WKY rats. It has been previously reported that the SHR model shows variations in oxidative stress depending on sex (154–158). Male SHR exhibits higher renal O_2^- production and H_2O_2 levels than females of the same group (154,157,158) and has increased all measures of ROS production in response to chronic infusion with angiotensin II (155). Other authors describe that oxidative stress reduces eNOS activity in the inner renal medulla of SHR through decreased levels of BH_4, a cofactor for NOS activation, which would lead to a worsening of hypertension in male rats but not in females (159). Our results show higher oxidative stress in hypertensive males, suggesting that the female sex may provide protection against hypertension-induced oxidative stress; however, this does not translate into an improvement in vascular function since hypertension induced endothelial dysfunction in both sexes.

The endothelial dysfunction found in the renal artery of the SHR model likely contributes to the increase in blood pressure seen around 9-12 weeks of age in SHR (160,161). Hypertension did not affect receptor-independent contraction to KCl, but increased phenylephrine-induced contraction only in females. This may reflect the essential role of NO in α_1-adrenergic contraction for females.

Following the hypothesis that T-type VGCCs are up-regulated in situations of low NO bioavailability (58–60), as demonstrated previously in rabbit renal artery, we tested this in the SHR model in both sexes. Our results suggest that T-type VGCCs participate in α_1-adrenergic contraction in rat renal artery. Furthermore, we noticed a greater involvement of T-type VGCCs

in female SHR, which does not occur in males. These discrepancies between both sexes could be linked to the reduced NO levels in the female SHR compared to WKY. If NO has an inhibitory effect on the function of T-type VGCCs, lower NO levels in SHR would make these channels more active. In this regard, we showed that additional blockage of NO synthesis with L-NAME increased the involvement of T-type VGCCs in the response to phenylephrine in female WKY but not in male WKY or SHR groups, since the contribution of NO in these groups was reduced.

In male SHR, the elevated gene expression of the two subtypes of T-type VGCCs studied could be attributed to the higher oxidative stress observed in this group. According to other authors, oxidative stress could up-regulate the gene expression of T-type VGCCs. For instance, the connexin 40-deficient mouse, which exhibits hypertension caused by increased activity of the renin-angiotensin system and presents high levels of oxidative stress due to NOX enzyme activation, shows a higher expression of T-type VGCCs than normotensive mice (62). These authors described that increased oxidative stress would enhance the contribution of T-type VGCCs over L-type VGCCs in the maintenance of myogenic tone. However, they did not perform the study in females. Studies are usually performed in male animals, so the effects in females are unknown. Our results show that the expression of T-type VGCCs changes with hypertension differently according to sex since we found an underexpression of *$Ca_V3.1$* and *$Ca_V3.2$* in female SHR. Nevertheless, this reduced expression does not translate into reduced activity, as we found an increased involvement of these channels in female SHR. Precisely, this could be the cause of such underexpression, i.e., the increased activity of T-type VGCCs in hypertensive females would exert an inhibitory

effect on *$Ca_V3.1$* and *$Ca_V3.2$* gene expression that would explain the gene underexpression shown in this group.

On the other hand, *Nos3* overexpression observed in male SHR could represent a compensatory mechanism against oxidative stress. However, this mechanism may not be sufficient to reverse the endothelial dysfunction in this group, possibly due to the involvement of other mechanisms. In contrast, hypertension does not change *Nos3* expression in females despite the lower NO involvement. This finding would indicate the inability of hypertensive females to up-regulate *Nos3* gene expression, leading to endothelial dysfunction and increased sensitivity to phenylephrine.

Finally, we found a positive correlation between the gene expression of the two subtypes of T-type VGCCs and *Nos3*, which represents another explanation for the increased expression of T-type VGCCs and eNOS observed in male SHR. Moreover, if there is a modulation between $Ca_V3.1$ and $Ca_V3.2$ by NO or vice versa, an increase in T-type gene expression could lead to a compensatory increase in eNOS to form more NO to control excess vasoconstriction due to the activity of these channels.

4. Final considerations.

The vascular role of T-type VGCCs is complex. These channels allow calcium to enter endothelial and muscle cells, and their function is essential for regulating α_1-adrenergic contraction in the aorta and renal artery under physiological conditions. Moreover, in the renal artery, T-type VGCCs are involved in the endothelium-dependent relaxation with colocalisation of $Ca_V3.1$ and eNOS in the endothelium. In hypertension, T-type VGCCs exhibit increased activity only in females, suggesting a sex-specific modulation of these channels. The regulation of T-type VGCCs could be affected by NO, and their gene expression could be modified differently in response to hypertension and depending on sex. Although there is still much to be explored about the function of the T-type VGCCs and their relationship with NO, this doctoral thesis provides new insight into the role of T-type VGCCs in regulating vascular tone.

CONCLUSIONS

Conclusions

1. T-type VGCCs participate in the vasoconstriction induced by phenylephrine and angiotensin II in the aorta and renal artery of male healthy rabbits. T-type VGCCs become more active in the absence of NO in response to α_1-adrenergic stimulation only in the renal artery.

2. T-type VGCCs are involved in endothelium-dependent vasodilation, without affecting endothelium-independent vasodilation, in the renal artery of male healthy rabbits.

3. T-type VGCCs are expressed in both the aorta and renal artery of male healthy rabbits. $Ca_V3.1$ colocalises with eNOS in the endothelium of the renal artery.

4. Hypertension induces endothelial dysfunction and decreases NO release in response to α_1-adrenergic stimulation in rat renal artery of both sexes, especially in females, where there is an evident increase in the involvement of T-type VGCCs.

BIBLIOGRAPHY

Bibliography

1. Zhao Y, Vanhoutte PM, Leung SWS. Vascular nitric oxide: Beyond eNOS. J Pharmacol Sci. 2015 Oct 1;129(2):83–94.

2. Berridge MJ. Smooth muscle cell calcium activation mechanisms. J Physiol. 2008 Nov 1;586(21):5047–61.

3. Somlyo AP. Excitation-contraction coupling and the ultrastructure of smooth muscle. Circ Res. 1985 Oct;57(4):497–507.

4. Furchgott RF, Zawadzki JV. The obligatory role of endothelial cells in the relaxation of arterial smooth muscle by acetylcholine. Nature. 1980 Nov 27;288(5789):373–6.

5. Ignarro LJ, Buga GM, Wood KS, Byrns RE, Chaudhuri G. Endothelium-derived relaxing factor produced and released from artery and vein is nitric oxide. Proc Natl Acad Sci U S A. 1987 Dec;84(24):9265–9.

3. Badimón L, Martínez-González J. [Endothelium and vascular protection: an update]. Rev Esp Cardiol. 2002;55 Suppl 1:17–26.

7. Ignarro LJ. Biological actions and properties of endothelium-derived nitric oxide formed and released from artery and vein. Circ Res. 1989 Jul;65(1):1–21.

8. Oliveira-Paula GH, Lacchini R, Tanus-Santos JE. Endothelial nitric oxide synthase: From biochemistry and gene structure to clinical implications of *NOS3* polymorphisms. Gene. 2016 Jan 10;575(2, Part 3):584–99.

9. Fleming I, Busse R. Molecular mechanisms involved in the regulation of the endothelial nitric oxide synthase. Am J Physiol-Regul Integr Comp Physiol. 2003 Jan;284(1):R1–12.

10. Félétou M. The Endothelium: Part 1: Multiple Functions of the Endothelial Cells—Focus on Endothelium-Derived Vasoactive Mediators [Internet]. San Rafael (CA): Morgan & Claypool Life Sciences; 2011 [cited 2024 Apr 8]. (Integrated Systems Physiology: from Molecule to

Function to Disease). Available from: http://www.ncbi.nlm.nih.gov/books/NBK57149/

11. Michel T, Li GK, Busconi L. Phosphorylation and subcellular translocation of endothelial nitric oxide synthase. Proc Natl Acad Sci U S A. 1993 Jul 1;90(13):6252–6.

12. Fleming I, Busse R. Molecular mechanisms involved in the regulation of the endothelial nitric oxide synthase. Am J Physiol-Regul Integr Comp Physiol. 2003 Jan 1;284(1):R1–12.

13. Beckman JS, Koppenol WH. Nitric oxide, superoxide, and peroxynitrite: the good, the bad, and ugly. Am J Physiol-Cell Physiol. 1996 Nov;271(5):C1424–37.

14. Fleszar MG, Wiśniewski J, Krzystek-Korpacka M, Misiak B, Frydecka D, Piechowicz J, et al. Quantitative Analysis of l-Arginine, Dimethylated Arginine Derivatives, l-Citrulline, and Dimethylamine in Human Serum Using Liquid Chromatography–Mass Spectrometric Method. Chromatographia. 2018;81(6):911–21.

15. Wong V (Wai C, Lerner E. Nitric oxide inhibition strategies. Future Sci OA. 2015 Aug 1;1(1):FSO35.

16. Ignarro LJ, Lippton H, Edwards JC, Baricos WH, Hyman AL, Kadowitz PJ, et al. Mechanism of vascular smooth muscle relaxation by organic nitrates, nitrites, nitroprusside and nitric oxide: evidence for the involvement of S-nitrosothiols as active intermediates. J Pharmacol Exp Ther. 1981 Sep;218(3):739–49.

17. Sheng Y, Zhu L. The crosstalk between autonomic nervous system and blood vessels. Int J Physiol Pathophysiol Pharmacol. 2018;10(1):17–28.

18. Guimarães S, Moura D. Vascular adrenoceptors: an update. Pharmacol Rev. 2001 Jun;53(2):319–56.

19. Søndergaard AM, Overgaard CB, Mazur A, Postnov DD, Matchkov VV, Aalkjaer C. Rat mesenteric small artery neurogenic dilatation is predominantly mediated by β1-adrenoceptors in vivo. J Physiol. 2019 Apr 1;597(7):1819–31.

20. Vanhoutte PM. Endothelial adrenoceptors. J Cardiovasc Pharmacol. 2001 Nov;38(5):796–808.

21. Garland C, Yarova P, Jiménez-Altayó F, Dora K. Vascular hyperpolarization to β-adrenoceptor agonists evokes spreading dilatation in rat isolated mesenteric arteries. Br J Pharmacol. 2011;164(3):913–21.

22. Rapoport RM, Draznin MB, Murad F. Endothelium-dependent relaxation in rat aorta may be mediated through cyclic GMP-dependent protein phosphorylation. Nature. 1983 Nov 10;306(5939):174–6.

23. Burnham MP, Bychkov R, Félétou M, Richards GR, Vanhoutte PM, Weston AH, et al. Characterization of an apamin-sensitive small-conductance Ca(2+)-activated K(+) channel in porcine coronary artery endothelium: relevance to EDHF. Br J Pharmacol. 2002 Mar;135(5):1133–43.

24. Bonventre JV. Phospholipase A2 and signal transduction. J Am Soc Nephrol JASN. 1992 Aug;3(2):128–50.

25. Clapham DE. Calcium signaling. Cell. 2007 Dec 14;131(6):1047–58.

26. Nelson MT, Cheng H, Rubart M, Santana LF, Bonev AD, Knot HJ, et al. Relaxation of arterial smooth muscle by calcium sparks. Science. 1995 Oct 27;270(5236):633–7.

27. Ottolini M, Sonkusare SK. The Calcium Signaling Mechanisms in Arterial Smooth Muscle and Endothelial Cells. Compr Physiol. 2021 Apr 1;11(2):1831–69.

28. Catterall WA. Voltage-gated calcium channels. Cold Spring Harb Perspect Biol. 2011 Aug 1;3(8):a003947.

29. Moosmang S, Schulla V, Welling A, Feil R, Feil S, Wegener JW, et al. Dominant role of smooth muscle L-type calcium channel Cav1.2 for blood pressure regulation. EMBO J. 2003 Nov 17;22(22):6027–34.

30. Sather WA, Tanabe T, Zhang JF, Mori Y, Adams ME, Tsien RW. Distinctive biophysical and pharmacological properties of class A (BI) calcium channel alpha 1 subunits. Neuron. 1993 Aug;11(2):291–303.

31. Ertel EA, Campbell KP, Harpold MM, Hofmann F, Mori Y, Perez-Reyes E, et al. Nomenclature of voltage-gated calcium channels. Neuron. 2000 Mar;25(3):533–5.

32. Talavera K, Nilius B. Biophysics and structure-function relationship of T-type Ca2+ channels. Cell Calcium. 2006 Aug;40(2):97–114.

33. Perez-Reyes E, Lory P. Molecular biology of T-type calcium channels. CNS Neurol Disord Drug Targets. 2006 Dec;5(6):605–9.

34. Knot HJ, Nelson MT. Regulation of arterial diameter and wall [Ca2+] in cerebral arteries of rat by membrane potential and intravascular pressure. J Physiol. 1998 Apr 1;508(Pt 1):199–209.

35. Navarro-Gonzalez MF, Grayson TH, Meaney KR, Cribbs LL, Hill CE. Non-L-type voltage-dependent calcium channels control vascular tone of the rat basilar artery. Clin Exp Pharmacol Physiol. 2009 Jan;36(1):55–66.

36. Hansen PBL. Functional and pharmacological consequences of the distribution of voltage-gated calcium channels in the renal blood vessels. Acta Physiol Oxf Engl. 2013 Apr;207(4):690–9.

37. Abd El-Rahman RR, Harraz OF, Brett SE, Anfinogenova Y, Mufti RE, Goldman D, et al. Identification of L- and T-type Ca2+ channels in rat cerebral arteries: role in myogenic tone development. Am J Physiol Heart Circ Physiol. 2013 Jan 1;304(1):H58-71.

38. Hansen PBL. Functional importance of T-type voltage-gated calcium channels in the cardiovascular and renal system: news from the world of knockout mice. Am J Physiol Regul Integr Comp Physiol. 2015 Feb 15;308(4):R227-237.

39. Björling K, Morita H, Olsen MF, Prodan A, Hansen PB, Lory P, et al. Myogenic tone is impaired at low arterial pressure in mice deficient in the low-voltage-activated CaV 3.1 T-type Ca(2+) channel. Acta Physiol Oxf Engl. 2013 Apr;207(4):709–20.

40. Braunstein TH, Inoue R, Cribbs L, Oike M, Ito Y, Holstein-Rathlou NH, et al. The Role of L- and T-Type Calcium Channels in Local and

Remote Calcium Responses in Rat Mesenteric Terminal Arterioles. J Vasc Res. 2008 Sep 2;46(2):138–51.

41. Kuo IY, Ellis A, Seymour VAL, Sandow SL, Hill CE. Dihydropyridine-insensitive calcium currents contribute to function of small cerebral arteries. J Cereb Blood Flow Metab Off J Int Soc Cereb Blood Flow Metab. 2010 Jun;30(6):1226–39.

42. Harraz OF, Visser F, Brett SE, Goldman D, Zechariah A, Hashad AM, et al. CaV1.2/CaV3.x channels mediate divergent vasomotor responses in human cerebral arteries. J Gen Physiol. 2015 May;145(5):405–18.

43. Perez-Reyes E. Molecular physiology of low-voltage-activated t-type calcium channels. Physiol Rev. 2003 Jan;83(1):117–61.

44. Weiss N, Zamponi GW. T-type calcium channels: From molecule to therapeutic opportunities. Int J Biochem Cell Biol. 2019 Mar;108:34–9.

45. Todorovic SM, Lingle CJ. Pharmacological properties of T-type Ca2+ current in adult rat sensory neurons: effects of anticonvulsant and anesthetic agents. J Neurophysiol. 1998 Jan;79(1):240–52.

46. Mangoni ME, Traboulsie A, Leoni AL, Couette B, Marger L, Le Quang K, et al. Bradycardia and slowing of the atrioventricular conduction in mice lacking CaV3.1/alpha1G T-type calcium channels. Circ Res. 2006 Jun 9;98(11):1422–30.

47. Bohn G, Moosmang S, Conrad H, Ludwig A, Hofmann F, Klugbauer N. Expression of T- and L-type calcium channel mRNA in murine sinoatrial node. FEBS Lett. 2000 Sep 8;481(1):73–6.

48. Wu S, Haynes J, Taylor JT, Obiako BO, Stubbs JR, Li M, et al. Cav3.1 (α1G) T-Type Ca2+ Channels Mediate Vaso-Occlusion of Sickled Erythrocytes in Lung Microcirculation. Circ Res. 2003 Aug 22;93(4):346–53.

49. Nikitina E, Zhang ZD, Kawashima A, Jahromi BS, Bouryi VA, Takahashi M, et al. Voltage-dependent calcium channels of dog basilar artery. J Physiol. 2007 Apr 15;580(Pt 2):523–41.

50. Perez-Reyes E, Cribbs LL, Daud A, Lacerda AE, Barclay J, Williamson MP, et al. Molecular characterization of a neuronal low-voltage-activated T-type calcium channel. Nature. 1998 Feb 26;391(6670):896–900.

51. Ball CJ, Wilson DP, Turner SP, Saint DA, Beltrame JF. Heterogeneity of L- and T-channels in the vasculature: rationale for the efficacy of combined L- and T-blockade. Hypertens Dallas Tex 1979. 2009 Apr;53(4):654–60.

52. Poulsen CB, Al-Mashhadi RH, Cribbs LL, Skøtt O, Hansen PB. T-type voltage-gated calcium channels regulate the tone of mouse efferent arterioles. Kidney Int. 2011 Feb;79(4):443–51.

53. Jensen LJ, Holstein-Rathlou NH. Is there a role for T-type Ca2+ channels in regulation of vasomotor tone in mesenteric arterioles? Can J Physiol Pharmacol. 2009 Jan;87(1):8–20.

54. El-Lakany MA, Haghbin N, Arora N, Hashad AM, Mironova GYu, Sancho M, et al. CaV3.1 channels facilitate calcium wave generation and myogenic tone development in mouse mesenteric arteries. Sci Rep. 2023 Nov 21;13:20407.

55. Mullan B, Pettis J, Jackson WF. T-type voltage-gated Ca2+ channels do not contribute to the negative feedback regulation of myogenic tone in murine superior epigastric arteries. Pharmacol Res Perspect. 2017 Jun;5(3):e00320.

56. VanBavel E, Sorop O, Andreasen D, Pfaffendorf M, Jensen BL. Role of T-type calcium channels in myogenic tone of skeletal muscle resistance arteries. Am J Physiol Heart Circ Physiol. 2002 Dec;283(6):H2239-2243.

57. Hashad AM, Harraz OF, Brett SE, Romero M, Kassmann M, Puglisi JL, et al. Caveolae Link CaV3.2 Channels to BKCa-Mediated Feedback in Vascular Smooth Muscle. Arterioscler Thromb Vasc Biol. 2018 Oct;38(10):2371–81.

58. Howitt L, Matthaei KI, Drummond GR, Hill CE. Nox1 upregulates the function of vascular T-type calcium channels following chronic nitric oxide deficit. Pflugers Arch. 2015 Apr;467(4):727–35.

59. Howitt L, Kuo IY, Ellis A, Chaston DJ, Shin HS, Hansen PB, et al. Chronic deficit in nitric oxide elicits oxidative stress and augments T-type calcium-channel contribution to vascular tone of rodent arteries and arterioles. Cardiovasc Res. 2013 Jun 1;98(3):449–57.

60. Smith JF, Lemmey HAL, Borysova L, Hiley CR, Dora KA, Garland CJ. Endothelial Nitric Oxide Suppresses Action-Potential-Like Transient Spikes and Vasospasm in Small Resistance Arteries. Hypertens Dallas Tex 1979. 2020 Sep;76(3):785–94.

61. McNeish AJ, Jimenez Altayo F, Garland CJ. Evidence both L-type and non-L-type voltage-dependent calcium channels contribute to cerebral artery vasospasm following loss of NO in the rat. Vascul Pharmacol. 2010;53(3–4):151–9.

62. Howitt L, Chaston DJ, Sandow SL, Matthaei KI, Edwards FR, Hill CE. Spreading vasodilatation in the murine microcirculation: attenuation by oxidative stress-induced change in electromechanical coupling. J Physiol. 2013 Apr 15;591(Pt 8):2157–73.

63. Marchio P, Guerra-Ojeda S, Vila JM, Aldasoro M, Victor VM, Mauricio MD. Targeting Early Atherosclerosis: A Focus on Oxidative Stress and Inflammation. Oxid Med Cell Longev. 2019 Jul 1;2019:8563845.

64. Chen CC, Lamping KG, Nuno DW, Barresi R, Prouty SJ, Lavoie JL, et al. Abnormal coronary function in mice deficient in alpha1H T-type Ca2+ channels. Science. 2003 Nov 21;302(5649):1416–8.

65. Fan G, Kaßmann M, Hashad AM, Welsh DG, Gollasch M. Differential targeting and signalling of voltage-gated T-type Cav 3.2 and L-type Cav 1.2 channels to ryanodine receptors in mesenteric arteries. J Physiol. 2018 Oct;596(20):4863–77.

66. Hashad AM, Sancho M, Brett SE, Welsh DG. Reactive Oxygen Species Mediate the Suppression of Arterial Smooth Muscle T-type Ca2+ Channels by Angiotensin II. Sci Rep. 2018 Feb 22;8(1):3445.

67. Harraz OF, Abd El-Rahman RR, Bigdely-Shamloo K, Wilson SM, Brett SE, Romero M, et al. CaV3.2 Channels and the Induction of Negative Feedback in Cerebral Arteries. Circ Res. 2014 Sep 12;115(7):650–61.

68. Svenningsen P, Andersen K, Thuesen AD, Shin HS, Vanhoutte PM, Skøtt O, et al. T-type Ca(2+) channels facilitate NO-formation, vasodilatation and NO-mediated modulation of blood pressure. Pflugers Arch. 2014 Dec;466(12):2205–14.

69. Enfermedades cardiovasculares [Internet]. [cited 2024 Apr 8]. Available from: https://www.who.int/es/health-topics/cardiovascular-diseases

70. INE [Internet]. [cited 2024 Apr 8]. INEbase / Sociedad /Salud /Estadística de defunciones según la causa de muerte / Últimos datos. Available from: https://www.ine.es/dyngs/INEbase/es/operacion.htm?c=Estadistica_C&cid=1254736176780&menu=ultiDatos&idp=1254735573175

71. Weintraub WS. High costs of cardiovascular disease in the European Union. Eur Heart J. 2023 Dec 1;44(45):4768–70.

72. Prevention, Use of Health Data and Healthcare Equity: Key Factors for Improving Cardiovascular Health in Spain [Internet]. [cited 2024 Apr 8]. Available from: https://efpia.eu/news-events/the-efpia-view/statements-press-releases/prevention-use-of-health-data-and-healthcare-equity-key-factors-for-improving-cardiovascular-health-in-spain/

73. Kearney PM, Whelton M, Reynolds K, Muntner P, Whelton PK, He J. Global burden of hypertension: analysis of worldwide data. Lancet Lond Engl. 2005 Jan 15;365(9455):217–23.

74. Writing Group Members, Mozaffarian D, Benjamin EJ, Go AS, Arnett DK, Blaha MJ, et al. Heart Disease and Stroke Statistics-2016 Update: A Report From the American Heart Association. Circulation. 2016 Jan 26;133(4):e38-360.

75. Hipertensión [Internet]. [cited 2024 Apr 8]. Available from: https://www.who.int/es/news-room/fact-sheets/detail/hypertension

76. Flack JM, Adekola B. Blood pressure and the new ACC/AHA hypertension guidelines. Trends Cardiovasc Med. 2020 Apr 1;30(3):160–4.

77. Villa Estébanez R, Tranche Iparraguirre S, Marín Iranzo R, Prieto Díaz MA, Hevia Rodríguez E, Oviedo de Hipertensión G. La presión de pulso como marcador de riesgo cardiovascular en población anciana. Aten Primaria. 2002 Oct 15;30(6):374–80.

78. Tranche Iparraguirre S, Marín Iranzo R, Prieto Díaz MA, Hevia Rodríguez E. La presión de pulso como marcador de riesgo cardiovascular. Hipertens Riesgo Vasc. 2001 Jun 1;18(5):218–24.

79. Ryan SM, Waack BJ, Weno BL, Heistad DD. Increases in pulse pressure impair acetylcholine-induced vascular relaxation. Am J Physiol-Heart Circ Physiol. 1995 Jan;268(1):H359–63.

80. Menéndez SS. Enfermedades Cardiovasculares.

81. Azcárraga PA, Latorre MA, Montalvo JFM, Gutierrez ML, Chamizo VV, Calleja JAB, et al. Base de Datos Clínicos de Atención Primaria – BDCAP Sistema Nacional de Salud.

82. Menéndez E, Delgado E, Fernández-Vega F, Prieto MA, Bordiú E, Calle A, et al. Prevalencia, diagnóstico, tratamiento y control de la hipertensión arterial en España. Resultados del estudio Di@bet.es. Rev Esp Cardiol. 2016 Jun 1;69(6):572–8.

83. Jaffe MG, Lee GA, Young JD, Sidney S, Go AS. Improved blood pressure control associated with a large-scale hypertension program. JAMA. 2013 Aug 21;310(7):699–705.

84. Jaffe MG, Young JD. The Kaiser Permanente Northern California Story: Improving Hypertension Control From 44% to 90% in 13 Years (2000 to 2013). J Clin Hypertens Greenwich Conn. 2016 Apr;18(4):260–1.

85. Zhang Y, Moran AE. Trends in the Prevalence, Awareness, Treatment, and Control of Hypertension Among Young Adults in the United States, 1999 to 2014. Hypertens Dallas Tex 1979. 2017 Oct;70(4):736–42.

86. Chambliss KL, Shaul PW. Estrogen modulation of endothelial nitric oxide synthase. Endocr Rev. 2002 Oct;23(5):665–86.

87. Mozaffarian D, Benjamin EJ, Go AS, Arnett DK, Blaha MJ, Cushman M, et al. Heart disease and stroke statistics--2015 update: a report from the American Heart Association. Circulation. 2015 Jan 27;131(4):e29-322.

88. Holjak EJB, Savinova I, Nelson VL, Ogilvie LM, Ng AM, Edgett BA, et al. An Evaluation of Cardiac Health in the Spontaneously Hypertensive Rat Colony: Implications of Evolutionary Driven Increases in Concentric Hypertrophy. Am J Hypertens. 2022 Mar 8;35(3):264–71.

89. Okamoto K, Aoki K. Development of a strain of spontaneously hypertensive rats. Jpn Circ J. 1963 Mar;27:282–93.

90. Martínez JLM, Mendoza LB, Hernández TG, Moreno VJH, Gómez CF, Martínez DP. La hipertensión arterial en animales de laboratorio. Medicentro Electrónica. 2022 Nov 18;27(1):e3798.

91. Elmarakby AA, Sullivan JC. Sex differences in hypertension: lessons from spontaneously hypertensive rats (SHR). Clin Sci Lond Engl 1979. 2021 Aug 13;135(15):1791–804.

92. Zhang Z, Zhao L, Zhou X, Meng X, Zhou X. Role of inflammation, immunity, and oxidative stress in hypertension: New insights and potential therapeutic targets. Front Immunol. 2023 Jan 10;13:1098725.

93. Costa TJ, Barros PR, Arce C, Santos JD, da Silva-Neto J, Egea G, et al. The homeostatic role of hydrogen peroxide, superoxide anion and nitric oxide in the vasculature. Free Radic Biol Med. 2021 Jan;162:615–35.

94. Förstermann U, Xia N, Li H. Roles of Vascular Oxidative Stress and Nitric Oxide in the Pathogenesis of Atherosclerosis. Circ Res. 2017 Feb 17;120(4):713–35.

95. Förstermann U. Oxidative stress in vascular disease: causes, defense mechanisms and potential therapies. Nat Clin Pract Cardiovasc Med. 2008 Jun;5(6):338–49.

96. Förstermann U. Nitric oxide and oxidative stress in vascular disease. Pflugers Arch. 2010 May;459(6):923–39.

97. Lee EM. Calcium channel blockers for hypertension: old, but still useful. Cardiovasc Prev Pharmacother. 2023 Oct 30;5(4):113–25.

98. Weir MR. Incidence of pedal edema formation with dihydropyridine calcium channel blockers: issues and practical significance. J Clin Hypertens Greenwich Conn. 2003;5(5):330–5.

99. Koh KK, Quon MJ, Lee SJ, Han SH, Ahn JY, Kim J a, et al. Efonidipine Simultaneously Improves Blood Pressure, Endothelial Function, and Metabolic Parameters in Nondiabetic Patients With Hypertension. Diabetes Care. 2007 Jun 1;30(6):1605–7.

100. Ohta M, Sugawara S, Sato N, Kuriyama C, Hoshino C, Kikuchi A. Effects of benidipine, a long-acting T-type calcium channel blocker, on home blood pressure and renal function in patients with essential hypertension: a retrospective, "real-world" comparison with amlodipine. Clin Drug Investig. 2009;29(11):739–46.

101. Feng MG, Li M, Navar LG. T-type calcium channels in the regulation of afferent and efferent arterioles in rats. Am J Physiol Renal Physiol. 2004 Feb;286(2):F331-337.

102. Sasaki H, Saiki A, Endo K, Ban N, Yamaguchi T, Kawana H, et al. Protective effects of efonidipine, a T- and L-type calcium channel blocker, on renal function and arterial stiffness in type 2 diabetic patients with hypertension and nephropathy. J Atheroscler Thromb. 2009 Oct;16(5):568–75.

103. Lee DS, Goodman S, Dean DM, Lenis J, Ma P, Gervais PB, et al. Randomized comparison of T-type versus L-type calcium-channel blockade on exercise duration in stable angina: results of the Posicor Reduction of Ischemia During Exercise (PRIDE) trial. Am Heart J. 2002 Jul;144(1):60–7.

104. Major TC, Dhamija S, Black N, Liachenko S, Morenko B, Sobocinski G, et al. The T- and L-Type Calcium Channel Blocker (CCB) Mibefradil Attenuates Leg Edema Induced by the L-Type CCB Nifedipine in the Spontaneously Hypertensive Rat: A Novel Differentiating Assay. J Pharmacol Exp Ther. 2008 Jun 1;325(3):723–31.

105. Niyonsaba E, Moussa M, Rusch N, Hill B. Estrogen Induces Coronary Arterial Dilation via Downregulation of Voltage-gated, Ca2+ Channels. FASEB J. 2015;29(S1):953.8.

106. Filgueira FP, Lobato NS, Nascimento DL, Ceravolo GS, Giachini FRC, Lima VV, et al. Equilin displays similar endothelium-independent vasodilator potential to 17β-estradiol regardless of lower potential to inhibit calcium entry. Steroids. 2019 Jan;141:46–54.

107. Vega-Vela NE, Osorio D, Avila-Rodriguez M, Gonzalez J, García-Segura LM, Echeverria V, et al. L-Type Calcium Channels Modulation by Estradiol. Mol Neurobiol. 2017 Sep;54(7):4996–5007.

108. Buñag RD. Validation in awake rats of a tail-cuff method for measuring systolic pressure. J Appl Physiol. 1973 Feb;34(2):279–82.

109. Lee JH, Gomora JC, Cribbs LL, Perez-Reyes E. Nickel block of three cloned T-type calcium channels: low concentrations selectively block alpha1H. Biophys J. 1999 Dec;77(6):3034–42.

110. Gilda JE, Gomes AV. Stain-Free total protein staining is a superior loading control to β-actin for Western blots. Anal Biochem. 2013 Sep 15;440(2):186–8.

111. Chomczynski P, Sacchi N. Single-step method of RNA isolation by acid guanidinium thiocyanate-phenol-chloroform extraction. Anal Biochem. 1987 Apr;162(1):156–9.

112. Livak KJ, Schmittgen TD. Analysis of relative gene expression data using real-time quantitative PCR and the 2(-Delta Delta C(T)) Method. Methods San Diego Calif. 2001 Dec;25(4):402–8.

113. Díez I, Calatayud S, Hernández C, Quintana E, O'Connor JE, Esplugues JV, et al. Nitric oxide, derived from inducible nitric oxide synthase, decreases hypoxia inducible factor-1alpha in macrophages during aspirin-induced mesenteric inflammation. Br J Pharmacol. 2010 Apr;159(8):1636–45.

114. Lampiao F, Strijdom H, du Plessis SS. Direct nitric oxide measurement in human spermatozoa: flow cytometric analysis using the fluorescent probe, diaminofluorescein. Int J Androl. 2006 Oct;29(5):564–7.

115. Emmendörffer A, Hecht M, Lohmann-Matthes ML, Roesler J. A fast and easy method to determine the production of reactive oxygen

intermediates by human and murine phagocytes using dihydrorhodamine 123. J Immunol Methods. 1990 Aug 7;131(2):269–75.

116. Crow JP. Dichlorodihydrofluorescein and dihydrorhodamine 123 are sensitive indicators of peroxynitrite in vitro: implications for intracellular measurement of reactive nitrogen and oxygen species. Nitric Oxide Biol Chem. 1997 Apr;1(2):145–57.

117. Kalyanaraman B. Oxidative chemistry of fluorescent dyes: implications in the detection of reactive oxygen and nitrogen species. Biochem Soc Trans. 2011 Oct;39(5):1221–5.

118. Kleinbongard P, Dejam A, Lauer T, Jax T, Kerber S, Gharini P, et al. Plasma nitrite concentrations reflect the degree of endothelial dysfunction in humans. Free Radic Biol Med. 2006 Jan 15;40(2):295–302.

119. Zaragoza C, Gomez-Guerrero C, Martin-Ventura JL, Blanco-Colio L, Lavin B, Mallavia B, et al. Animal Models of Cardiovascular Diseases. J Biomed Biotechnol. 2011;2011:497841.

120. Li Y, Xie D, Li L, Jiang P. Comprehensive analysis of metabolic changes in spontaneously hypertensive rats. Clin Exp Hypertens N Y N 1993. 2023 Dec 31;45(1):2190529.

121. Li Q, Fang Y, Peng DW, Li LA, Deng CY, Yang H, et al. Sacubitril/valsartan reduces susceptibility to atrial fibrillation by improving atrial remodeling in spontaneously hypertensive rats. Eur J Pharmacol. 2023 Aug 5;952:175754.

122. Zhou X, Frohlich ED. Analogy of cardiac and renal complications in essential hypertension and aged SHR or L-NAME/SHR. Med Chem Shariqah United Arab Emir. 2007 Jan;3(1):61–5.

123. He X, Zhang HL, Zhao M, Yang JL, Cheng G, Sun L, et al. Amlodipine ameliorates endothelial dysfunction in mesenteric arteries from spontaneously hypertensive rats. Clin Exp Pharmacol Physiol. 2011 Apr;38(4):255–61.

124. Ho JH, Baskaran R, Wang MF, Mohammedsaleh ZM, Yang HS, Balasubramanian B, et al. Dipeptide IF and Exercise Training Attenuate Hypertension in SHR Rats by Inhibiting Fibrosis and Hypertrophy and

Activating AMPKα1, SIRT1, and PGC1α. Int J Mol Sci. 2022 Jul 25;23(15):8167.

125. Mlinar B, Enyeart JJ. Block of current through T-type calcium channels by trivalent metal cations and nickel in neural rat and human cells. J Physiol. 1993 Sep;469:639–52.

126. Huang L, Keyser BM, Tagmose TM, Hansen JB, Taylor JT, Zhuang H, et al. NNC 55-0396 [(1S,2S)-2-(2-(N-[(3-benzimidazol-2-yl)propyl]-N-methylamino)ethyl)-6-fluoro-1,2,3,4-tetrahydro-1-isopropyl-2-naphtyl cyclopropanecarboxylate dihydrochloride]: a new selective inhibitor of T-type calcium channels. J Pharmacol Exp Ther. 2004 Apr;309(1):193–9.

127. Thuesen AD, Andersen H, Cardel M, Toft A, Walter S, Marcussen N, et al. Differential effect of T-type voltage-gated Ca2+ channel disruption on renal plasma flow and glomerular filtration rate in vivo. Am J Physiol Renal Physiol. 2014 Aug 15;307(4):F445-452.

128. Garcha RS, Sever PS, Hughes AD. Mechanism of action of angiotensin II in human isolated subcutaneous resistance arteries. Br J Pharmacol. 2001 Sep;134(1):188–96.

129. Ozawa Y, Hayashi K, Nagahama T, Fujiwara K, Saruta T. Effect of T-type selective calcium antagonist on renal microcirculation: studies in the isolated perfused hydronephrotic kidney. Hypertens Dallas Tex 1979. 2001 Sep;38(3):343–7.

130. Harraz OF, Brett SE, Zechariah A, Romero M, Puglisi JL, Wilson SM, et al. Genetic Ablation of CaV3.2 Channels Enhances the Arterial Myogenic Response by Modulating the RyR-BKCa Axis. Arterioscler Thromb Vasc Biol. 2015 Aug;35(8):1843–51.

131. Mikkelsen MF, Björling K, Jensen LJ. Age-dependent impact of CaV 3.2 T-type calcium channel deletion on myogenic tone and flow-mediated vasodilatation in small arteries. J Physiol. 2016 Oct 15;594(20):5881–98.

132. Collins EM, Walsh MP, Morgan KG. Contraction of single vascular smooth muscle cells by phenylephrine at constant [Ca2+]i. Am J Physiol. 1992 Mar;262(3 Pt 2):H754-762.

133. Unger T, Chung O, Csikos T, Culman J, Gallinat S, Gohlke P, et al. Angiotensin receptors. J Hypertens Suppl. 1996 Dec 1;14(5):S95-103.

134. Lee SH, Ok SH, Subbarao RB, Kim JY, Bae SI, Hwang Y, et al. Nitric oxide-mediated inhibition of phenylephrine-induced contraction in response to hypothermia is partially modulated by endothelial Rho-kinase. Int J Med Sci. 2020 Jan 1;17(1):21–32.

135. Dora KA, Doyle MP, Duling BR. Elevation of intracellular calcium in smooth muscle causes endothelial cell generation of NO in arterioles. Proc Natl Acad Sci. 1997 Jun 10;94(12):6529–34.

136. Tuttle JL, Falcone JC. Nitric oxide release during alpha1-adrenoceptor-mediated constriction of arterioles. Am J Physiol Heart Circ Physiol. 2001 Aug;281(2):H873-881.

137. Ball CJ, Wilson DP, Turner SP, Saint DA, Beltrame JF. Heterogeneity of L- and T-channels in the vasculature: rationale for the efficacy of combined L- and T-blockade. Hypertens Dallas Tex 1979. 2009 Apr;53(4):654–60.

138. Kuo IYT, Howitt L, Sandow SL, McFarlane A, Hansen PB, Hill CE. Role of T-type channels in vasomotor function: team player or chameleon? Pflugers Arch. 2014 Apr;466(4):767–79.

139. Moncada S, Palmer RM, Higgs EA. Nitric oxide: physiology, pathophysiology, and pharmacology. Pharmacol Rev. 1991 Jun;43(2):109–42.

140. Iepsen UW, Hjortdal AR, Thuesen AD, Finsen SH, Hansen PBL, Mortensen SP. The role of T-type calcium channels in elderly human vascular function: A pilot randomized controlled trial. Exp Physiol. 2024 May;109(5):779–90.

141. Doris PA. Genetics of hypertension: an assessment of progress in the spontaneously hypertensive rat. Physiol Genomics. 2017 Nov 1;49(11):601–17.

142. Rizzoni D, Castellano M, Porten E, Bettoni G, Muiesan ML, Agabiti-Rosei E. Vascular Structural and Functional Alterations Before and After

the Development of Hypertension in SHR. Am J Hypertens. 1994 Feb 1;7(2):193–200.

143. Butts CA, Hedderley DI, Martell S, Dinnan H, Middlemiss-Kraak S, Bunn BJ, et al. Influence of oral administration of kukoamine A on blood pressure in a rat hypertension model. PLOS ONE. 2022 May 6;17(5):e0267567.

144. Hohl M, Lauder L, Sevimli Ö, Tokcan M, Wagmann L, Götzinger F, et al. Efficacy of Antihypertensive Drugs of Different Classes After Renal Denervation in Spontaneously Hypertensive Rats. Hypertension. 2023 Jun;80(6):e90–100.

145. Safar M, Chamiot-Clerc P, Dagher G, Renaud JF. Pulse Pressure, Endothelium Function, and Arterial Stiffness in Spontaneously Hypertensive Rats. Hypertension. 2001 Dec;38(6):1416–21.

146. Wu CC, Yen MH. Higher level of plasma nitric oxide in spontaneously hypertensive rats. Am J Hypertens. 1999 May;12(5):476–82.

147. Ling WC, Murugan DD, Lau YS, Vanhoutte PM, Mustafa MR. Sodium nitrite exerts an antihypertensive effect and improves endothelial function through activation of eNOS in the SHR. Sci Rep. 2016 Sep 12;6(1):33048.

148. Cerecedo D, Martínez-Vieyra I, Hernández-Rojo I, Hernández-Cruz A, Rincón-Heredia R, Millán-Aldaco D, et al. Reactive oxygen species downregulate dystroglycans in the megakaryocytes of rats with arterial hypertension. Exp Cell Res. 2023 Dec 15;433(2):113847.

149. Cuzzocrea S, Mazzon E, Dugo L, Di Paola R, Caputi AP, Salvemini D. Superoxide: a key player in hypertension. FASEB J Off Publ Fed Am Soc Exp Biol. 2004 Jan;18(1):94–101.

150. Souza Bomfim GH, Musial DC, Rocha K, Jurkiewicz A, Jurkiewicz NH. Red wine but not alcohol consumption improves cardiovascular function and oxidative stress of the hypertensive-SHR and diabetic-STZ rats. Clin Exp Hypertens. 2022 Aug 18;44(6):573–84.

151. Randriamboavonjy JI, Rio M, Pacaud P, Loirand G, Tesse A. Moringa oleifera Seeds Attenuate Vascular Oxidative and Nitrosative Stresses in Spontaneously Hypertensive Rats. Oxid Med Cell Longev. 2017;2017:4129459.

152. Wu T, Zheng Y, Huang Q, Tian S. Paeonol improves renal and vascular angiotensin II type 1 receptor function via inhibiting oxidative stress in spontaneously hypertensive rats. Clin Exp Hypertens N Y N 1993. 2023 Dec 31;45(1):2182884.

153. Wu L, de Champlain J. Effects of superoxide on signaling pathways in smooth muscle cells from rats. Hypertens Dallas Tex 1979. 1999 Dec;34(6):1247–53.

154. Sartori-Valinotti JC, Iliescu R, Fortepiani LA, Yanes LL, Reckelhoff JF. Sex differences in oxidative stress and the impact on blood pressure control and cardiovascular disease. Clin Exp Pharmacol Physiol. 2007 Sep;34(9):938–45.

155. Bhatia K, Elmarakby AA, El-Remessy AB, Sullivan JC. Oxidative stress contributes to sex differences in angiotensin II-mediated hypertension in spontaneously hypertensive rats. Am J Physiol Regul Integr Comp Physiol. 2012 Jan 15;302(2):R274-282.

156. Reckelhoff JF, Romero DG, Yanes Cardozo LL. Sex, Oxidative Stress, and Hypertension: Insights From Animal Models. Physiol Bethesda Md. 2019 May 1;34(3):178–88.

157. Sullivan JC, Semprun-Prieto L, Boesen EI, Pollock DM, Pollock JS. Sex and sex hormones influence the development of albuminuria and renal macrophage infiltration in spontaneously hypertensive rats. Am J Physiol Regul Integr Comp Physiol. 2007 Oct;293(4):R1573-1579.

158. Sullivan JC, Sasser JM, Pollock JS. Sexual dimorphism in oxidant status in spontaneously hypertensive rats. Am J Physiol Regul Integr Comp Physiol. 2007 Feb;292(2):R764-768.

159. Gillis EE, Brinson KN, Rafikova O, Chen W, Musall JB, Harrison DG, et al. Oxidative stress induces BH4 deficiency in male, but not female, SHR. Biosci Rep. 2018 Aug 31;38(4):BSR20180111.

160. Anishchenko AM, Aliev OI, Sidekhmenova AV, Shamanaev AYu, Plotnikov MB. Dynamics of Blood Pressure Elevation and Endothelial Dysfunction in SHR Rats During the Development of Arterial Hypertension. Bull Exp Biol Med. 2015 Sep 1;159(5):591–3.

161. Lataro RM, Silva MAB, Mestriner FL, Cau SBA, Tostes RCA, Salgado HC. Chronic Treatment With Acetylcholinesterase Inhibitors Attenuates Vascular Dysfunction in Spontaneously Hypertensive Rats. Am J Hypertens. 2019 May 9;32(6):579–87.

ANNEXES

Annexe I: Supplementary data

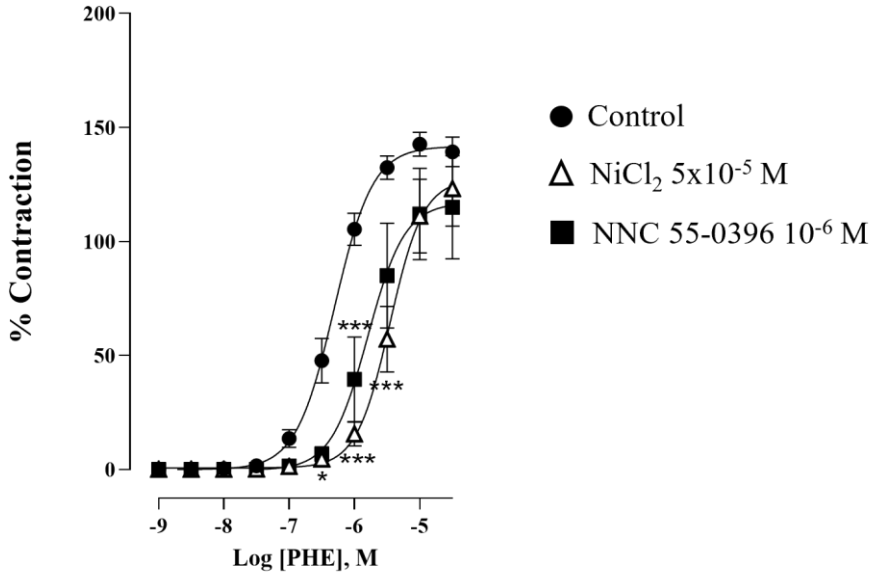

*Supplementary Figure 1: Concentration-response curve to phenylephrine in the rabbit renal artery in the absence (control) and presence of nickel chloride ($5x10^{-5}$ M) and NNC 55-0396 (10^{-6} M). n=6. Data are shown as mean ± SEM. *P<0.05; **P<0.01; ***P<0.001 compared to control.*

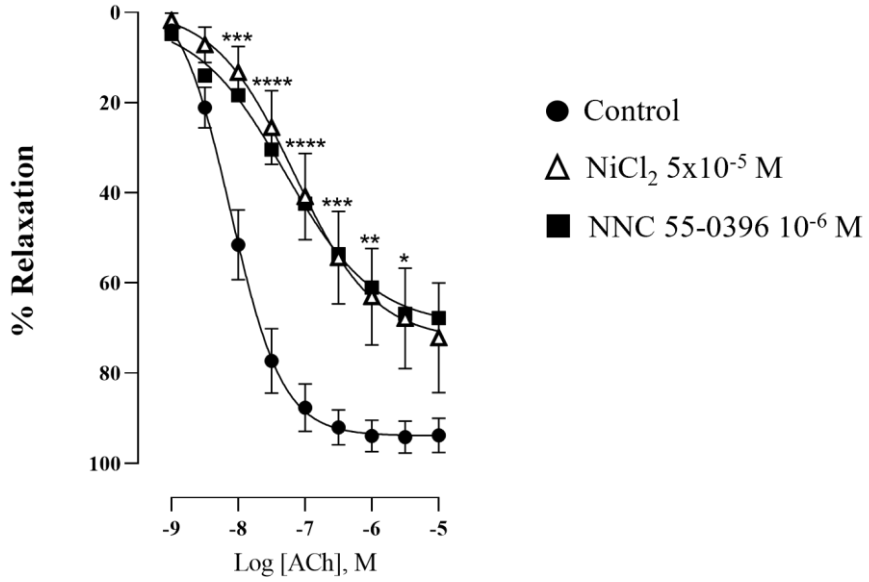

*Supplementary Figure 2: Concentration-response curve to acetylcholine in the rabbit renal artery in the absence (control) and presence of nickel chloride ($5x10^{-5}$ M) and NNC 55-0396 (10^{-6} M). n=6. Data are shown as mean ± SEM. *P<0.05; **P<0.01; **P<0.01; ***P<0.001 compared to control.*